NEURODEGENERATION IN CEREBELLAR GRANULE CELLS OF P/Q TYPE VOLTAGE GATED CALCIUM CHANNEL MUTANT LEANER MICE

A Dissertation

by

BHUPINDER BAWA

Submitted to the Office of Graduate Studies of
Texas A&M University
in partial fulfillment of the requirements for the degree of

DOCTOR OF PHILOSOPHY

December 2007

Major Subject: Veterinary Anatomy

NEURODEGENERATION IN CEREBELLAR GRANULE CELLS OF P/Q TYPE VOLTAGE GATED CALCIUM CHANNEL MUTANT LEANER MICE

A Dissertation

by

BHUPINDER BAWA

Submitted to the Office of Graduate Studies of
Texas A&M University
in partial fulfillment of the requirements for the degree of

DOCTOR OF PHILOSOPHY

Approved by:

Chair of Committee,	Louise C. Abbott
Committee Members,	William Griffith
	C. Jane Welsh
	W. Les Dees
Head of Department,	Evelyn Tiffany Castiglioni

December 2007

Major Subject: Veterinary Anatomy

ABSTRACT

Neurodegeneration in Cerebellar Granule Cells of P/Q Type Voltage Gated Calcium Channel Mutant Leaner Mice. (December 2007)

Bhupinder Bawa,

B.V.Sc. & A.H., Punjab Agricultural University; M.V.Sc., Punjab Agricultural University

Chair of Advisory Committee: Dr. Louise C. Abbott

Mutations of the α_{1A} subunit of Ca_V 2.1 voltage gated calcium (VGCC) channels are responsible for several inherited disorders affecting humans, including familial hemiplegic migraine, episodic ataxia type and spinocerebellar ataxia type. The leaner mouse also carries an autosomal recessive mutation in the α_{1A} subunit of Ca_V 2.1 VGCCs, which, in the homozygous condition, results in a severe cerebellar atrophy and ataxia. The leaner mutation results in reduced calcium influx through Ca_V 2.1 VGCCs. To better understand cerebellar neurodegeneration and cerebellar dysfunction we focused our research on elucidating the relationship between mitochondrial function/dysfunction and calcium channel mutations. The aims of this dissertation were: 1) to estimate the extent of neuronal cell death, basal intracellular calcium and mitochondrial (dys)function in cerebellar granule cells (CGC) of adult leaner mice; 2) to analyze the role of the leaner calcium channel mutation on postnatal development of CGCs; and 3) to test whether inducing increased calcium influx by exposing cultured granule cells to potassium chloride can eliminate or reduce the CGC death.

By using mechanism independent Fluoro-Jade staining and apoptosis specific TUNEL staining, we demonstrated that leaner CGC death continues into adulthood and the spatial pattern of granule cell death observed during postnatal development also continues into adulthood. The present investigation showed a reduced resting intracellular calcium in CGC from leaner mice as compared to age matched wild type mice, and tottering mice. The tottering mouse is another mutant mouse that carries a mutation in the α_{1A} subunit of Ca_V 2.1 VGCCs like leaner mouse. However, these mice do not show any neurodegeneration and therefore they were used as a second control. Our results also showed that even though CGC of leaner mice have dysfunctional $Ca_V2.1$ channels, there is no change in depolarization induced Ca^{2+} influx, which suggests a functional compensation for $Ca_V2.1$ calcium channels by other VGCCs. Our results showed reduced mitochondrial membrane potential at the time of peak CGC death in leaner mice as compared to wild type CGCs and tottering CGCs. The results of this investigation suggest mitochondrial mediated but reactive oxygen species independent cell death in CGCs of leaner mice.

ACKNOWLEDGEMENTS

I feel privileged to express gratitude to my revered guide Dr. Louise C. Abbott for her keen supervision, persistent encouragement, excellent and dexterous guidance, invaluable suggestions, judicious attitude and constructive criticism during every phase of my graduate study. I humbly place on record my respect and gratitude to Drs. Griffith, Dees and Welsh for their valuable suggestions during my research work leading to successful completion of my dissertation work. I extend my sincere thanks to my colleagues Tamy Catherine Frank-Cannon, Kerry Thuett, Sairam Bellum, Sarah Wills, and Pei-San Huang for their association and cooperation.

With great pleasure I express my profound sense of gratitude to Drs. Ruoff, Hoffman, Herman and Jaeger for their valuable advice and guidance during the years of my graduate study as a teaching assistant in Veterinary Anatomy. My heartiest thanks are due to Dr. Mark Zoran for his valuable advice and guidance in my research work. Special thanks to Dr. Gerald Frye and Haiying Wang (TAMU-HSC) for providing instrumentation and Christine McCoy for technical support.

Lastly, no words are enough to express my profound gratitude, love and affection to my beloved wife, Manveen. Words alone cannot express how truly thankful I am to her for her patience and love. I take pride in myself for being the son of great parents whose everlasting desire, selflessness, sacrifice, infinite encouragement, affection, blessing and help throughout my academic exploration brought me here. It would not have been possible for the present study to see the light of the day without them. I shall be failing in my duties if special thanks are not expressed to my brother, his wife and

two wonderful kids and my sister, her husband and their two lovely kids for their appreciation, encouragement and good wishes for the completion of this study.

Words fail to express my feelings for all those who love and care for me. All may not have been mentioned, but none is forgotten. Last but not the least; I thank the Almighty God for giving me patience and strength to overcome the difficulties which crossed my way in accomplishment of this endeavor.

TABLE OF CONTENTS

CHAPTER Page

LIST OF FIGURES

FIGURE Page

LIST OF TABLES

CHAPTER I

INTRODUCTION

THE BASIC NEUROANATOMY OF THE CEREBELLUM

The word cerebellum comes from Latin, which means “little brain” and that is a very apt description of this neural center. The cerebellum contributes to only 10% of total brain volume however; it has more neurons than the rest of the brain (Ghez and Thach, 2000). The cerebellum is situated caudal to the cerebral hemispheres and dorsal to the fourth ventricle and occupies most of the posterior cranial fossa (Ghez and Thach, 2000; Nolte, 1999). The primary function of the cerebellum is integration of sensory signals delivered from various regions of the brain and spinal cord in order to serve as a coordination center for movement of the eyes, head and body. The cerebellum does not initiate or execute movement, but it is responsible for controlling the rate, range and force of every movement (Ito, 1984a; Middleton and Strick, 1998; Gilbert, 2001). The cerebellum is attached to the pons by three pairs of tracts: the superior, middle and inferior cerebellar peduncles.

This dissertation follows the style of Journal of Neuroscience.

The fundamental anatomical organization of the cerebellum and its circuitry was established more than a century ago by Cajal (Cajal 1888a; Cajal 1888b) whose detailed description has been only slightly modified thereafter. At a gross anatomical level, this bilaterally symmetric structure can be divided into several distinct areas. Mediolaterally, there is a midline vermis, two lateral expansions known as the hemispheres and flocculi. These anatomical divisions have functional significance, since the primary modalities subserved by the specific regions are different (Herrup and Kuemerle, 1997). The vermis is primarily responsible for spinocerebellar or somatosensory functions, while the hemispheres are responsible for motor planning to coordinate motor function in the limbs and motor learning (Nolte, 1999). The flocculonodular lobe is most closely associated with vestibular function and thus is responsible for balance and equilibrium (Nolte, 1999).

In the anterior-posterior (A-P axis) direction, the subdivisions of cerebellum are: the anterior cerebellum (rostral to the primary fissure), the posterior cerebellum (caudal to the primary fissure), and the flocculonodular lobe (caudal to the posterolateral fissure) (Herrup and Kuemerle, 1997). The A-P axis is further divided by the process of lobulation. Ten lobules are recognized at the midline, while eight are recognized in each hemisphere (Herrup and Kuemerle, 1997) (Figure I-1). Lobules in the vermis are denoted by roman numerals positioned at the midline. Lobules in the hemispheres are indicated by their Latin names. Different nomenclature for these lobules is used between human and other mammalian species (Table I-1). In the mouse cerebellar vermis (Figure

I-2), lobules I and II are fused as are lobules IV and V where as, lobule III remains separate (Marani and Voogd, 1979).

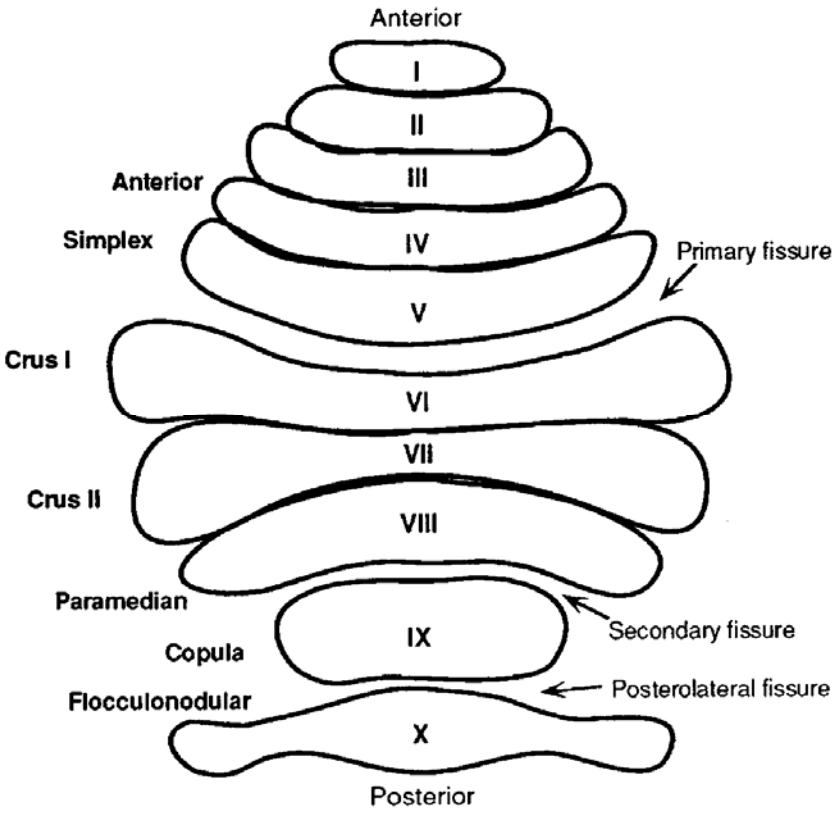

Figure I-1. Schematic presentation showing cerebellar lobules. Cerebellum is unrolled to view all the lobules from the dorsal surface. Lobules in the vermis are denoted by Roman numerals positioned at the midline. Lobules in the hemispheres are indicated by their Latin names. Arrows indicate the three major fissures that divide the cerebellum anterior-posteriorly (Modified from Herrup and Kuemerle, 1997).

Microscopic anatomy of cerebellum

Microscopically, the cerebellar cortex is arranged into three layers starting with the most external: molecular layer, Purkinje cell body layer, and granule cell layer (Figure I-2). The molecular layer, a region of low cellular density but of high synaptic

incidence, primarily consists of interneurons (stellate and basket cells), dendritic processes of Purkinje cells and axons of granule cells (parallel fibers) and inferior olive neurons (climbing fibers) (Nolte, 1999; Altman and Bayer, 1997a). The granule cell layer includes granule cell neurons, unipolar brush cell interneurons and Golgi cell interneurons; whereas, the Purkinje cell layer consists of the cell bodies of Purkinje neurons (Nolte, 1999; Altman and Bayer, 1997a).

Table I-1: Nomenclature of cerebellar lobules

Vermis		**Hemisphere**	
Human	**Other mammals**	**Human**	**Other mammals**
Lingula	Lobule I	Vincingulum lingulae	Anterior lobule
Centralis	Lobule II & III	Ala lobulus centralis	Anterior lobule
Culmen	Lobule IV & V	Ant. quadrangulate lobule	Anterior lobule
Declive	Lobule VI	Post. quadrangulate lobule	Lobule simplex
Folium	Lobule VIIA	Sup. semilunar lobule	Ansiform lobule Crus I
Tuber	Lobule VIIB	Inf. Semilunar & Gracile lob	Ansiform lobule Crus I
Pyramis	Lobule VIII	Biventral lobule	Paramedian lobule
Uvula	Lobule IX	Tonsilla	Dorsal paraflocculus
Nodulus	Lobule X	Accessory paraflocculu	Ventral paraflocculus

Ant. = anterior, Post. = posterior, Sup. = superior, Inf.= inferior, Lob= lobule (Altman and Bayer, 1997b; Voogd and Glickstein, 1998).

A characteristic Purkinje cell has a pear-shaped cell body and a fan-shaped dendritic arbor that is oriented in the sagittal plan and which extends throughout the width of the cerebellar molecular layer. Purkinje cells are among the largest neurons of the brain, with their somata measuring approximately 50-80μm in diameter (Parent 1996).

Granule cells are approximately 5-8 µm in diameter with scarce cytoplasm. They are the most numerous neurons present in the brain (Ito, 1984c). Each granule cell extends 3 to 5 dendrites, which terminate to synapse with mossy fiber and other terminal axons. The axons of granule cells pass through the granule and Purkinje cell layers to a particular level in the molecular layer where they bifurcate to form parallel fibers. The deepest granule cells send axon to innermost molecular layer and granule cells close to Purkinje cell layer have axon in the outermost molecular layer.

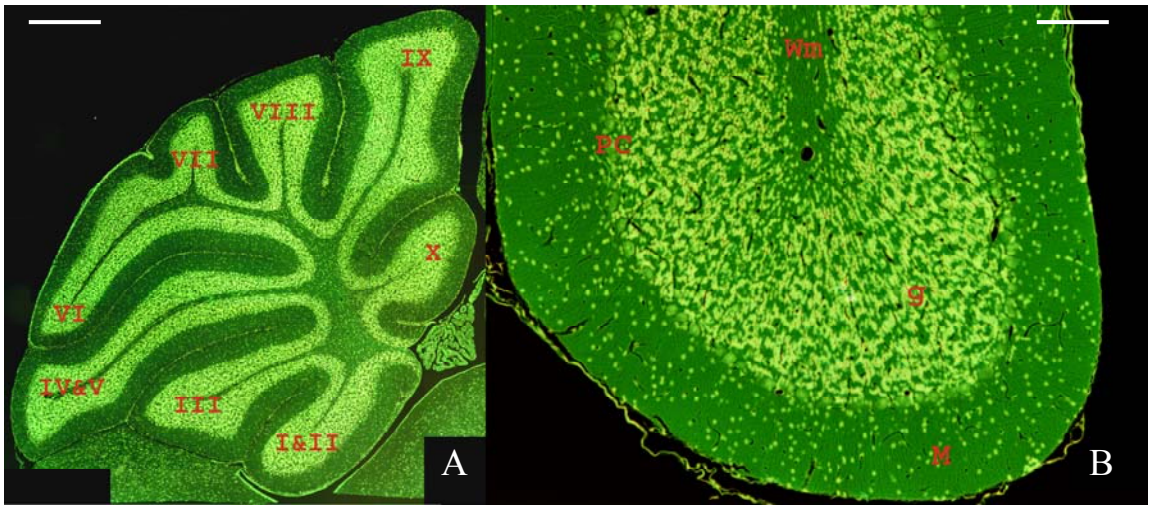

Figure I-2. Light microscopic section of adult mouse cerebellum. (A) is showing a midsagittal view of mouse cerebellar vermis identifying various lobules (I – X). (B) is showing the three layers of cerebellum at high magnification. "A" and "B" are images from a 5 µm thick sagittal section take from a paraformaldehyde fixed, paraffin embedded mouse brain. The section was stained with H&E. The images are color inverted using Adobe photoshop for visual clarity. M represents molecular layer, PC is Purkinje cell body layer, g is granule cell layer and Wm is white matter. Scale bar in A is 500 µm. Scale bar in B is 100 µm.

The cerebellum receives inputs from various parts of the nervous system via three major regions or systems of the central nervous system (CNS) (Figure I-3). These are: 1) climbing fibers, 2) mossy fibers and 3) the monoaminergic fiber systems. The inferior olive is the source of climbing fiber input into the contralateral cerebellum and relay information from the spinal cord, red nucleus and cerebral motor cortex through the caudal cerebellar peduncles. Each climbing fiber, after entering the cerebellum, divides and sends one branch to a cerebellar Purkinje cell and the other branch provides collateral innervation to deep cerebellar nuclei neurons (O'Leary et al., 1970; Altman and Bayer, 1997a). The projections from the inferior olive to the cerebellum are topographically organized. Climbing fibers use aspartate and corticotrophin releasing factor (CRF) as neurotransmitter (NT) and are excitatory to Purkinje cells and it is known to make 1:1 contact with a Purkinje cell along the dendritic tree (Larramendi and Victor, 1967).

Mossy fibers are the most numerous axons entering the cerebellum. They originate from neurons in the brain stem reticular formation, pontine nuclei, vestibular nuclei and spinal cord to relay information through the middle and caudal cerebellar peduncles to cerebellar granule cells, unipolar brush cells, and collateral innervation to the deep cerebellar nuclei neurons (Chan-Palay et al., 1977; Olschowka and Vijayan, 1980; Altman and Bayer, 1997a; Morin et al., 2001). Mossy fibers on reaching granule cells form a rosette-like structure and synapse on granule cell dendrites. Mossy fibers use glutamate as NT and are excitatory to granule and unipolar brush cells (Olschowka and Vijayan, 1980).

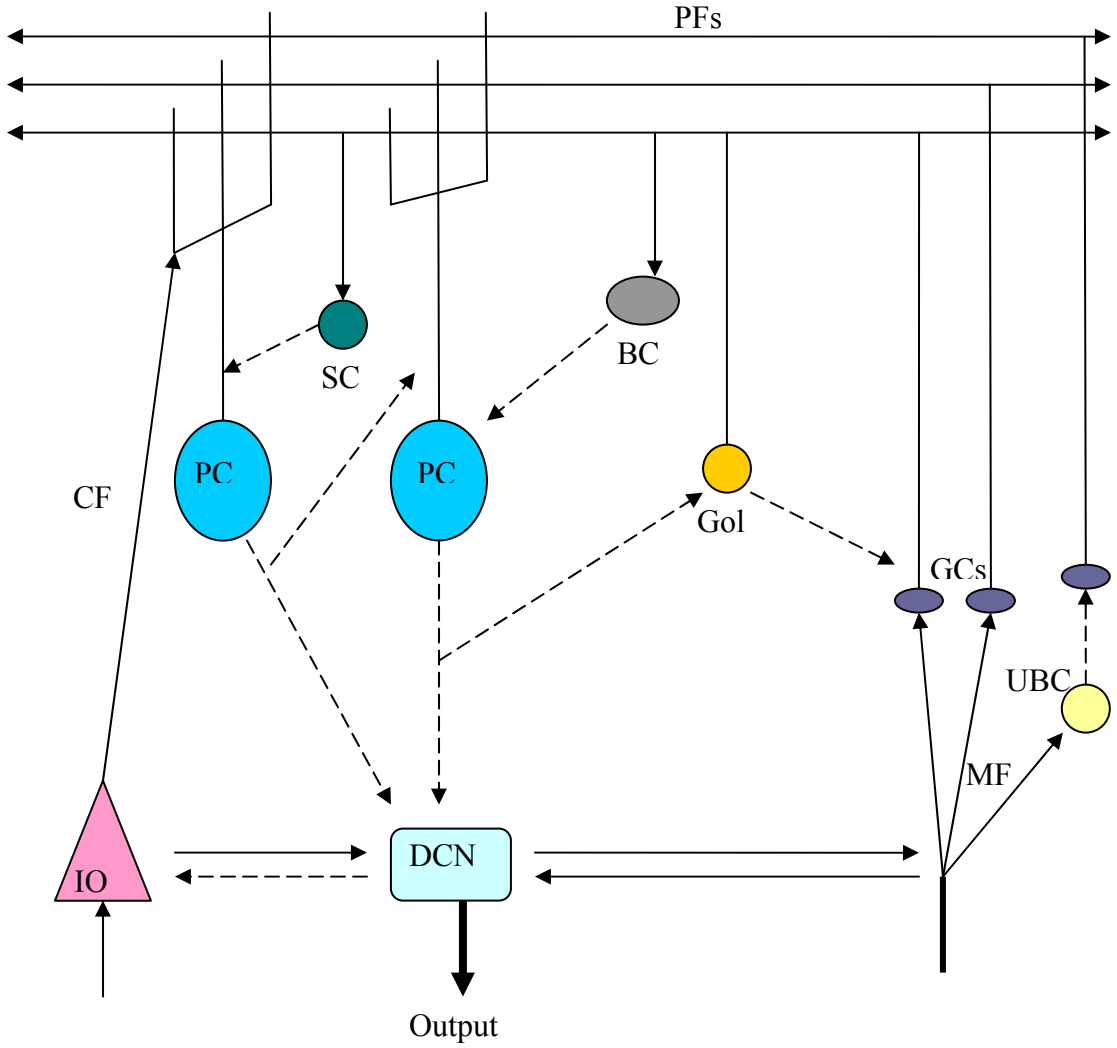

Figure I-3. Schematic presentation of basic circuitry of cerebellum. The arrows represent flow of signal. Solid lines represent excitatory innervation and dashed lines represent inhibitory innervation. IO is inferior olive, DCN is deep cerebellar nuclei, MF are mossy fibers, CF are climbing fibers, UBC are unipolar brush cells, GCs are granule cells, Gol are Golgi cells, PC are Purkinje cells, BC are basket cells, SC are stellate cells, and PFs are parallel fibers.

Parallel fibers from cerebellar granule cells make excitatory synapses on perpendicularly oriented Purkinje cell dendrites, primarily on the tertiary dendrites (Palkovits et al., 1971). The summary of neurotransmitters involved in cerebellar circuitry is given in Table I-2. Parallel fibers also have glutamate mediated excitatory synapse on basket and stellate cells, which are located in the molecular layer (Eccles et al., 1967; Ito, 1984c) and Golgi cells located in the granule cell layer. The axons of stellate cells terminate on the primary dendrite of Purkinje cells. Parallel fibers provide excitatory input to stellate cells, which in turn use GABA to produce inhibitory signals to Purkinje cells (Martin, 1996). Basket cells receive excitatory parallel fiber input and their axons synapse on Purkinje cell bodies, and also exert strong inhibition on Purkinje cells (Altman and Bayer, 1997a). Golgi cells receive input from parallel fibers along with collateral GABA mediated inhibitory input from Purkinje cells and then make inhibitory synapses on granule cell dendrites in the cerebellar glomeruli (Altman and Bayer, 1997a). Since Golgi cells are inhibitory to cerebellar granule cells, this provides a negative feedback loop for Purkinje cell excitability and further modulates Purkinje cell activity. Because all the neurons contacted by parallel fibers (Purkinje cells, basket, stellate cells and Golgi cells) are inhibitory neurons, the net effect of granule cells excitation is the inhibition of discharges by their target neurons.

In addition to climbing fiber and mossy fibers, diffuse monoaminergic fibers also reach the cerebellum. Noradrenergic, serotonergic and dopaminergic fibers originate from the locus coeruleus, raphe nuclei and ventral mesencephalic tegmentum,

respectively and extend from the white matter into all layers of the cerebellar cortex (Ghez and Thach, 2000; Parent, 1996).

Purkinje cells are the sole generator of output signals from the cerebellar cortex and their axons synapse on the deep cerebellar nuclei (DCN) and vestibular nuclei. Purkinje cell input to the DCN exerts powerful inhibition on the deep cerebellar neurons (Ito, 1984b).

Table I-2: Neurotransmitters involved in cerebellar circuitry.

Presynaptic fibers	Neurotransmitter	Postsynaptic targets
Mossy fibers	Glutamate, Acetylcholine	Granule cells
	Glutamate	Unipolar brush cells
Climbing fibers	Aspartate, CRF	Purkinje cells
	CRF	Deep cerebellar nuclei
Granule cells	Glutamate	Purkinje cells
Purkinje cells	GABA	Deep cerebellar nuclei
		Golgi cells
Golgi cells	GABA, Glycine	Granule cells
Basket cells	GABA	Purkinje cells
Stellate cells	GABA, Taurine	Purkinje cells
Deep cerebellar nuclei	GABA	Inferior olivary nuclei (ION)
	Aspartate, Glutamate	Other than ION
Unipolar brush cells	Glutamate*	Granule cells

CRF = corticotrophin releasing factor, GABA = gamma amino butyric acid (Altman and Bayer, 1997a), * (Dino et al., 2000; Billups et al., 2002)

The DCN are composed of bilateral pairs of fastigial, interpositus (emboliform and globus in humans) and dentate nuclei (Marani and Voogd, 1979). The fastigial nuclei receive axons from the cerebellar vermis, while the interpositus and dentate nuclei receive axons from the paravermis and hemispheres, respectively (Nolte, 1999). DCN

send their axons to the red nucleus, thalamic nuclei, vestibular nuclei, reticular formation and pons. Some axons of the DCN project directly to the spinal cord (Voogd et al., 1990). Most of the efferent fibers from the DCN exit the cerebellum through the superior cerebellar peduncle. Purkinje cell axons from the flocculonodular lobe project directly to the medial and lateral vestibular nuclei. Through the lateral vestibular nucleus Purkinje cells are able to modulate lateral and medial vestibulospinal tracts, which control axial muscles and limb extensors that regulate gait and stance. Purkinje cells control head and eye movements through the medial vestibular nucleus (Kandel and Siegelbaum, 2000).

A number of neuromodulators influence the cerebellar circuitry. Neuromodulation is defined as chemical communication between neurons that is either not fast, not point to point, or not simply excitation or inhibition (Schweighofer et al., 2004). Traditionally, the cerebellum has been thought to receive only serotonergic and noradrenergic neuromodulatory afferents (Ito, 1984a). Besides these two major projections, however, there are projections from the other long-range neuromodulatory groups including dopamine, acetylcholine, histamine and endocannabinoids.

The cholinergic input to the cerebellum is sparser than to the forebrain and midbrain area so it makes a diffuse plexus of beaded fibers in the cerebellar cortex and cerebellar nuclei (Barmack et al., 1992a, 1992b) that originate in the pedunculopontine tegmental nucleus, the lateral paragigantocellular nucleus, and to a lesser extent, in various raphe nuclei (Jaarsma et al., 1997). Acetylcholine potentiates granule cell-

Purkinje cell synapses, presumably via muscarinic acetylcholine receptors (Andre et al., 1993).

The cerebellum receives it dopaminergic innervation from the ventral tegmental area (Ikai et al., 1992). In the cerebellar cortex Purkinje cells are known to express dopaminergic receptors (Barili et al., 200), which presumably influence the plasiticity in Purkinje cells (Schweighofer et al., 2004). Histamine is found in nerve cell bodies of the tuberomammillary nucleus in the mammalian brain and has been shown to send projections to both the Purkinje cell and granule cell layer (Xu et al., 1987; Panula et al., 1993). Histamine exerts an excitatory effect via both H1 and H2 receptors on granule cells (Li et al., 1999) and via H2 receptors on Purkinje cells (Tian et al., 1999).

The cerebellum also contains several intrinsic neuromodulators like cannabinoids (Kreitzer et al., 2002; Yoshida et al., 2002) and nitric oxide (Crepel and Jaillard, 1990). Endocannabinoids are released from postsynaptic cells in a calcium-dependent manner after brief depolarizing input. Once released, endocanabinoids inhibit neurotransmitter release via the retrograde activation of cannabinoid CB1 receptors located on axon terminals (Wilson and Nicoll, 2001; Good, 2007). Two endocannabionoids, anandamide and 2-arachidonyl glycerol have been studied in depth so far (Fride, 2005) and two cannabinoid receptors, CB1 and CB2 have been identified and cloned (Fride, 2005). In the cerebellum, CB1 receptors immunuoreactivity has been shown in the molecular layer and Purkinje cell layer (Tsou et al., 1998; Freund et al., 2003). The interneurons of molecular layer, stellate and basket cells, are thought to sharpen the parallel fiber inputs

to Purkinje cells by temporally limiting this excitatory input through release of endocannabinoids (Good, 2007).

DEVELOPMENT OF CEREBELLAR GRANULE CELLS

The cerebellum is derived from the alar (dorsal, sensory) plate of the neural tube at the mesencephalon-metencephalon junction (also called the isthmus) shortly after neural tube closure at embryonic day (E) 8.5 in rats and mice (McMahon and Bradley, 1990; Herrup and Kuemerle, 1997; Goldwitz and Hamre, 1998). The isthmus has been shown, using a chick-quail chimera paradigm, to have organizing potential on surrounding neural tissue by virtue of its morphogenetic properties and expression of many regulatory genes like *Fgf8*, *Wnt1*, *Gbx2* and *Otx2* (Sotelo, 2004).

During the embryonic phase of murine cerebellar development, a gap in the dorsal neural plate combined with bending of the pontine flexure leads to formation of two cerebellar anlages on the roof of IV^{th} ventricle. These anlages are first extended in anteroposterior axis and then rotate to adopt a mediolateral orientation, which leads to fusion of anterior parts at the midline by E16.5 in mice to form precursors of the central cerebellar vermis and bilaterally paired cerebellar hemispheres (Narboux-Neme et al., 2005; Sgaier et al., 2005).

The cerebellum is one of the unusual structures in the brain where the neuronal population arises from at least two different germinal zones; the initial germinal matrix and the secondary germinal matrix. The initial germinal matrix, which is bounded

anteriorly by the isthmus and posteriorly by the choroid plexus, consists of neuroepithelial ventricular zone rostrally and the rhombic lip caudally (Goldwitz and Hamre, 1998). The first neurons to be generated in the mouse cerebellum are the DCN neurons and then the Purkinje cells are generated from E11 to E14 (Sotelo, 2004; Goldwitz and Hamre, 1998). Purkinje cells attain their characteristic size and single layered arrangement only ten days after birth (Altman and Bayer, 1997c). The Golgi cells that are produced over a longer period of time are thought to share a similar origin as Purkinje cells and DCN neurons (Narboux-Neme et al., 2005).

The rhombic lip leads to formation of the secondary germinal matrix, which forms the external granule cell layer (EGL). Basket cells and stellate cells appear postnatally between postnatal day (P) 1 to P15 (Miale and Sidman, 1961). These neuronal cell types where originally thought to be generated from EGL since it is the only active germinal zone for cerebellar neurons at postnatal ages. However, fate mapping experiments using chick and quail chimera have established that, unlike granule cells, these molecular layer interneurons were generated from both mesencephalon and metencephalon. Zhang and Goldman (1996) were the first to identify that cerebellar white matter has dividing neuronal precursors, which migrate to cerebellar cortex and differentiate into molecular layer interneurons. Unipolar brush cell interneurons also called Lugaro cells develop around E14, migrate to the internal granule cell layer of the vestibulocerebellum by P2 to P9 where they complete their differentiation and maturation by P20 (Abbott and Jacobowitz, 1995; Morin et al., 2001; Ito, 2006). These are rounded cell (9-12μm in diameter) having a single thin axon and a

short dendrite that divides only at the tip, giving rise to tightly packed branchlets resembling a paintbrush (Mugnaini and Floris, 1994).

Around E13 in the mouse embryo, granule neuron precursors from the rhombic lip migrate tangentially to cover the superficial zone of cerebellar anlage to form the EGL. By E15, granule cell precursors cover most of the cerebellar surface and undergo clonal expansion to produce, perinatally, postmitotic granule cells (Sotelo, 2004; Hatten et al., 1997). During this process the EGL becomes bilayered, forming a superficial zone containing actively proliferating granule cells and a deep zone containing undifferentiated postmitotic granule cells (Cajal, 1911). Postmitotic granule cells undergo radial migration along the radially aligned Bergmann glial fibers to reach their final destination in the internal granule cell layer (IGL) (Hatten et al., 1997). The stacking of granule cells in IGL follows a "inside-out" settling pattern, with the earlier-generated and earlier-settling granule cells occupying the base of IGL and later produced and later arriving granule cells settling above them close to Purkinje cell layer (Altman and Bayer, 1997d). The EGL disappears by P15, which means that the proliferative period for granule cells is from E10 to P15 (Stoleo, 2004). The developmental stages of granule cells are shown in Figure I-4.

The cerebellum is a highly ordered structure with tight regulation of the ratio of Purkinje cells to granule cells (Wetts and Herrup, 1983). However, the mechanism that regulates the massive cell division in granule cell precursors and their differentiation is still elusive. A number of studies have suggested that Purkinje cells may be responsible for regulating the proliferation of granule cell precursor cells and determining the size of

the granule cell population. The classical studies done on neurological mutant mice affecting either the number (*staggerer*) or location (*reeler*) of Purkinje cells in the developing cerebellum suggest the role of Purkinje cells in proliferation of granule cell precursors (Mallet et al., 1976; Mariani et al., 1977). Studies done on meander tail↔wild type and weaver↔wild type chimeric mice suggests a feedback mechanism between EGL and Purkinje cells to control proliferation of granule cells (Goldowitz, 1989; Hamre and Goldowitz, 1997). Recent studies on identification of genes, particularly transcription factors that mark the granule cell lineage from precursors to mature neurons have suggested that Purkinje cell- derived Sonic hedgehog morphogen plays a role in proliferation of granule cell precursors (Wallace, 1999; Wechsler-Reya and Scott, 1999).

Postnatal cerebellar development processes include Purkinje cell maturation, inward migration of external granule cells and refinement of precerebellar synaptic connections (Altman and Bayer, 1997e; Goldowitz and Hamre, 1998). Granule cells migrate from the EGL to form the internal granule cell layer, which is first evident at P7 (Miale and Sidman, 1961). During this period, differentiation of stellate and basket cells occurs and Purkinje cell bodies become aligned in a monolayer between the molecular and granule cell layers (Miale and Sidman, 1961). Purkinje cells undergo extensive dendritic arborization and achieve synaptic association with parallel fibers originating from granule cells and climbing fibers from the inferior olive (Altman, 1972). Due to extensive cell proliferation, the external granule cell layer also is thicker by P10.

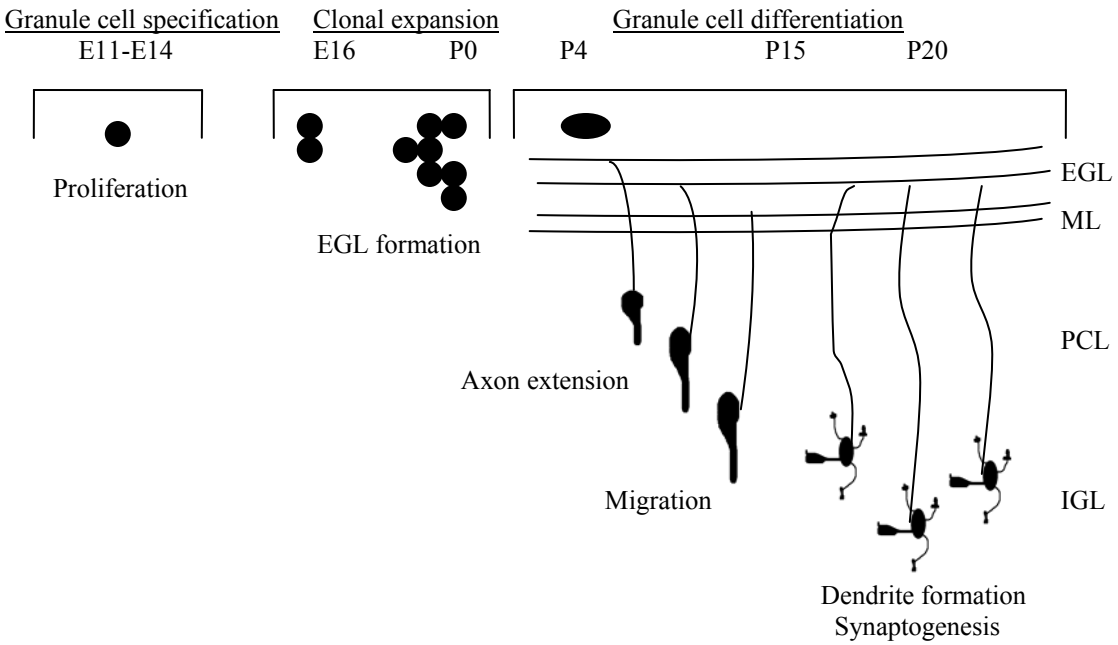

Figure I-4. Developmental stages of cerebellar granule cell shown schematically. Early precursors of granule cells arise from rhombic lip between E11-E14. The granule cell precursors move on the surface of the cerebellar anlage to form a single cell layer by E16 and then undergo clonal expansion between P0-P8. Between P4-P15 the precursors in the deeper aspect of EGL begin to differentiate and migrate to form the IGL under the PCL by P20. Abbreviations: EGL – external granule cell layer, ML - molecular layer, PCL - Purkinje cell layer, IGL – internal granule cell layer. (Modified from Hatten et al., 1997)

Granule cells begin to migrate inwards across the Purkinje cell body layer starting at P11, and by P15 the majority of migration has taken place. These migrating granule cells express a neural glycoprotein called astrotactin. Astrotactin acts a ligand and helps with inward migration of granule cells along the ascending Bergman glia (Hasel and Sutcliffe, 1990). Development of the cerebellum is complete in rodents by P21 (Fujita et al., 1966).

ROLE OF CALCIUM IONS AND CALCIUM HOMEOSTASIS

Calcium ions (Ca^{2+}) are a universal second messenger, controlling a diverse range of cellular processes and functions (Berridge, 1998; Berridge et al., 2000; Carafoli, 2004, Montell, 2005). In neurons these processes include neurotransmitter release, excitability, neurite outgrowth, synaptogenesis, activity dependent gene expression, differentiation, plasticity, cell death and survival (Pietrobon, 2002). There are a few notable facts that make Ca^{2+} a universal second messenger. The calcium ion concentration gradient between various cellular compartments is particularly important for calcium signaling. There is 10,000 fold difference in Ca^{2+} concentration across the plasma membrane (1.5mM outside the cell and 0.1 μm inside the cell), which drives Ca^{2+} into the cell (Berridge et al., 2000; Montell, 2005). Secondly, Ca^{2+} is small in size and rapidly diffuses, which is also a key for being a second messenger. Other factors that enable Ca^{2+} to serve as a versatile signaling molecule includes its ability to autoregulate its own concentration and physiological effect. Ca^{2+} as a second messenger can operate over a wide dynamic range and variety of time scales (Berridge et al., 2003; Montell, 2005). Spatially and temporally controlled changes in Ca^{2+}concentration are central to the ability of this messenger molecule to regulate processes ranging from synaptic transmission to apoptosis, muscle contraction, fertilization, cell division and sensory signaling (Blackstone and Sheng, 2002; Montell, 2005). Cellular Ca^{2+} homeostasis is regulated by numerous molecular cascades which balance Ca^{2+} influxes

through extracellular and intracellular membranes and cytoplasmic Ca^{2+} buffering. A diagrammatic presentation of Ca^{2+} homeostasis in neurons is illustrated on page 19.

Calcium influxes

Ca^{2+} entry in the cell is driven by the presence of a large electrochemical gradient across the plasma membrane using three channel families: (i) voltage gated channels (VGCC) (ii) Ligand gated channels (LGCC) and (iii) transient receptor potential ion channels (TRP) (Carafoli, 2004; Bezin et. al., 2006). VGCCs are operated when the cells are depolarized, during which sodium (Na^+) channels open allowing Na^+ influx and depolarization of the plasma membrane (Koester and Siegelbaum, 2000; Bear et al., 2001). Following depolarization VGCC open allowing Ca^{2+} to move down its concentration gradient from the extracellular space into the neuron.

Depolarization is followed by repolarization, where voltage-gated potassium (K^+) channels open and K^+ exits the cell repolarizing the membrane and closing the VGCC (Koester and Siegelbaum, 2000; Bear et al., 2001). In addition, during synaptic transmission, LGCCs, such as the N-methyl-D-aspartate (NMDA) receptor, open a cation channel permeable to Ca^{2+} in response to neurotransmitter binding (Kandel and Siegelbaum, 2000). Another class of calcium ion influx channels, the TRP channels, is activated primarily by signal transduction pathways. Calcium ion influx through these channels is regulated through dynamic movement of these channels to the plasma membrane (Clapham, 2003; Montell, 2004). This shuttling requires the activity of phospholipase C and Di-acyl glycerol (Minke, 2006). Although the exact function of

most TRP channels and their regulation has not been established, increasing data suggest that they are localized and regulated within spatially distinct Ca^{2+} signaling microdomains (Ambudkar, 2006; Minke, 2006).

In addition to extracellular calcium influx following depolarization, intracellular calcium ion ($[Ca^{2+}]_i$) increase can also take place by mobilization of calcium ions from intracellular stores (Fig. I-5). These stores accumulate Ca^{2+} using energy driven systems, and release it through coupled transporters or LGCC (Carafoli, 2004). Three main intracellular calcium ion stores in neurons are the mitochondria, the smooth endoplasmic reticulum (SER) and Golgi bodies. Mitochondria serve as low affinity, high-capacity system driven by mitochondrial membrane potential. The SER on the other hand serves as a high-affinity, low capacity calcium ion store (Somlyo et al., 1985). In neurons, the SER can take up calcium ions from the cytosol even at very low concentrations while mitochondria need at least 500nM of local extra mitochondrial calcium ions in order to take up calcium ions (Nicholls and Scott, 1980).

Golgi bodies take up calcium ions using a secretory pathway Ca^{2+}-ATPase pump and release it through a channel sensitive to inositol triphosphate (IP3) (Pinton et al., 1998; Sudbrak et al., 2000). SER takes up Ca^{2+} using a SER Ca^{2+}-ATPase (SERCA) pump and releases it through two ligand-gated calcium channels, which are responsible for calcium induced calcium release (CICR), IP3 receptors and ryanodine receptors (RyR) (Berridge et al., 2000; Carafoli 2004). Activation of these receptors is through second messengers. Apart from IP3, which acts as a second messenger for IP3 receptors, the discovery of two new Ca^{2+} mobilizing second messengers, cyclic ADP-ribose

(cADPR) and nicotinic acid adenine dinucleotide phosphate (NAADP), has really increased the understanding of calcium ion signaling (Montell, 2005; Bezin et al., 2006). Emerging evidence suggests that cADPR enhances the Ca^{2+} sensitivity of RyR to produce prolonged Ca^{2+} signals through CICR, while NAADP acts on a novel Ca^{2+} release mechanism to produce a local trigger Ca^{2+} signal, which can be amplified by CICR through recruitment of other Ca^{2+} release mechanisms (Galione and Churchill, 2002; Bezin et al., 2006). The coordinated action of NAADP, cADPR and IP3 contribute to repetitive increases and decreases in $[Ca^{2+}]_i$ concentration through CICR (Montell, 2005; Galione and Ruas, 2005).

Ca^{2+} uptake by mitochondria is through two known transport systems. First is the uniporter system, which transports unbound calcium ions down the calcium gradient between the cytosol and mitochondria (Gunter et al., 2000). Second is a fast calcium ion uptake system, which allows calcium ion uptake from submicromolar, pulsed calcium ion transients and decodes the frequency as well as the amplitude of the signals (Gunter et al., 2000). Efflux of Ca^{2+} from mitochondria is through ion exchangers that are coupled with sodium or hydrogen ions (Carafoli et al., 1974; Sparagna et al., 1995).

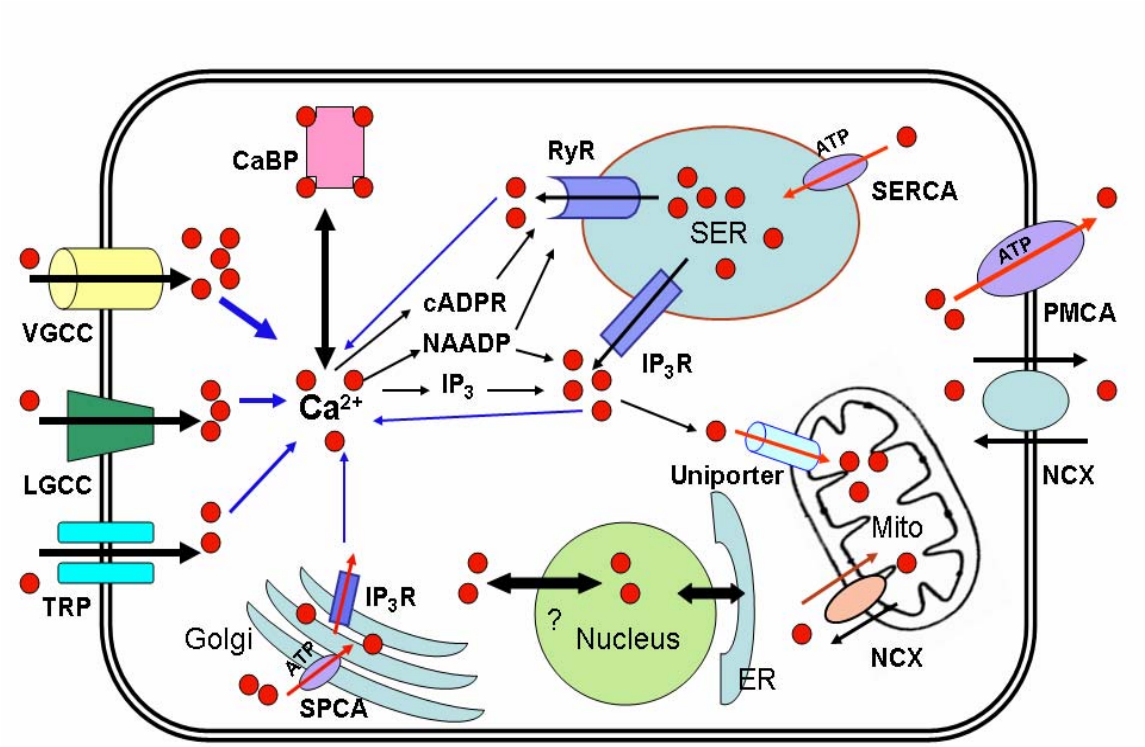

Figure I-5. Schematic drawing illustrating calcium ion homeostasis in neurons. Extracellular calcium ions enter neurons primarily through VGCC, LGCC and TRP channels. SER is responsible for calcium induced calcium release through IP3, cADPR and NAADP molecules. Increased cytosolic calcium ions are buffered primarily by calcium-binding proteins. Subsequent rise in cytosolic calcium ion concentration is further buffered by smooth endoplasmic reticulum and mitochondria. Efflux of cytosolic calcium ions into the extracellular space is regulated by calcium ion pumps and exchangers present on the plasma membrane. Abbreviations: VGCC= voltage-gated calcium ion channel, LGCC= ligand-gated calcium ion channel, TRP= transient receptor potential, CaBP= calcium-binding proteins, IP_3= inositol 1,4,5-triphosphate, cADPR= cyclic ADP-ribose, NAADP= nicotinic acid adenine dinucleotide phosphate, IP_3R= inositol 1,4,5-triphosphate receptor, RyR= ryanodine receptors, SER= smooth endoplasmic reticulum, SERCA= sarcoplasmic and endoplasmic reticulum calcium ATPase, PMCA= plasma membrane calcium ion ATPase, SPCA= secretary pathway calcium ion ATPase, NCX= Sodium calcium exchanger, ER= endoplasmic reticulum, Mito= Mitochondria (Carafoli, 2004; Montell, 2005)

Calcium buffering

Increased cytosolic Ca^{2+} following influx need to be buffered in order to maintain proper Ca^{2+} homeostasis. The rate at which Ca^{2+} is cleared from the cytoplasm affects the duration, amplitude and spread of Ca^{2+} signals (Thayer et al., 2002). Of the Ca^{2+} entering the cytosol, only a very small proportion ends as free calcium ions, because most of it is rapidly bound to buffering agents (Berridge et al., 2003). Calcium buffers can be categorized as rapid buffers that limit the peak $[Ca^{2+}]_i$ or slow buffers that clear calcium ions from the cytoplasm and restore resting $[Ca^{2+}]_i$ (Murchison et al., 2002). Slow buffers, which act to maintain physiological $[Ca^{2+}]_i$ in the cytosol, include calcium pumps and sodium/calcium exchangers present in the plasma membrane (Carafoli, 2002).

Neuronal $[Ca^{2+}]_i$ is regulated by a well developed calcium ion buffering system, which includes the SER, mitochondria, the nucleus and cytosolic calcium-binding proteins (CaBP) (Carafoli, 2002) (Figure I-5). In the CNS, CaBPs act as intracellular calcium ion acceptors and share a common Ca^{2+} binding motif, called the EF-hand (Bastianelli, 2003). In addition to buffering the influx of Ca^{2+}, these CaBPs are key components of several second messenger signaling pathways and control diverse cellular functions (Berridge et al., 2000). Functionally, CaBPs act either as calcium ion sensors (calmodulin) or buffers (calretinin, calbindin and parvalbumin) (Baimbridge et al., 1992). These proteins respond to sudden increases in $[Ca^{2+}]_i$ and buffer this excess calcium ion so that only 0.05-2.0% of calcium ions entering the cytosol remains unbound. The distribution pattern of CaBPs in the cerebellum varies depending upon the

specific cell type and so serves as excellent neuronal markers (Andressen et al., 1993). Table I-3 shows the Cerebellar distribution of calcium binding proteins.

Recently, a new calcium-binding protein, caldendrin has been shown to act as a calcium sensor and may play an important role in different aspects of synapto-dendritic Ca^{2+} signaling (Seidenbecher et al., 1998; Mikhaylova et al., 2006). Caldendrin has a bipartite structure with a highly basic N-terminus and a C-terminal part that resembles the EF-hand-structure of calmodulin (Seidenbecher et al., 1998; Laube et al., 2002). Mikhaylova et al. (2006) have introduced two new EF-hand calcium sensor proteins prominently expressed in neurons, which they termed calneurons. Calneurons have a different EF-hand organization compared to other calcium sensor proteins and bind Ca^{2+} with higher affinity than caldendrin.

Table I-3: Cerebellar distribution of calcium binding proteins.

	Purkinje Cells	**Granule cells**	**Golgi cells**	**Basket & Stellate cells**
Calmodulin	++	+	?	+
Calbindin	+++	–	++	–
Parvalbumin	++	–	+/–	+++
Calretinin	+/–	+++	+	+/–

"+++" = present in large amounts, "++" = present in moderate amounts, "+" = present in small amounts and "–"= protein is not present, "+/–" may be present in extremely small amounts and "?" indicates presence or absence is unknown (Bastianelli, 2003).

Cytosolic Ca^{2+} buffers modify propagation of the Ca^{2+} wave through the cytosol, but cellular organs like mitochondria, the SER and the nucleus not only buffer Ca^{2+} but

also contribute generation of subcellular domains with different Ca^{2+} concentrations (Alonso et al., 2006). Since SER is a high-affinity, low capacity Ca^{2+} store, it can sequester large amounts of calcium ions, which is vital because rapid intracellular calcium ion mobilization from intracellular depots is required for calcium ion signaling (Meldolesi and Pozzan, 1998; Meldolesi, 2001). Ca^{2+} enters the lumen of SER via SERCA pumps present on the SER membrane (Carafoli, 2004). Inside the SER lumen, calcium ions are buffered by calreticulin and calsequetrin, which belong to another group of EF-hand CaBPs present in the SER. These proteins are involved in calcium ion homeostasis within ER to regulate the pool of available free calcium ions to be liberated upon stimulation (Meldolesi, 2001).

Nuclear calcium ion uptake and release occurs in close association with the SER because the outer nuclear membrane is continuous with the SER membrane. The nuclear envelope contains SERCA pumps, IP3 receptors and RyRs (Carafoli, 2004). Calcium ions in the SER are mobilized into the nucleoplasm through IP3 receptors and RyRs and taken back by the SER through calcium ion-ATPases (Santella and Bolsover, 1999). Investigations with isolated nuclei have provided evidence in support of autonomous regulation of nuclear calcium ion signaling (Malviya and Klein, 2006). Two calcium ion transporting systems located on the outer nuclear membrane, an ATP-dependant nuclear Ca^{2+}-ATPase and an IP4-mediated inositol 1,3,4,5-tetrakisphosphate receptor, are responsible for filling the nuclear envelope calcium ion pool (Malviya and Klein, 2006). Recent studies have shown that the nucleus has its own calcium ion signaling

mechanism, which is independent from cytosolic calcium ion signaling (Leite et al., 2003; Gomes et al., 2006; Malviya and Klein, 2006).

Mitochondrial calcium ion uptake occurs when there is a much higher increase in $[Ca^{2+}]_i$ as seen in calcium ion waves generated from the SER. Moreover, mitochondrial calcium uptake takes place in the proximity of the SER. Therefore mitochondria serve as a second line for calcium buffering that is activated in conjunction with SER calcium signaling processes (Gunter et al., 2000; Meldolesi, 2001). As mentioned previously, mitochondria have two Ca^{2+} intake systems, one is the uniporter system and the other is a fast calcium ion uptake system. Efflux of Ca^{2+} from mitochondria is through two ion exchangers that are coupled with sodium or hydrogen ions (Carafoli et al., 1974; Sparagna et al., 1995). Mitochondria are called biosensors of Ca^{2+} microdomains, as they avidly take up Ca^{2+} from the high cytosolic Ca^{2+} microdomains generated during cell activation near Ca^{2+} channels of the plasma membrane and prevent propagation of the high Ca^{2+} signal to the bulk cytosol. This shaping of cytosolic Ca^{2+} signaling is essential for independent regulation of compartmentalized cell functions (Alonso et al., 2006).

The inner mitochondrial membrane has permeablitiy transition pores (PTP) which are known to operate distinctly at two physiological states by changing its confirmation. One confirmation is low conductance where PTP is involved in normal regulation of intracellular calcium ion homeostasis influenced through changes in the mitochondrial matrix pH (Davidson and Halestrap, 1990; Ichas et al., 1994). Under the high-conductance state opening of PTP results in irreversible changes in the membrane potential, eventually rupturing the outer mitochondrial membrane and causing release of

proapoptotic factors into the cytosol (Scarlett and Murphy, 1997; Ichas and Mazat, 1998).

APOPTOSIS (OR) PROGRAMMED CELL DEATH

Cell death, a fundamental and an integral part of biological processes, has been classified into two major categories; necrosis and programmed cell death (PCD) (Gerschenson and Rotello, 1992). PCD has emerged as an important regulator of development and homeostasis in multicellular organisms and occurs in numerous physiological and pathological processes. Apoptosis also called PCD, though the meanings of these terms are not identical, is a common phenomenon induced either by specific insults mediated through so-called “death receptors” (external pathway) or by non-specific insults leading to reduction of mitochondrial potential (internal pathway), whereas physiological cell death during normal development is typically referred to as PCD (Kajta, 2004).

Apoptosis is different from necrosis, although both lead to cell death. In the case of necrosis, which is an energy independent process, the main target of injury is the cell membrane whose breakdown is followed by enzyme release into the intracellular space/matrix and inflammation. In contrast to necrosis, apoptosis is an energy dependent, highly regulated process that is mainly related to cell nucleus and specific DNA fragmentation which results in apoptotic body formation and individual cell death without an inflammatory response to the damage (Sastry and Rao, 2000; Yuan and

Yankner, 2000; Kajta, 2004). The surface of apoptotic cells is altered such that they are swiftly recognized as dying cells and rapidly phagocytosed by macrophages. This not only avoids the damaging consequences of cell necrosis but also allows the organic components of the dead cells to be recycled by the cell that ingests them (Savill et al., 1993). So, apoptosis is a mechanism by which only dysfunctional or damaged cells are removed from a tissue without adversely affecting healthy cells in the tissue (Mattson, 2006). Although necrosis and apoptosis are mediated through different mechanisms, they may both be initiated by the same stimuli, e.g. Ca^{2+} influx into the cytoplasm (Kajta, 2004).

Schweichel and Merker (1973) divided cell death into three types, based on differences in ultrastructural morphological features. Apart from apoptosis and necrosis, the third type they mentioned was autophagy. Autophagy is a physiological and evolutionarily conserved phenomenon maintaining homeostatic functions like protein degradation and organelle turnover and is upregulated under conditions leading to cellular stress, such as nutrient or growth factor deprivation (Gozuacika and Kimchi, 2007). Accumulating data provide evidence that autophagic machinery can be also recruited to kill cells under certain conditions leading to a caspase-independent form of programmed cell death, named autophagic cell death (Gozuacika and Kimchi, 2007). Morphological and biochemical features of above mentioned three types of cell death are summarized in Table I-4.

Table I-4: Comparative features of different types of cell death (Bursch 2001; Yuan et al., 2003; Gozuacika and Kimchi, 2007).

	Necrosis	**Apoptosis**	**Autophagy**
ATP	early depletion	no depletion	no depletion +/- increases
Mitochondrial morphology	Swelling	Normal	Some swelling; Number decreased but some normal
ER/Golgi	Swelling	Normal	Some swelling Some normal
Cytoplasm	Empty spaces (nonlysosomal)	Condensation	Autophagic vacuoles; Loss of density
Plasma membrane	Fragmentation	Blebbing into apoptotic bodies	Minor blebbing late in process
Nucleus	Fragmentation +/– swelling	Pyknosis	Some pyknosis late in process
Chromatin/DNA	Lysis/diffuse degradation	Condensation/ Fragmentation	Late condensation/ No Fragmentation
Final Clean Up	Loss of membrane integrity & lysis; Removed by phagocytosis with inflammation	Membrane bound apoptotic bodies removed by phagocytosis without inflammation	Remaining cell removed by phagocytosis without inflammation

Autophagic cell death shares features with both necrosis and apoptosis. For example, there is a decrease in mitochondrial numbers and some mitochondrial swelling is observed in autophagy, however, enough normal mitochondria are retained to maintain ATP synthesis and complete a controlled break down of the cell (Bursch,

2001). It is speculated that the intracellular ATP levels actually increase during autophagy, probably due to the shutdown of energy-consuming processes such as protein translation (Gozuacika and Kimchi, 2007). Although, apoptosis and autophagy proceed through independent mechanisms, emerging lines of evidence point out the existence of crosstalk between the two pathways.

It is speculated that the cellular response to the same stimuli may manifest itself predominantly by autophagic or apoptotic characteristics depending on cellular context or experimental setting (Gozuacika and Kimchi, 2007). Furthermore, in some cases, apoptotic and autophagic morphologies may coexist in the same cells, and the cell death may show mixed characteristics even at the molecular level. On the other hand, apoptosis and autophagy may depend on each other in some systems, so that inhibition of one PCD type may lead to enhancement or inhibition of the other type (Gozuacika and Kimchi, 2007).

Apoptosis is crucial for the normal development of the nervous system, as excess of neurons produced, must die to ensure the precise formation of appropriately matching pre- and postsynaptic connections (Benn and Woolf, 2004). However, apoptosis on a large scale in the nervous system can result in various neurodegenerative disorders like Alzheimer's disease or Parkinson's disease (Savitz and Rosenbaum, 1998). Apoptosis can be broadly divided into two types i.e. extrinsic apoptotic signaling pathway and intrinsic apoptotic pathways. Extrinsic pathways are considered to be triggered by stimulus outside the cell, received by receptors called as death receptors. On the other hand intrinsic pathways has intracellular origin basically mitochondria. These two

pathways at some point do merge to each other or one pathway can trigger the other pathway (Benn and Woolf, 2004).

Neurons are very vulnerable to many kinds of external and internal insults. The external insults that cause neuronal apoptosis include neurotoxicants, DNA damaging agents and irradiation. Internal insults include neurotrophic factor withdrawal, changes in calcium homeostasis, glutamate excitotoxicity, oxidative stresses and others (Sastry and Rao, 2000). Initially, there is activation of pro-apoptotic genes that subsequently activate a family of proteases called "caspases". Caspases execute the final phase of apoptosis by cleaving key protein components of the cell so that cellular processes are disabled and the cell is phagocytosed (Thornberry and Lazebnik, 1998).

Apoptotic death in both developing and adult neurons occurs through a highly ordered sequence of signaling cascades (Benn and Woolf, 2004). Extrinsic signaling pathway is initiated by the binding of proapoptotic ligands to death receptors like the tumour necrosis factor (TNF) receptor, TNF-related apoptosis-inducing ligand receptor (TRAILR1) and FAS receptor (Benn and Woolf, 2004). Activation of these receptors will lead to cell death either by activation of caspase 8 or activation of JNK pathway, which may directly or indirectly activate effector caspases such as caspase 3 (Mattson, 2006). The extrinsic caspase-dependent apoptotic pathway converges with the intrinsic apoptotic pathway at the mitochondrion, through activated caspase 8 which lead to truncation of the pro-apoptotic Bcl-2 family protein BID (Polster and Fiskum, 2004). The truncated Bid (tBID) translocates to mitochondria leading to tBID-mediated opening

of mitochondrial permeability transition pores (PTP) and consequent release of apoptogenic proteins (Benn and Woolf, 2004; Polster and Fiskum, 2004).

The intrinsic apoptotic pathway or mitochondrial mediated apoptosis in adult neurons is regulated by both pro- and anti-apoptotic proteins, collectively called the Bcl-2 family (Adams and Cory, 1998). The Bcl-2 families of proteins are a group of proteins that share a conserved Bcl-2 homology (BH) domain (Cory and Adams, 2002). The Bcl-2 subfamily of proteins having BH domains 1 – 4, which includes Bcl-2, Bcl-xL, and Bcl-w, are anti-apoptotic (Cory and Adams, 2002). The Bax subfamily proteins having BH domains 1 – 3, are pro-apoptotic, and include proteins such as Bax, Bak, and Bok (Cory and Adams, 2002). The second group of pro-apoptotic protein contains only the BH 3 domain and are refer to as BH3 proteins (Cory and Adams, 2002). BH3 proteins include members such as Bid, Bad, Bik and Bim (Ward et al., 2004). Anti-apoptotic Bcl family members are localized primarily in the outer mitochondrial membrane (OMM) and retain cytochrome C and other apoptogenic factors within the mitochondrial intermembrane space (Nakai et al., 1993). Proapoptotic family members, like Bax, reside primarily in the cytoplasm of healthy cells and translocate to the OMM during apoptosis. Once at the OMM, these proteins promote release of apoptogenic factors from the mitochondria into the cytoplasm (Wolter et al., 1997; Putcha et al., 1999).

Once released from mitochondria, apoptogenic factors such as cytochrome C and second mitochondrial activator of caspase (SMAC), activate caspase proteases, which carry out degradation of the cell (Liu et al., 1996; Du et al., 2000). In the cytosol, cytochrome C in presence of ATP and Apoptosis inducing factor-1 (Apaf-1) binds to and

activates caspase 9, which in turn cleaves and activates caspase 3 (Kirkland and Franklin, 2003). Caspase 3 further activates a down stream caspase cascade to induce apoptosis in a dying cell (Li et al., 1997; Liu et al., 1996). SMAC alternatively blocks the action of inhibitor of apoptosis proteins (IAP) to free caspases for activation (Du et al., 2000). Other proteins such as apoptosis inducing factor (AIF) act independent of caspases to breakdown the cell (Susin et al., 1999; Joza et al., 2001).

Caspases are cysteine aspartases, which become activated in most forms of apoptosis. All caspases are synthesized as inactive zymogens that require activation. Earlier it was thought that cleavage is a required step for activation of all caspases (Shi, 2002). However, recent studies suggest that the long prodomain containing caspases do not require cleavage for activation while caspases with short prodomains do (Boatright et al. 2003; Shi, 2004).

In cells, caspases are found in the nucleus, cytoplasm and the mitochondrial intermembrane space. There are 13 mammalian caspases which can be classified based on structure, cleavage specificity, mode of activation and presumed function (Prunell et al., 2005). Structural classification divides the caspases into two groups, the long prodomain containing initiators and the short prodomain containing effectors (Prunell et al., 2005). Functionally, the initiator group of caspases is further subdivided into death initiators (caspases-2, -8, -9 and -10) and inflammation mediators (caspases-1, -4, -5, -11) (Martinon and Tschopp, 2004). The effector caspases, which includes caspases 3, 6, and 7, are mainly responsible for further activation of their down stream caspase effectors and targets cytoplasmic and nuclear proteins to carrying out degradation of the

cell. They also lead to activation of DNases responsible for breaking DNA into fragments (Earnshaw et al., 1999).

ROLE OF MITOCHONDRIA IN CELL LIFE AND DEATH

Mitochondria have long been considered to play a critical role in the life of the cell by carrying out energy-yielding oxidative reactions to create the vast majority of ATP necessary to support all cellular functions. However, a variety of apoptotic events focus on mitochondria, suggesting that mitochondria are pivotal in controlling cell life and also death. As discussed above mitochondria plays an essential role in maintaining Ca^{2+} homeostasis. There are numerous other reactions taking place in mitochondria that are essential for human life including; break down of sugars and long chain fatty acids, recycling of ADP back into ATP, synthesis of steroids and lipids, DNA replication, transcription and translation of proteins (McBride et al., 2006).

From a structural perspective, the mitochondrion contains two membranes that separate four distinct compartments, the outer membrane, intermembrane space, inner membrane and the matrix. The inner membrane is highly folded into cristae, which house the megadalton complexes of the electron transport chain and ATP synthase that control the basic rates of cellular metabolism (McBride et al., 2006). Mitochondrial cristae are not staggered into neat folds but are a complex array of tubules that divide and fuse continuously (Griparic and Van Der Bliek, 2001; Perkins et al., 2001; Duguez

et al., 2002). The functional significance of the outer membrane is less well understood but it is known to be selectively permeable to ions and small molecules (Duchen, 2004).

Mitochondria form a functional reticulum and their morphology, distribution, and activity is regulated by dynamic fission, fusion and motility events (Chan, 2006). Recent studies indicate that mitofusin 1, mitofusin 2, present in outer mitochondrial membrane, and OPA1, present in inner mitochondrial membrane, are essential for mitochondrial fusion, whereas Fis1, present in outer mitochondrial membrane and Drp1, present primarily in cytosol are essential for mitochondrial fission (Chen and Chan, 2005; Chan, 2006). Perturbation of mitochondrial fusion results in defects in mitochondrial membrane potential and respiration, poor cell growth and increased susceptibility to cell death, whereas mitochondrial fission accompanies several types of apoptotic cell death and appears important for progression of the apoptotic pathway (Chen and Chan, 2005).

Mitochondrial membrane potential

The enzymatic components of mitochondria include the citric acid cycle or tricarboxylic acid (TCA) cycle and respiratory (electron transport) chain. During aerobic respiration, mitochondrial enzymes accept electrons from electron carriers (NADH and $FADH_2$) reduced in glycolysis and the TCA cycle. These electrons are ultimately transferred to O_2 to produce water. The series of redox reactions involves four enzyme complexes embedded in the inner mitochondrial membrane (Figure I-6). The electron carriers NADH and succinate donate electrons to NADH dehydrogenase (Complex I) and succinate dehydrogenase (Complex II) respectively (Das, 2006).

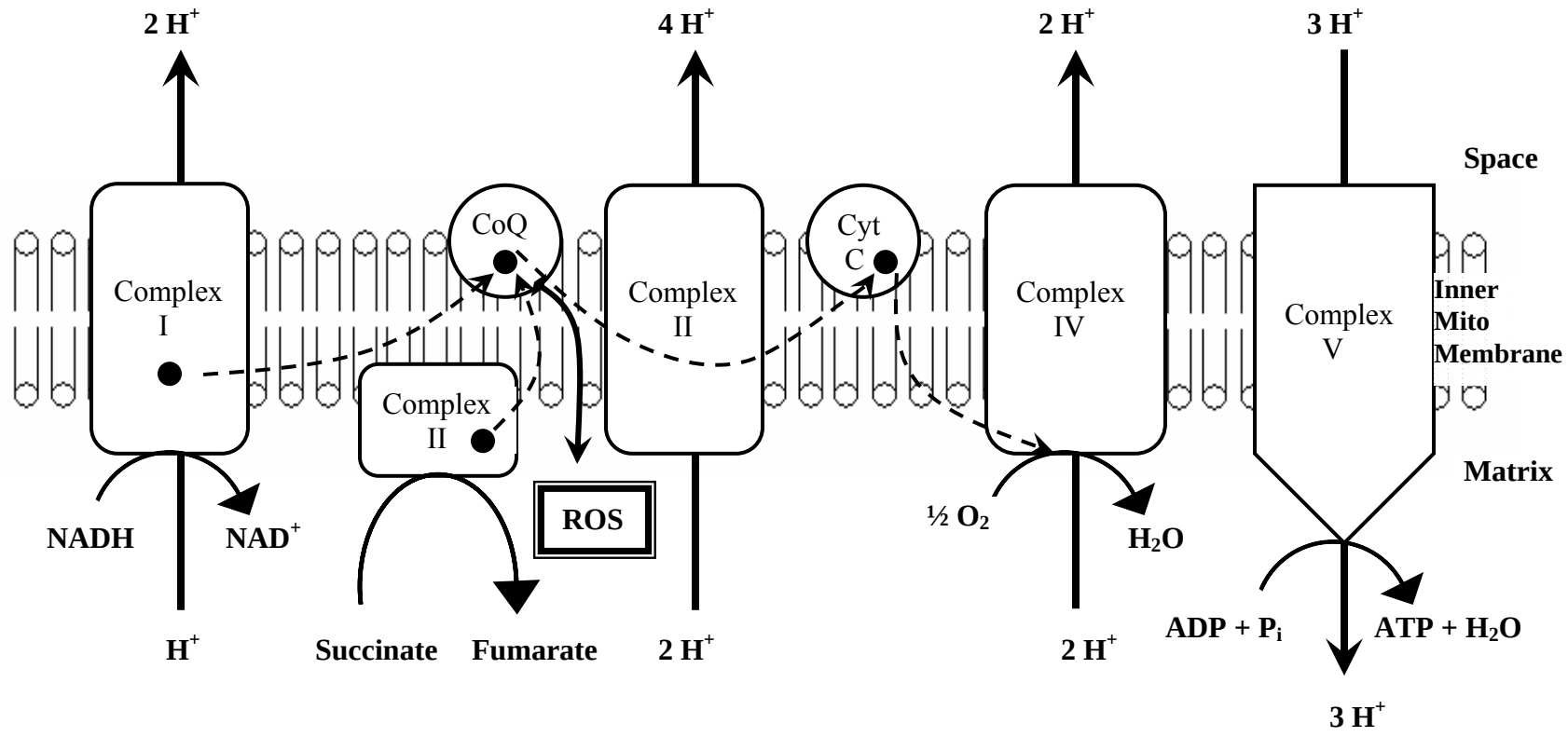

Figure I-6. An overview of electron transport chain in mitochondria. Complexes I and II transfer electrons from NADH and succinate, respectively, to CoQ to form ubiquinol. Complex III catalyzes electron transfer to Complex IV which reduces molecular oxygen to form water. The path of electrons (Solid black circles) is shown in dotted arrows. Complexes I, III and IV use the energy from electron transfer to pump protons into the intermembrane space, creating an electrochemical gradient or mitochondrial membrane potential. Complex V uses the energy stored in this electrochemical gradient to condense ADP and Pi into ATP. Abbreviation; Cyc C = cytochrome C, CoQ = Coenzyme (Das, 2006).

The electrons are then transferred to coenzyme Q to form ubiquinol, which donates them to the cytochrome bc1 complex (Complex III). Cytochrome c is the next electron acceptor and donates electrons to cytochrome c oxidase (Complex IV). In the final step, the electrons are accepted by molecular oxygen to produce water (Das, 2006).

During the process of electron transport, the substrates viz., NADH and $FADH_2$, get reduced and generate protons at complexes I, III and IV, which are pumped into the intermembrane space and establishes an electrochemical proton gradient or proton motive force or mitochondrial membrane potential (Duchen, 2004). The fifth enzyme complex, ATP synthase (Complex V) uses the energy stored in this electrochemical gradient to condense ADP and Pi into ATP (Das, 2006). This proton motive force has two components to it: (a) a pH gradient, because protons are acidic and (b) ionic gradient, because protons are charged. The ionic gradient represents the mitochondrial membrane potential and is usually 150 -180 mV negative relatively to the cytosol (Duchen, 2004). This membrane potential drives the major bioenergetic functions of mitochondria, which include ATP synthesis and accumulation of calcium ions.

Oxidative phosphorylation is most efficient when excess ADP is available, since all available oxygen is consumed in order to maintain membrane potential to drive ATP synthesis. When ADP is in limiting quantity, some of the molecular oxygen is reduced to form toxic reactive oxygen species (ROS) (Figure I-6) (Das, 2006). Oxidative stress occurs due to excess ROS in mitochondria. Within the mitochondria ROS mainly target the protein components of the membranes and polyunsaturated fatty acids. Hydroxyl radicals are known to initiate lipid peroxidation and generate peroxyl-radical and

alkoxyl-radical intermediates. Mitochondrial DNA is probably the preferred target of ROS owing to its close proximity to the respiratory chain and absence of mitochondrial DNA-protecting mechanisms (Shoji et al., 1995; Zamzami and Kroemer; 2001).

Severe damage to mitochondria can lead to cell death because mitochondria are the main sources of ATP. Once ATP levels drop, energy dependent processes in the cell like maintaining calcium ion homeostasis, ion gradients, secretion of transmitters etc., will be disrupted. Disruption of ionic gradients will result in inability of the cell to maintain osmolarity. Eventually the cells will swell and die due to necrosis. Mitochondria also determine the mode of cell death (apoptosis or necrosis) because ATP is required to execute apoptosis. The switch between necrotic pathways and apoptotic pathways is at the level of available ATP (Magistretti et al., 1999).

Apoptosis is achieved through the mitochondrial permeability transition pore (PTP) or megachannel, which is a large maximal conductance pore formed at the contact site between the inner and outer mitochondrial membrane (Crompton and Costi, 1990). Its core components are the adenine nucleotide translocator (ANT), found in the inner mitochondrial membrane and the volt age-dependent anion channel (VDAC) located in the outer mitochondrial membrane (Zamzami and Kroemer; 2001). The opening of this megachannel is believed to increase the inner membrane permeability to solutes of molecular mass up to 1.5 kDa (Bernardi et al., 1999; Zamzami and Kroemer; 2001). The PTP functions as a sensor for voltage, divalent cations, matrix pH, metabolites, ANT ligands, anti and pro-apoptotic members of Bcl-2 family (Zamzami and Kroemer; 2001).

Direct interactions have been shown for the ANT and cyclophilin D (located in the mitochondrial matrix) as well as between the ANT and VDAC (Crompton, 1999; Woodfield et al., 1998). As a consequence of such interactions, changes in the conformation of the ANT may indirectly impinge on the function of the VDAC, or vice versa. So the PTP simultaneously controls permeability of the outer and inner mitochondrial membrane (Zamzami and Kroemer; 2001; Vyssokikh and Brdiczka; 2003). Two conformational states of PTP have been reported. One is low conductance where PTP is involved in normal regulation of intracellular calcium ion homeostasis influenced through changes in the mitochondrial matrix pH (Davidson and Halestrap, 1990; Ichas et al., 1994). Under the high-conductance state opening of PTP results in irreversible changes in the membrane potential, eventually rupturing the outer mitochondrial membrane and causing release of proapoptotic factors into the cytosol (Scarlett and Murphy, 1997; Ichas and Mazat, 1998).

The VDAC structure that is specific for contact sites generates a signal at the surface for several proteins in the cytosol to bind with high capacity, such as hexokinase, glycerol kinase and Bax (Vyssokikh and Brdiczka, 2003). If the VDAC binding site is not occupied by hexokinase, the VDAC–ANT complex changes conformation such that Bax gets access to cytochrome C and causes its release and secondly the ANT changes conformation into an unspecific channel (uniporter) causing permeability transition (Vyssokikh and Brdiczka, 2003).

VOLTAGE GATED CALCIUM CHANNELS

Voltage gated calcium channels (VGCC) are membrane proteins that mediate Ca^{2+} entry into a excitable cell in response to membrane depolarization, transducing an electrical signal into a chemical one (Randall and Benham, 1999; Catterall, 2000; Bezanilla, 2005; Bidaud et al., 2006). Based on biophysical and pharmacological features, VGCCs are subdivided into high-voltage activated (Ca_V1, $Ca_V2.1$, $Ca_V2.2$ and $Ca_V2.3$ previously called as L, P/Q, N and R-type respectively) and low-voltage activated (Ca_V3 or T-type) (Catterall, 2000; Ertel et al., 2000; Bidaud et al., 2006). VGCCs are composed of a pore forming α_1 subunit, which is associated – in the case of Ca_V1, $Ca_V2.1$, $Ca_V2.2$ and $Ca_V2.3$ channels – with regulatory $\alpha_2\delta$, β and γ subunits (Biduad et al., 2006). Ten genes (named CACNA1A-I and CACNA1S) code for the α_1 subunits (Lory et al., 1997; Biduad et al., 2006). Table I-5 illustrates the physiological function and pharmacology of voltage gated calcium channels.

The α_1 subunit of 190 to 250 kDa is the largest subunit, and it incorporates the conduction pore, the voltage sensor and gating apparatus, and most of the known sites of channel regulation by second messengers, drugs, and toxins (Catterall et al., 2005). It is organized in four homologous domains (I-IV), with six transmembrane segments (S1-S6) in each. Figure I-7 shows a schematic presentation of α_1 subunit. The S4 segment serves as the voltage sensor. When the membrane is depolarized, S4 senses changes in the membrane potential and rotates due to the charge change. S4 rotation further elicits structural changes in surrounding transmembrane repeats to open the pore. VGCCs are

inactivated as membrane depolarization diminishes (Horn, 2000). The pore loop between transmembrane segments S5 and S6 in each domain determines ion conductance and selectivity (Catterall et al., 2005).

The auxiliary subunits interact with α1 subunit to modulate VGCC kinetics. However, the properties of the channel complex, the pharmacological and electrophysiological diversity of calcium channels arises primarily from the existence of multiple α1 subunits (Hofmann et al., 1994). The β subunit binds a conserved domain between transmembrane domains I and II α_1 subunit and profoundly affects multiple channel properties such as voltage-dependent activation, inactivation rates, G-protein modulation, drug sensitivity and cell surface expression (Van Petegem et al., 2004). Recently two reports (Hibino et al., 2003; Berggren et al., 2004) have suggested that β subunit may not be an "auxiliary" subunit and may regulate Ca^{2+} homeostasis or gene regulation without α_1 subunit (Rousset et al., 2005).

The α2 is an extracellular subunit that is linked to the δ subunit by disulfide bonds. The α2δ subunits together have an effect on channel activation/inactivation speed upon β subunit binding to α1 subunit. The modulatory effect of γ subunit on the VGCCs is to downregulate calcium channel activity by causing a hyperpolarizing shift in the inactivation curve (Black, 2003). Recent studies revealed the presence of isoforms of each auxiliary subunit. Currently, three α2δ (1 - 3), four β (1 - 4) and five γ (1 - 5) subunit isoforms have been identified (Walker and De Waard, 1998).

Table I-5: Physiological function and pharmacology of VGCCs (Catterall, 2000; Biduad et al., 2006).

Channel	Current	Gene name	Localization	Specific Antagonists	Cellular Functions
$Ca_V1.1$	L	CACANA1S	Skeletal muscle; transverse tubules	Dihydropyridines; phenylalkylamines; benzothiazepines	Excitation-contraction coupling
$Ca_V1.2$	L	CACANA1C	Cardiac myocytes; smooth muscle myocytes; endocrine cells; neuronal cell bodies; proximal dendrites	Dihydropyridines; phenylalkylamines; benzothiazepines	Excitation-contraction coupling hormone release; regulation of transcription; synaptic integration
$Ca_V1.3$	L	CACANA1D	Endocrine cells; neuronal cell bodies and dendrites; cardiac atrial myocytes & pacemaker cells; cochlear hair cells	Dihydropyridines; phenylalkylamines; benzothiazepines	Hormone release; transcription; synaptic regulation; cardiac pacemaking; hearing; Neurotransmitter release
$Ca_V1.4$	L	CACANA1F	Retinal rod and bipolar cells; spinal cord; adrenal gland; mast cells	Dihydropyridines; phenylalkylamines; benzothiazepines	Neurotransmitter release from photoreceptors
$Ca_V2.1$	P/Q	CACANA1A	Nerve terminals and dendrites; neuroendocrine cells	ω-Agatoxin IVA	Neurotransmitter release; dendritic Ca^{2+} transients; hormone release
$Ca_V2.2$	N	CACANA1B	Nerve terminals and dendrites; neuroendocrine cells	ω-Conotoxin-GVIA	Neurotransmitter release; dendritic Ca^{2+} transients; hormone release
$Ca_V2.3$	R	CACANA1E	Neuronal cell bodies and dendrites	SNX-482	Repetitive firing; dendritic calcium transients
$Ca_V3.1$	T	CACANA1G	Neuronal cell bodies and dendrites; cardiac and smooth muscle myocytes	None	Pacemaking; repetitive firing
$Ca_V3.2$	T	CACANA1H	Neuronal cell bodies and dendrites; cardiac and smooth muscle myocytes	None	Pacemaking; repetitive firing
$Ca_V3.3$	T	CACANA1I	Neuronal cell bodies and dendrites; cardiac and smooth muscle myocytes	None	Pacemaking; repetitive firing

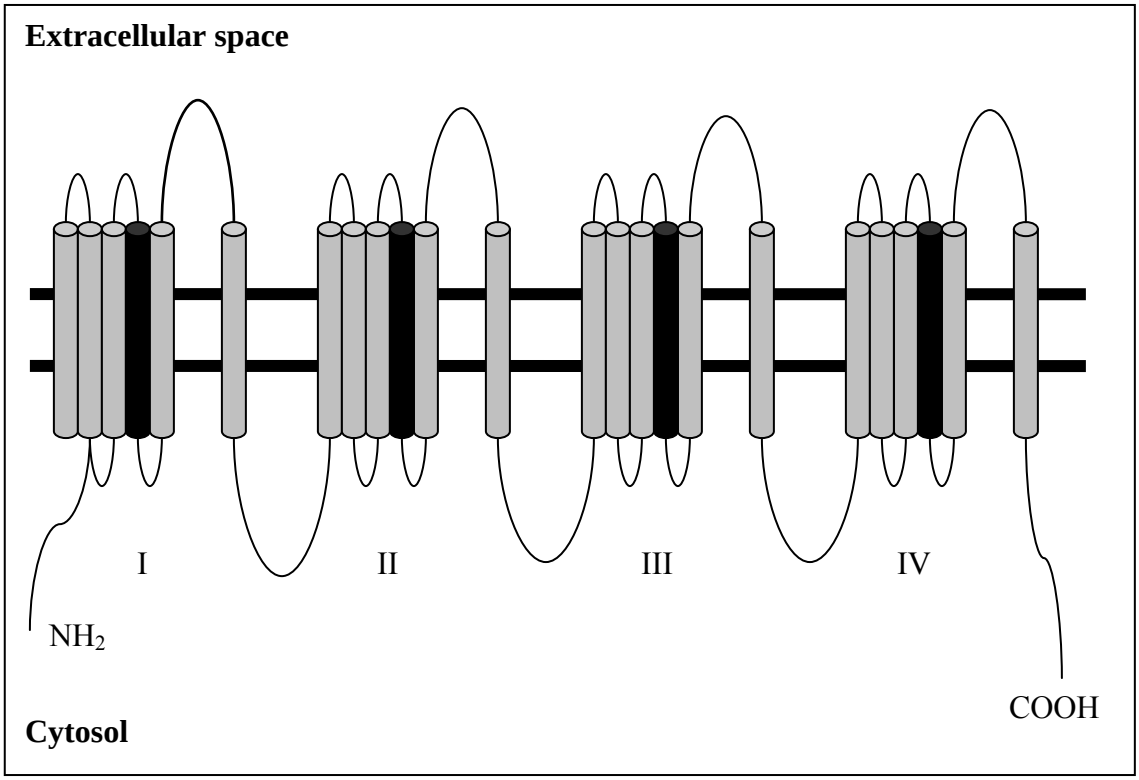

Figure I-7. Structure of the α1 subunit of voltage-gated calcium channels. The α_1 subunit is composed of four internal homologous domains (I - IV) labeled in Roman numerals and each domain contains six transmembrane repeats (S1 – S6) where S4 being a voltage sensor (Black). The α_1 subunit contains the Ca^{2+} pore, which is formed by the loops that fold within the membrane between transmembrane domains 5 and 6. NH2 represents the N-terminus of the α_1 protein and COOH represent the C-terminus. (Catterall, 2000; Pietrobon, 2002; Carafoli, 2004)

In addition to the auxiliary subunits, the pore forming subunit is modulated by phosphorylation (Li et al., 2005), Ca^{2+} and calmodulin binding and synaptic vesicle proteins (Lee et al., 1999). $Ca_V2.1$, $Ca_V2.2$ and $Ca_V2.3$ channels can also be regulated by G proteins (Herlitze et al., 1996; Zhou, et al., 2003; Tedford and Zamponi, 2006).

Channelopathies associated with Ca_V 2.1 (P/Q type) VGCCs

The P-type voltage calcium channels were first identified in cerebellar Purkinje cells and are highly expressed in the dentate gyrus and CA fields of the hippocampus, the cerebellar cortex, pontine nucleus, olfactory bulb and cerebral cortex layers II and VI (Stea, et al., 1994). They are preferentially located at presynaptic terminals where they play a central role in neurotransmitter release, especially excitatory neurotransmitters, as well as at somatodendritic membranes, where they contribute to neuronal excitability (Pietrobon and Striessnig, 2003). These P-type calcium channels mediate a relatively strong current that is blocked by ω-Agatoxin (Llinas et al., 1989). Similar currents, but less sensitive to ω-Agatoxin, were later found in cerebellar granule cells and were named Q-type channels (Randall and Tsien, 1995). $Ca_V2.1$ calcium channels share $\alpha_1 2.1$ as their pore-forming subunits. The CACNA1A gene encodes alternate splice isoforms of the $Ca_V2.1$ subunit that generate the P- and Q-type channels (Bourinet et al., 1999). Molecular and functional studies have showed that more than 90% of the calcium current in Purkinje cell somata is mediated by P-type calcium channels (Mintz et al., 1992). In cerebellar granule cell somata, 35% and 11% of calcium current is mediated by Q- and P-type calcium channels, respectively (Randall and Tsien, 1995).

Because of the critical role which Ca^{2+} channels play in signaling processes within the nervous system disruption of their function will lead to profound disturbances in neuronal function. Recent progress in molecular techniques has identified many human diseases related to ion channel mutations. These diseases are collectively referred to as “channelopathies”. Spontaneous mutations in the CACNA1A gene, which encodes

human $Ca_V2.1$ α1 subunits, cause several autosomal dominant neurological diseases including familial hemiplegic migraine (FHM-1), episodic ataxia type 2 (EA-2), spinocerebellar ataxia type 6 (SCA6) and certain cases of absence epilepsy (Ophoff et al., 1996; Zhuchenko et al., 1997; Imbrici et al., 2004; Pietrobon, 2005). The mutations causing episodic ataxia and absence epilepsy lead to loss-of-function of recombinant human $Ca_V2.1$ channels, whereas those causing FHM-1 lead to gain-of-function of human $Ca_V2.1$ channels (Pietrobon, 2005). FHM-1 is a rare subtype of inherited migraine that is associated with 12 different mutations in the $\alpha_1 2.1$ gene (Ophoff et al., 1996; Pietrobon, 2002). FHM-1 patients suffer from migraine accompanied by characteristic transient hemiparesis and some patients exhibit permanent cerebellar ataxia as well (Pietrobon, 2002; Pietrobon, 2005). The onset is often in childhood or adolescence (Carrera et al., 2001).

EA-2 has been linked to 15 different mutations in the α1A gene. Most of these mutations disrupt the open reading frame resulting in truncation, intron inclusion or exon skipping of the $\alpha_1 2.1$ subunit (Ophoff et al., 1996; Klockgether and Evert, 1998). These changes cause episodes of ataxia that may be progressive and cerebellar atrophy localized to the anterior vermis (Klockgether and Evert, 1998; Pietrobon, 2002). The latter effects are similar to those of the rolling Nagoaya (tg^{rol}), leaner (tg^{la}) or tottering (*tg*) mutations; however, for unclear reasons, the mutations are dominant in humans and recessive in mice (Pietrobon, 2005). SCA6 is caused by inheritance of expansion of polymorphic CAG repeats in the CACNA1A gene (Zhuchenko et al., 1997). It results in a slowly progressive cerebellar ataxia with marked cerebellar atrophy (Pietrobon, 2002).

SCA-6 cerebellar atrophy is concentrated in the anterior cerebellar vermis and includes a severe loss of cerebellar Purkinje cells and granule cells (Pietrobon, 2002).

There are several mutations of the CACNA1A gene found in mice in which the phenotype or clinical signs closely resemble those in humans and have therefore been used as animal models to investigate the cellular and molecular consequences of $\alpha_1$2.1 mutations in FHM-1, EA-2 and SCA-6 (Fletcher et al., 1996). Other then $Ca_V2_{\alpha1}^{-/-}$ knockout, there are four spontaneous autosomal recessive mouse mutants (tottering: *tg/tg*, leaner: tg^{la}/tg^{la}, rolling Nagoya*:* tg^{rol}/tg^{rol} and rocker: tg^{rkr}/tg^{rkr}) that harbor loss-of-function mutations in the $Ca_V2_{\alpha1}$ gene leading to a reduced P/Q current density in neurons (Pietrobon, 2005). Table I-6 summaries the phenotypes of Ca_V2.1 mouse models.

The *tg/tg* mutation is due to an amino acid substitution (leucine for proline) in the P-loop of domain II of the $\alpha_1$2.1 (Fletcher et al., 1996). Tottering mice show reduced cerebellar weight and volume at a young age however, these mice do not show any noticeable neuronal loss in the cerebellum (Isaacs and Abbott, 1995). The tottering mouse has been most extensively studied as a model of absence seizures (Barclay and Rees, 1999). Phenotypically, these mice also show mild to moderate cerebellar ataxia and a stereotyped movement disorder called as paroxysmal dyskinesia, which as been referred differently by different others like intermittent myoclonic movement disorders (Lau et al., 1998; Abbott et al., 2000), dystonia (Campbell and Hess, 1999), and motor seizures (Fletcher et al., 1996).

Paroxysmal dyskinesia is a sudden, episodic, involuntary movement disorder that may include any combination of dystonia, chorea, athetosis, or ballism and it is not considered as a part of any generalized seizures that cause loss of consciousness (Guerrini, 2001; Blakeley and Jankovic, 2002). A typical paroxysmal dyskinesia event exhibited by tottering mice is initiated from the hind limbs as "paddling motions" and progressively spreads into the fore limbs. As the episode progresses, the "paddling motions" alternate between hind and fore limbs, then may be followed by arching of the neck and back (Green and Sidman, 1962). Paroxysmal dyskinesia is often induced when tottering mice are exposed to caffeine, alcohol and stress, such as novel environment or restraint (Fureman et al., 2002).

The etiology of paroxysmal dyskinesia in tottering mice involves the cerebellum as it has been shown that immediate early gene c-fos is activated within the cerebellar circuitry during these episodes (Campbell and Hess, 1998). The episodes of paroxysmal dyskinesia in tottering mice were blocked by L-type calcium channel blockers, which suggest that these channels compensate for dysfunctional P/Q-type VGCC (Campbell and Hess, 1999).

The rocker (tg^{rkr}) mutation results in an amino acid substitution (lysine for threonine) in the P-loop of domain III (Zwingman et al., 2001). Rocker mice also show mild to moderate cerebellar ataxia, without any sign of cerebellar neuronal loss (Zwingman et al., 2001). Topographical presentation of mutations associated with α_{1A} subunit of $Ca_V2.1$ channel is shown in Figure I-8. The Nagoya rolling (tg^{rol}) mouse

mutation is an arginine to glycine substitution in the voltage sensor of domain III (Oda, 1981).

The rolling mouse phenotype is a moderate to severe ataxia with a minor loss of granule cells in the rostral cerebellum (Suh et al., 2002). Although, Purkinje cell death is not observed in these mice (Suh et al., 2002), Rhyu et al. (1999a) demonstrated multiple Purkinje cell dendritic spines synapsing with single parallel fiber suggesting abnormal Purkinje/parallel fiber synapses.

THE LEANER MOUSE

The leaner mouse was named for its motor dysfunction, which caused the mouse to "lean" against a wall to prevent it from falling while walking (Sidman et al., 1965). The leaner mouse carries a naturally occurring autosomal recessive mutation at $\alpha_1$2.1 gene on mouse chromosome 8 (Fletcher et al., 1996; Doyle et al., 1997). The mutation is a guanine to adenine substitution at the 5' end of the unspliced intron in the $\alpha_1$2.1 gene and results in truncation of the carboxy terminal of the normal protein giving rise to two $\alpha_1$2.1 splice variants (Fletcher et al., 1996). The aberrant splicing event lead to formation of two unequal sized fragments; the larger fragment results from failure to splice out intron and the smaller fragment results from skipping of one exon, leading to formation of two abnormal proteins (Fletcher et al., 1996). The $\alpha_1$2.1 gene encodes the pore forming subunit of Ca_V 2.1 or P/Q-type VGCCs (Westenbroek et al., 1995; Dove et al., 1998; Wakamori et al., 1998; Lorenzon et al., 1998).

Table I-6: Phenotypes of the $Ca_V2.1$ mouse models. Symbols and abbreviations: CSD = cortical spreading depression; TH = tyrosine hydroxylase; PC = Purkinje cell; PF = parallel fiber; + = mild phenotype; +++ = severe phenotype; ↓ = decreased; ↑ = increased; ↓* and ↑* = P/Q current density is either decreased or increased over a broad voltage range at low voltages near the threshold of activation, but unchanged at high voltages (V); n.d.= not determined; Yes (No?) = controversial findings (Adapted from Pietrobon, 2005).

	$Ca_V2.1^{-/-}$	**$Ca_V2.1^{+/-}$**	***tg/tg***	***tg^{la}/tg^{la}***	***tg^{rol}/tg^{rol}***	***tg^{rkr}/tg^{rkr}***	**FHM1 knock in**
Absence seizures	Yes	No	Yes	Yes	No?	Yes	No
Ataxia	Yes (+++) and dystonia	No	Yes (+)	Yes (+++) and dystonia	Yes (++)	Yes (+)	No
Cerebellar cell death	Yes	No	No	Yes	Yes (No?)	No	No
Episodic dyskinesia	No	No	Yes	No	No	No	No
Susceptibility to CSD	n.d.	n.d.	↓	↓	n.d.	n.d.	↑
Inflammatory pain responses	↓[2]	↓[2]	n.d.	n.d.	n.d.	n.d.	n.d.
Abnormal TH expression in Purkinje cells	n.d.	n.d.	Yes	Yes	Yes	No	n.d.
Abnormal organization of PF–PC synapses	Yes	n.d.	Yes	Yes	Yes	No	n.d.
Neuronal P/Q current	0	↓(50%)	↓	↓	↓*	n.d.	↑*
Shift of P/Q channel activation	No	No	No	Yes (No?) to more positive V	Yes to more positive V	n.d.	Yes to more negative V

Phenotypically, the most apparent sign in leaner mice is extreme ataxia, which is recognized at around postnatal day (P) 10 and becomes progressively worse until stabilizing at about P40 to P50 (Sidman et al., 1965). These mice show reduced survivability and death occurs by P21 due to their inability to move about their environment (Sidman et al., 1965; Meier et al., 2000), unless special care is given to support these mice through this critical period (Abbott and Jacobowitz, 1999). Leaner mice also exhibit absence seizures and intermittent dyskinesia (Sidman et al., 1965; Hess and Wilson, 1991). Generalized absence seizures begin as early as P14 and are similar to those in the tottering mouse, consisting of 6 – 7Hz spike wave discharges at a rate of 40 to 60 bursts an hour (Noebels, 1984).

The most notable phenotype and consequence of the leaner mutation is extensive neurodegeneration in the leaner cerebellum, which shows a significant reduction in size and volume (Sidman et al., 1965). Even though the overall cytoarchitecture of the cerebellum is maintained, leaner cerebellar granule cells, Purkinje cells and Golgi cells die during postnatal development (Herrup and Wilczynski, 1982). Also, the number of granule cells per unit area in the leaner mouse cerebellum is unchanged when compared to wild-type mice, even after significant granule cell loss has taken place in leaner mice (Nahm et al., 2002). There is abnormal synaptic connectivity between parallel fibers and Purkinje cell dendritic spines; however the physiological consequence of the synaptic modification is not clearly understood (Rhyu et al., 1999b). The Purkinje and granule cell loss are more prominent in the anterior cerebellum. However, Golgi cell loss does not show any anterior-posterior gradient pattern (Herrup and Wilczynski, 1982).

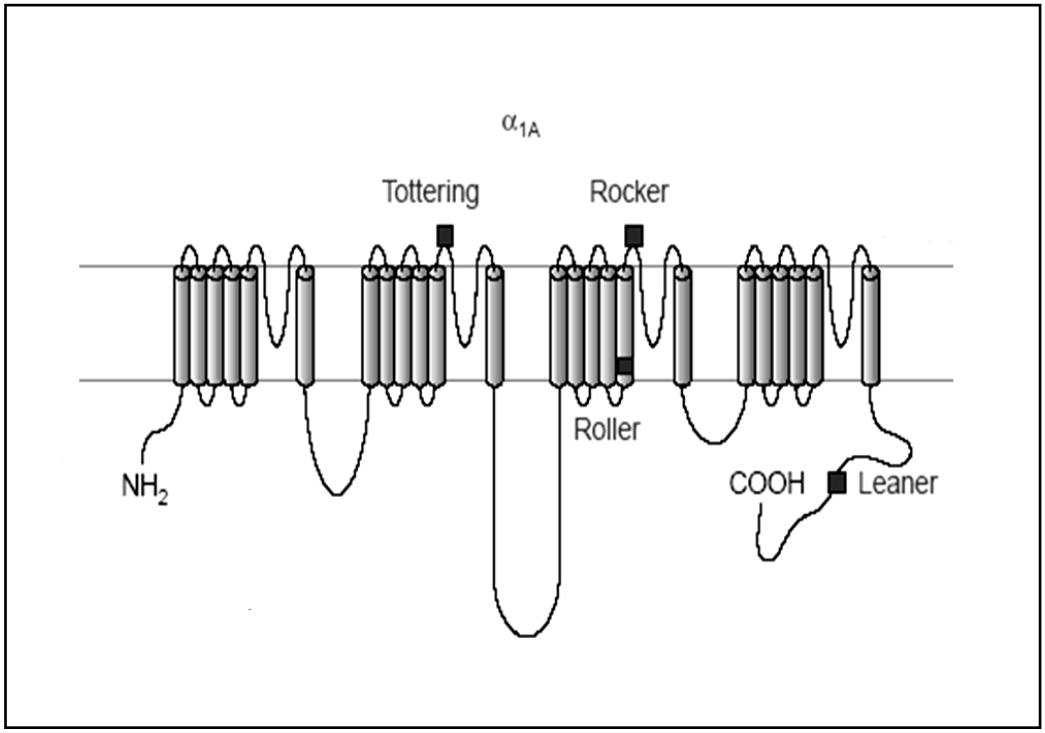

Figure I-8. Topographical presentation of mutations associated with α_{1A} subunit of $Ca_V2.1$ channel. (Modified from Carafoli, 2004)

Leaner cerebellar granule cells begin to die at P10 – 12 and peak cell death occurs at P20 (Herrup and Wilczynski, 1982; Lau et al., 2004), which is concomitant with ataxic signs shown by these animals. The granule cell death remains noticeable until about P40 and becomes infrequent by 4 months of age (Herrup and Wilczynski, 1982). Fletcher et al. (1996) provided evidence with terminal deoxytransferase-mediated dUTP nick end-labeling (TUNEL) that granule cells undergo apoptotic cell death. The results where confirmed using electron microscopic observation of leaner granule cells,

which revealed the morphological hallmark of apoptosis including condensed nuclei and convoluted membranes (Lau, 1999). The results were further confirmed by Lau et al. (2004), which showed that granule cells die via an apoptotic cell death process that includes activation of caspase 3 (Lau et al., 2004).

Herrup and Wilczynski's (1982) study found that dying leaner Purkinje cells were not reliably identifiable, so they used counts of surviving Purkinje cells to determine the timing of Purkinje cell death. Their study found that Purkinje cells begin dying after P26, with approximately half of the Purkinje cells gone by P60 and death continuing at lower levels until at least 1 year of age (Herrup and Wilczynski, 1982). Frank et al. (2003) conducted a developmental study of Purkinje cell death in these mice by using Fluoro-Jade dye, which is an anionic fluorochrome and selectively labels degenerating neurons through an unknown mechanism (Schmued et al., 1997; Schmued and Hopkins, 2000). Fluoro-Jade-positive Purkinje cells were first seen at P25 and maximum Purkinje cell death observed at P40 (Frank et al., 2003). The Purkinje cell loss was more in anterior cerebellum and was seen until P80, which was the latest age examined (Frank et al., 2003). The temporospatial pattern of leaner cerebellar granule and Purkinje cell death has been examined; however, the molecular mechanism underneath the cell death has not been examined.

In spite of the mutation, mRNA and protein expression of the leaner $\alpha_1 2.1$ subunit is not altered (Wakamori et al., 1998; Lau et al., 1998). The main effect of the mutation is alteration in $Ca_V 2.1$ channel activity. Experiments done on Purkinje neurons of leaner mice showed a 60% decrease in Ca^{2+} currents, beginning as early as P7 – 9,

just prior to the onset of ataxia (Dove et al., 1998; Lorenzon et al., 1998; Wakamori et al., 1998). The voltage dependent gating, mean channel open time and Ca^{2+} conductance through the $Ca_V2.1$ channel are unaffected (Dove et al., 1998; Lorenzon et al., 1998; Wakamori et al., 1998). However, it was observed that due to this mutation the open probability of $Ca_V2.1$ type calcium channels is reduced threefold and therefore decreasing the amount of overall Ca^{2+} entering the Purkinje cells following depolarization (Dove et al., 1998; Lorenzon et al., 1998; Wakamori et al., 1998). P-type calcium channels contribute approximately 90% of whole cell Ca^{2+} current in wild type Purkinje somata (Dove et al, 1998), so due to this mutation there is profound decrease in whole cell calcium current.

Unlike Purkinje cells, the basal forebrain (BF) neurons express all of the Ca^{2+} channel α_1 subunits, with $Ca_V2.1$ contributing approximately 30% to the whole-cell current (Griffith et al., 1994). Recently, it was shown that the whole cell current densities in BF neurons are not reduced in the leaner mice despite a reduction in the $Ca_V2.1$ contribution (Etheredge et al., 2007). There was a significant increase in the proportion of Ca_V1/L-type Ca^{2+} current in basal mutant phenotypes, which is probably compensating for the deficient $Ca_V2.1$ current. Similarly, cerebellar granule cells express all the α_1 subunits with $Ca_V2.1$ constituting 46% of whole cell current (Randall and Tsien, 1995). However, it is not known how much of whole cell calcium current is changed in leaner cerebellar granule cells, if it is changed at all.

Jun et al. (1999) constructed $\alpha_1$2.1-deficient mice ($\alpha_{1A}^{-/-}$) and showed that whole cell current in cerebellar granule cells is significantly reduced in knockout mice. There is

elevation in L- and N-type current density in cerebellar Purkinje cell bodies and reduction of R-type current density in cerebellar granule cell bodies. These findings in the knockout are unexpected perhaps, considering the results obtained from reduced function mutants. Dove et al. (1998) found no change in the current fraction supported by Ca_V1 channels in leaner Purkinje neurons. Also, Fletcher et al. (2001) showed an increase in L and N-type current density in cerebellar granule cells of $\alpha_1$2.1-deficient mice. There were no changes in R-type current in cerebellar granule cells of knockout mice. One of the remarkable finding of this study was that mice heterozygous for $\alpha_1$2.1 targeted disruption, exhibit similar reductions in Ca_V2.1 current density, but have normal cerebellar function and morphology; hence suggesting that the cell death may not be due to reduced VGCC currents (Fletcher et al., 2001)

The $\alpha_1$2.1 C-terminus participates in a number of protein–protein interactions and plays a prominent role in modulating channel activity (Walker and De Waard, 1998). Thus, its alteration by proteolytic cleavage or genetic mutation would have significant functional consequence. The C-terminus of Ca_V2.1 VGCC has regulatory sites which are modulated by G-protein coupled receptor Gβγ subunits (Hille, 1994; Herlitze, et al., 1996; Qin et al., 1997; Ikeda and Dunlap, 1999) and a site for Ca^{2+}- calmodulin binding (Lee et al., 1999). Gβγ subunits modulate gating properties while Ca^{2+}-calmodulin enhances Ca_V2.1 channel recovery from inactivation, facilitating Ca^{2+} entry. The leaner mutation likely alters these or other regulatory functions such as phosphorylation sites in the C-terminal tail, to modify Ca_V2.1 Ca^{2+} current. Recently, it was shown that the C-terminus of the $\alpha_1$2.1 subunit of the Ca_V2.1 VGCC is cleaved from the full-length protein

and translocated to the Purkinje cell nucleus (Kordasiewicz et al., 2006). This C-terminal cleavage product contains three nuclear localization signals that promote its localization to the nucleus (Kordasiewicz et al., 2006). The author speculated that this C-terminus may be required for survivability and its alteration in leaner mice may be the reason for cell death.

Reduced calcium ion influx alters calcium ion homeostasis and signaling in the leaner mouse. Dove et al. (2000) reported reduced calcium ion buffering capacity in leaner Purkinje cells. The observed changes include reduced calcium ion uptake into the ER and decreased cytosolic calbindin and parvalbumin expression. The changes in the calcium ion buffering system in leaner Purkinje cells are thought to be compensatory changes to maintain proper levels of calcium ions to elicit calcium ion signaling cascades (Murchison et al., 2002). Similarly, Nahm et al., (2002) reported a decreased expression of primary calcium ion binding protein, Calretinin, in leaner cerebellar granule cells, as a compensatory mechanism to maintain calcium ion homeostasis. In addition, T-type VGCCs are increased in leaner cerebellar Purkinje cells and decreased in leaner granule cells (Nahm et al., 2005). The differences between leaner Purkinje cells and granule cells likely represent different adaptive or compensatory processes within each cell type attempting to preserve cell function in presence of reduced Ca^{2+} currents.

Other changes in leaner mice include delayed response to nociceptic stimuli which is caused by a reduced ability to elicit action potentials in the dorsal root ganglion (Ogasawara et al., 2001). Ayata et al. (2000) reported that neurons in the neocortex of the leaner mouse show higher threshold for initiating cortical spreading depression

(CSD) and subsequent decrease in glutamate release. The CSD is also known to be involved in the generation of migraine attack. Leaner cerebellum exhibits aberrant tyrosine hydroxylase (TH) expression in Purkinje cells. TH, which converts tyrosine to L-DOPA, is the rate limiting enzyme in the synthesis of the neurotransmitter dopamine. TH is transiently expressed in wild cerebellar Purkinje cells between the third and fifth postnatal weeks (Hess and Wilson, 1991; Austin et al., 1992). However, in leaner cerebellar Purkinje cells, TH expression persists into adulthood (Hess and Wilson, 1991; Austin et al., 1992).

OBJECTIVES OF THE DISSERTATION

The objective of this dissertation was to better understand pathways associated with cerebellar neurodegeneration in the calcium channel mutant mouse, leaner. Our long term goal is to elucidate the molecular mechanisms and pathophysiology associated with mutations in CACNA1A gene which play significant roles in human diseases such as familial hemiplegic migraine, episodic ataxia type 2 and spinocerebellar ataxia type 6.

We have focused our research on understanding the relationship between mitochondrial function/dysfunction and calcium channel mutations and establishing a possible molecular pathway for cell death in leaner mice. The central hypothesis of this proposal is: **extensive cerebellar granule cell death in leaner mice is due to abnormal intracellular calcium homeostasis mediated by mitochondrial dysfunction**. To evaluate this hypothesis, this dissertation was subdivided into three specific aims:

1) To estimate the extent of cell death, basal intracellular calcium and mitochondrial (dys)function in cerebellar granule cells of adult leaner mice.

2) Determine the role of the leaner calcium channel mutation on postnatal development of cerebellar granule cells.

3) Test whether inducing increased calcium influx by exposing cultured granule cells to potassium chloride can eliminate or reduce the cell death**.**

The objective of specific aim #1 was to quantify cerebellar granule cell death in adult leaner mice. During postnatal development cerebellar granule cells in leaner mice showed a spatial pattern of cell death (Herrup and Wilczynski, 1982; Lau et al., 2004); thus we wanted to establish if this pattern would continue into adulthood. The second objective of this specific aim was to elucidate mitochondrial activity and calcium homeostasis in cerebellar granule cells of adult leaner mice and compare those results with tottering mutant mice. This would help us to establish if the cellular changes observed are directly related to cell death or not, as tottering mice carry a mutation in the same gene as leaner mice but no excessive neuronal cell death is observed in tottering mice (Isaacs and Abbott, 1995).

The primary objective of specific aim # 2 was to build on the results observed in specific aim #1 in order to develop a postnatal model of granule cell death in leaner mice. In the first part of this aim the mitochondrial function and basal intracellular calcium were observed in postnatally developing mice. We hypothesized that a decreased mitochondrial membrane potential and altered calcium homeostasis would coincide with the time of peak granule cell death, which is postnatal day (P) 20. We

studied four different ages: P10, P20, P30 and P40. The second objective of specific aim # 2 was to look for calcium transient currents when cerebellar granule cells are depolarized. By depolarizing the granule cells using potassium chloride and using P/Q type VGCC specific blocker, ω-Agatoxin IV A, we identified the contribution of P/Q type channel towards whole cell calcium current.

The objective of specific aim # 3 was to differentiate if decreased intracellular calcium or calcium influx is directly leading to neurodegeneration or the defective P/Q channel protein is causing an altered protein-protein interaction at the C-terminus triggering a lethal cascade of altered gene expression. To elucidate this, cerebellar granule cells were cultured under high potassium environment to induce increased calcium influx, and then cell death was quantified.

CHAPTER II

ESTIMATION OF THE EXTENT OF CELL DEATH, BASAL INTRACELLULAR CALCIUM AND MITOCHONDRIAL (DYS)FUNCTION IN CEREBELLAR GRANULE CELLS OF ADULT LEANER MICE

OVERVIEW

Excessive leaner cerebellar granule cell (CGC) death starts soon after postnatal day 10, but it is not known whether the degree of CGC death observed in adult leaner mice is significantly different from wild type mice. Also it is not known if the spatial pattern of granule cell death observed during postnatal development continues into adulthood or not. By using two cell death specific staining methods, Fluoro-Jade and TUNEL, we have shown that CGC death in adult leaner mice not only continues into adulthood, but is significantly greater than observed in the cerebella of age matched wild type mice. We also have shown that the spatial pattern of cell death, in which more cell death occurs in the anterior lobe as compared to the posterior lobe of the cerebellum, continues to adulthood. We know that altered calcium homeostasis, which could be due to dysfunctional P/Q type (Ca_V 2.1) voltage gated calcium channels (VGCC), can severely affect mitochondrial function, eventually causing neuronal cell death. By using indicator dyes Fura-2AM and TMRM to label acutely isolated CGCs we have shown a

reduced basal intracellular calcium and mitochondrial dysfunction respectively in CGC of leaner mice.

Reduced mitochondrial function could be either due to over all reduced cellular mitochondrial activity or a reduction in the total number of mitochondria. To investigate this, we assessed mitochondrial mass in two ways; first, by quantifying the mitochondrial protein, Cytochrome C, and second, by quantifying the mitochondrial phospholipid, Cardiolipin. Both experiments showed similar results, namely, that CGC from leaner mice have reduced mitochondrial activity and not a decreased number of mitochondria. Although the mitochondrial activity is reduced, our results using generation of reactive oxygen species (ROS) indicator dye CMH_2DCFDA, showed no change in ROS production in CGC of leaner mice as compared to wild type mice.

INTRODUCTION

Neurodegeneration underlies symptoms of many neurological disorders, including Alzheimer's, Parkinson's and Huntington's diseases, stroke and amyotrophic lateral sclerosis. Cell death in most of these neurodegenerative disorders takes place via apoptosis. Apoptosis or programmed cell death is an energy dependent, highly regulated process that allows for controlled dissolution of a cell without inducing an inflammatory response in the tissue surrounding the affected cell (Sastry and Rao, 2000; Yuan and Yankner, 2000; Yuan et al., 2003). Among the various pathways associated with apoptosis, one important pathway involves mitochondrial dysfunction. In neurons,

mitochondria are involved in regulation of calcium ion homoeostasis by buffering cells against high concentrations of free calcium ions (Budd and Nicholls, 1996). Calcium is a ubiquitous intracellular signaling messenger that is involved in essentially all events taking place in the cells of the nervous system (Berridge, 1998, Carafoli, 2002). Maintaining calcium homeostasis is crucial for normal neuronal function as any alteration will affect neuronal survival and may interfere with normal calcium signaling processes. Alterations in intracellular calcium ion concentration ($[Ca^{2+}]_i$) may severely affect mitochondrial function, leading to a cascade of events that eventually cause cell death (Nicholls and Ward, 2000).

Leaner and tottering mutant mice carry autosomal recessive mutations in the CACNA1A gene, coding for the α_{1A} pore forming subunit of Ca_v 2.1 (formerly known as P/Q-type, Ertel et al., 2000) voltage-gated calcium channels (VGCC). Ca_v 2.1 channels are highly expressed by cerebellar Purkinje and granule cells (Westenbroek et al., 1995). Inherited human neurological disorders caused by mutations in genes encoding calcium channel subunits are referred to as calcium channelopathies (Peitrobon, 2002). Several autosomal dominant human neurological disorders are associated with mutations in the CACNA1A gene, which encodes the $\alpha_1$2.1 subunit of Ca_v 2.1 calcium channels including; familial hemiplegic migraine, generalized epilepsy with ataxia, episodic ataxia type 2 and spinocerebellar ataxia type 6 (Ophoff et al., 1996; Klockgether and Evert, 1998; Ducros et al., 1999; Jouvenceau et al., 2001; Pietrobon, 2002). Leaner and tottering mutant mice provide powerful models to study the mechanisms by which defective Ca_v 2.1 VGCCs result in neurological disorders.

The cerebellar granule cell degeneration occurring in homozygous leaner mice is relatively slow, progressive and extensive, beginning shortly after P10 and peaking at P20 (Lau et al., 2004). However, granule cell death, while decreased at P30 and P40 compared to P20, is still significantly greater than seen in age-matched wild type mice (Lau et al., 2004). During postnatal development, neurodegeneration in leaner mice follows a spatial pattern with more cell death observed in anterior lobe as compared to posterior (Frank et al., 2003; Lau et al., 2004). Based on histological analysis, Herrup and Wilczynski (1982) reported that the size and density of the granule cell layer keeps decreasing and so hypothesized that the cell death is continuous throughout the life of leaner mice. However, it is unknown whether the granule cell death in adult leaner mouse is significantly different from the wild type mice; moreover it is not known whether spatial pattern of cell death continues into adulthood.

The goals of this study were two fold. The first objective was to elucidate the pattern and mode of cerebellar granule cell death in adult leaner mouse and the second objective was to investigate the effect of the calcium channel mutation on calcium homeostasis and mitochondrial function in leaner cerebellar granule cells. We used three mouse genotypes for this study: 1) wild type mice (controls), which lack any mutation in the CACNA1A gene and do not experience any significant neuronal cell death; 2) tottering mice, which act as a second control because they carry a calcium channel mutation in the CACNA1A gene, but do not exhibit excessive cerebellar granule cell death; and 3) leaner mice, which carry a mutation in the CACNA1A gene and exhibit significant cerebellar granule cell death.

MATERIALS AND METHODS

Animals

Wild type (+/+), homozygous leaner (tg^{la}/tg^{la} or Cacna1a$^{tg\text{-}la}$) and homozygous tottering (tg/tg or Cacna1a^{tg}) mice on an inbred C57BL/6J background were used. All mice were bred and housed at the Comparative medicine program facility at Texas A&M University. Homozygous leaner pups started to show ataxia at approximately postnatal day 12 (P12). As a result of their neurological deficits, these mice have limited ability to move about the cage and adequately access food and water, which increases their mortality due to hypothermia and dehydration. To increase their survival rate all homozygous leaner mice were supplemented with moistened rodent chow starting at P17-18. Additionally, since homozygous leaner females do not nurture their pups well, homozygous leaner pups were fostered to lactating Swiss White Webster mice at the age of P0 to P1. Male and female wild type, homozygous tottering and homozygous leaner mice at the age of 6–7 months were used for all experiments. Animals were maintained under a 12hr light/dark photoperiod with a constant room temperature (21-22^{o}C) and provided with access to food and water *ad libitum*. Procedures for animal use were approved by the Texas A&M University Laboratory Animal Use Committee and carried out in accordance with the National Institutes of Health Guide for the Care and Use of Laboratory Animals (National Institutes of Health Publication No. 85-23, revised 1996).

Fluoro-Jade staining

Four wild type and four homozygous leaner mice were anesthetized intraperitoneally with 150 mg/kg ketamine and 15 mg/kg xylazine. Once anesthetized, mice were perfused intracardially with 50 ml of Tyrode's saline, followed by 500 ml of 4% paraformaldehyde in 0.12 M phosphate buffer (pH 7.4). Brains were removed and cerebellum separated. Cerebella were dehydrated through a series of graded alcohols, then embedded in paraffin and sectioned sagittally at 5 μm. The sections obtained were used for Fluoro-Jade and TUNEL staining. Fluoro-Jade staining procedure is same as described in detail elsewhere (Frank et al., 2003). Briefly, paraffin embedded sections were deparaffinized by standard protocols using xylenes and graded alcohols. The sections were immersed in distilled water for 1 min and transferred to a 0.06% potassium permanganate solution for 15 minutes on a rotating platform. Slides were then washed in deionized water for 1 minute and incubated in 0.001% Fluoro-Jade (Histo-chem Inc., Jefferson, AR, USA) in deionized water with 0.1% acetic acid for 30 minutes on a rotating platform.

After staining with Fluoro-Jade, slides were rinsed with three 1-minute changes of deionized water, dried thoroughly in a hot-air stream, immersed in xylene and coverslipped using DPX mounting media (EMS, Fort Washington, PA, USA). Sections of testes from both genotypes were used as positive control. Sections were examined with an epifluorescence microscope using a FITC filter. Fluorescent images were acquired using a Zeiss Axioplot 2 research microscope (Carl Zeiss, Inc., Thornwood, NY, USA) equipped with a three-chip Hamamatsu video camera. Quantification was

done by counting the number of Fluoro-Jade positive granule cells per midsagittal cerebellar section without knowing the genotype of the mouse from which the sections were obtained. To compare regional/spatial differences, the same cerebellar sections were divided into the anterior lobe (lobules I through anterior portion of lobule VI) and the posterior lobe (posterior portion of lobule VI through X) (Herrup and Kuemerle, 1997). The number of Fluoro-Jade positive granule cells in each lobe was recorded and compared. A minimum of 10 sections per animal were assessed.

TUNEL staining

For TUNEL staining, sections were obtained as described above and processed using Apoptag *in situ* detection kit (Chemicon, Temecula, CA) following the manufacturer's instructions. Diaminobenzidine (0.05%, Sigma, St. Louis, MO, USA) was used as the chromogen and methyl green (0.5% in 0.1 M sodium acetate, pH 4.0) as a counter stain. Sections of testes from both genotypes were used as positive and negative controls. In each experiment both positive and negative controls sections were processed under identical conditions except for negative controls for which H_2O was used in place of Tdt enzyme. Cells were considered positive for apoptosis if the nucleus was stained brown and showed signs of chromatin condensation. Quantification was done by counting the number of apoptotic granule cells per midsagittal cerebellar section. To compare the regional/spatial differences each cerebellar section was divided into anterior lobe (lobules I through the anterior portion of lobule VI) and the posterior

lobe (posterior portion of lobule VI through X) (Herrup and Kuemerle, 1997). A minimum of 8 sections per animal were assessed for the presence of apoptotic cells.

Acute isolation of cerebellar granule cells

Cerebellar granule cells (CGC) were acutely isolated as described in Current Protocols in Toxicology (Oberdoerster, 2001) with some modifications. Briefly, at specified ages, mice were anesthetized using isoflurane and killed by decapitation. The brain was removed and the cerebellum isolated. The meninges were removed and the cerebellum was chopped in 6-8 pieces and transferred to a chilled 50 ml falcon tube containing minimum essential medium with Earle's salts (MEM; Life Technologies inc., Rockville, MD). The pieces of cerebellum were transferred to dissociation medium made of MEM and 1.5 U/ml protease (Sigma, St. Louis, MO, USA) and stirred. During the stirring 0.2% DNase (Sigma) was added to digest genomic DNA released by damaged cells. After the final stirring, media containing the cells were centrifuged at 1000g for 10 min and resuspended in MEM.

To confirm isolation of CGC, isolated cells were plated on to coverslips coated with 500 μg/ml of poly-D-lysine (Sigma, St. Louis, MO, USA) and fixed using 4% paraformaldehyde for 15 min at room temperature (RT). CGC were permeabilized with 0.3% Triton X-100 and then blocked with 5% normal goat serum (NGS). The cells were incubated with a specific neuronal nuclei marker, mouse anti-neuronal nuclei (NeuN, 0.1 μg/ml, Chemicon) overnight at 4^{o}C, diluted to 1:2,000 in sterile PBS containing 2% NGS, followed by a 2 hr RT incubation in 1:1,000 diluted secondary antibody (Goat-

Anti-mouse, Alexa fluor 568, Molecular Probes Inc. Eugene, OR). CGCs were then incubated for 2 min at RT with DAPI (Molecular Probes Inc. Eugene, OR) to label all cell nuclei. Coverslips were then mounted onto slides using Prolong antifade (Molecular Probes Inc.). The cells were evaluated using epi-fluorescence at excitation wavelengths of 560 nm and 350 nm. Digital images were captured using a Zeiss Axioplot 2 Research Microscope (Carl Zeiss, Inc., Thornwood, NY, USA) and a three-chip Hamamatsu video camera.

Basal intracellular calcium ion levels

For basal intracellular calcium ion ($[Ca^{2+}]_i$) measurements, CGC were acutely dissociated as described previously from wild type, leaner and tottering mice (n=4 per genotype). Isolated CGC were plated onto chambered slides (VWR, West Chester, PA, USA) and incubated at 37^oC for 20 min using 95% O_2 and 5% CO_2. Cells were loaded with 5 μM Fura-2 AM made in 20% pluronic acid (Sigma) and further incubated at 37^oC for 30 min. De-esterification of the dye was carried out by washing the cells with fresh MEM media and incubating at 37^oC for an additional 30 min. Fura-2AM changes fluorescence intensity differentially at excitation wavelengths of 340 and 380 nm upon binding Ca^{2+}. The cells were exposed to dual excitation at 340 and 380 nm and fluorescence was monitored at 510 nm. Fluorescent images were acquired using 40X UV objectives on an Olympus 1X-70 microscope and a three-chip Hamamatsu ORCA-ER cooled charge-coupled device camera. Image capturing and R-values were calculated

using Simple PCI Version 5.0.0.1503 Compix Inc. and Imaging System (Cranberry Township, PA). $[Ca^{2+}]_i$ was determined by the equation

$$[Ca^{2+}]_i = K_D (F_{min}/F_{max}) [(R - R_{min})/(R_{max} - R)]$$

where, R is the observed 340:380 fluorescence ratio and the dissociation constant (K_D) value used was 224 (Grynkiewicz et al., 1985). F_{min} and F_{max} indicate fluorescence intensity at 380nm in the absence of Ca^{2+} and high Ca^{2+} respectively. R_{min} and R_{max} represent the ratio of F340/380 in the absence of Ca^{2+} and high Ca^{2+}, respectively. The values used for F_{min}/F_{max}, R_{min} and R_{max} were 8.36, 0.2 and 8.47, respectively. The calibrations were done using a calcium calibration kit (Molecular Probes Inc.).

Mitochondria membrane potential (MMP) measurement

Cerebellar granule cells were isolated as described previously from wild type, leaner and tottering mice (n=5 per genotype). Dissociated granule cells were plated onto coverslips coated with poly-D-lysine (Sigma) and incubated in MEM in 95% O_2 and 5% CO_2 at 37^{o}C for 25 min. CGCs were loaded with tetramethyl rhodamine methyl ester (TMRM, Molecular Probes) at 150 nM made in 100% dimethyl sulfoxide (Sigma) and then incubated at 37^{o}C for 15 min. Fluorescent images were acquired using a 40X oil objective on an Olympus 1X-70 microscope and a Hamamatsu ORCA-ER cooled charge-coupled device camera at excitation and emission of 555nm and 600nm, respectively. CGC were illuminated minimally to reduce the photo bleaching. All images were corrected for background fluorescence. Image analysis was carried out to

determine mitochondrial membrane potential using the Simple PCI Imaging System (Compix).

Mitochondrial mass measurement

Two approaches were used to estimate mitochondrial mass. First, we measured cytochrome C protein expression in protein extracted from whole cerebella using Western blotting. Second, we estimated the content of the inner mitochondrial membrane phospholipid, cardiolipin, in mitochondria of CGC.

Cytochrome C expression: Three mice of each genotype, wild type, leaner and tottering mice, were anesthetized with isoflurane and killed by decapitation. The brains were rapidly removed and immediately frozen with powdered dry ice, then stored at -70 °C until used. Total protein from each cerebellum was extracted by sonication in 0.5ml of protein extraction reagent (M-PER; Pierce, Rockford, IL, USA) and one tablet of Complete, Mini, EDTA-free protease inhibitor cocktail (Roche Diagnostics Corp, Indianapolis, IN, USA) per 10 mL of M-PER. At the time of analysis, 30 µg of protein sample was denatured and loaded into a 4-20% gradient polyacrylamide gel. Protein was then transferred onto a PVDF blotting membrane (BioRad, Hercules, CA, USA) using a Mini Trans-Blot Electrophoretic Transfer Cell system (BioRad). Membranes were blocked with 5% skim milk in phosphate-buffered saline containing 0.1% Tween-20 for 2 hours at room temperature (RT), then were incubated with monoclonal mouse cytochrome C antibody (1 µg/ml, BD Pharmingen, San Diego, CA, USA) overnight at 4ºC, followed by peroxidase labeled secondary antibody (1:20,000, Anti-Mouse IgG,

Cell Signaling Technology, Danvers, MA) for 2 hours at RT. The immunoreactive bands were visualized by enhanced chemiluminescence substrate (Pierce, Rockford, IL, USA). The chemiluminescence signal was obtained by capturing images using the FluroChem 8800 Imaging System (Alpha Innotech, San Leandro, CA, USA). After detecting immunoreactive bands, the gels and membranes were stained with Coomassie blue using GelCode blue stain (Pierce) to ensure equal protein loading and transfer. Densitometric analysis was performed using the AlphaEase FC^{TM} Imaging system (Alpha Innotech) to determine the optical density of the immunoreactive bands. Gels were repeated at least three times and the integrated density value obtained was used as percent control for statistical analysis.

Cardiolipin: Cellular cardiolipin content was estimated by visualization of CGC stained with 10-*N*-Nonly acridine orange (NAO, Molecular Probes), a dye that binds with high affinity to cardiolipin (Petit et al., 1992, 1994). CGCs were isolated from four mice of each genotype (wild type, leaner and tottering), as described previously, plated onto chambered slides (VWR) and incubated at 37^{o}C for 25 min at 95% O_2 and 5% CO_2. Cells were loaded with 10 µl of 50 µM NAO made in 100% ethanol (ETOH) to reach a final concentration of 500 nM and further incubated at RT for 25 min. Fluorescent images were acquired using a 20X objective on an Olympus 1X-70 microscope and a Hamamatsu ORCA-ER cooled charge-coupled device camera at excitation and emission of 488 nm and 520nm, respectively. CGC were illuminated minimally to reduce photo bleaching. Image analysis was carried out to determine the fluorescent emitted by CGC

as an index of cardiolipin content potential using the Simple PCI Imaging System (Compix).

Reactive oxygen species (ROS) measurement

For determination of ROS we used Chloromethyl-dihydrodichlorofluorescein diacetate (CM-H_2DCFDA) (Molecular Probes Inc), which is a redox-sensitive dye. It is membrane permeable and gets trapped in cells by binding of the chloromethyl group to cellular thiols. Subsequently, the dye becomes fluorescent when oxidized by H_2O_2 and/or downstream free radical products of H_2O_2. CGC were acutely dissociated as described above, plated onto chambered slides (VWR International, Inc.) and incubated in 95% O_2 and 5% CO_2 at 37^{o}C for 25 min. The cells were loaded with CM-H_2DCFDA at a concentration of 500 nmol and incubated in 95% O_2 and 5% CO_2 at 37°C for 8 min. Sequential time course fluorescent image capturing was performed for 22.5 minutes using a 90 second interval with a 20X objective on an Olympus 1X-70 microscope and a Hamamatsu ORCA-ER cooled charge-coupled device camera at excitation and emission of 490 nm and 520 nm, respectively. Image capturing and ROS levels were analyzed using Simple PCI Version 5.0.0.1503 Compix Inc. and Imaging.

Statistics

Data are presented as means ± standard error of mean. All data were analyzed using statistical software SPSS Version 12.0.1 for windows. General Linear Model (GLM) - Univariate Analysis of Variance (ANOVA) at $\alpha = 0.05$ was used to analyze all

data except ROS, which was analyzed using the GLM - repeated measures analysis. Significant differences among genotypes were interpreted using the Tukey's honest significant difference (HSD) post hoc test.

RESULTS

To estimate the proportion and spatial pattern of cerebellar granule cell (CGC) death we used Fluoro-Jade and TUNEL staining. Fluoro-Jade is an anionic fluorescein derivative that selectively stains the degenerating neurons irrespective of the mechanism of cell death (apoptosis or necrosis) (Schmued et al., 1997; Frank et al., 2003). Figure II-1A shows the representative phototmicrographs of Fluoro-Jade staining. We used testis as the positive control, as seminiferous tubules consistently have numerous apoptotic cells (Blandchard et al., 1996). Our results showed a significantly higher number of Fluoro-Jade positive CGCs in adult leaner cerebellum as compared to age matched wild type (Figure. II-1B). We also observed that Fluoro-Jade positive granule cells were primarily located in the anterior lobe of the leaner cerebellum (Figure. II-2C).

To confirm Fluoro-Jade staining results and identify the mode of cell death, we used the TUNEL assay. The TUNEL assay specifically label the DNA strand breaks, a hallmark of apoptosis (Migheli et al., 1994). Fig. II-2 shows representative photomicrographs of TUNEL positive CGCs in leaner (Fig. II-2A) and wild type (Fig. II-2B) mice. We used testis as both positive (Fig. II-2C) and negative (Fig. II-2D) controls.

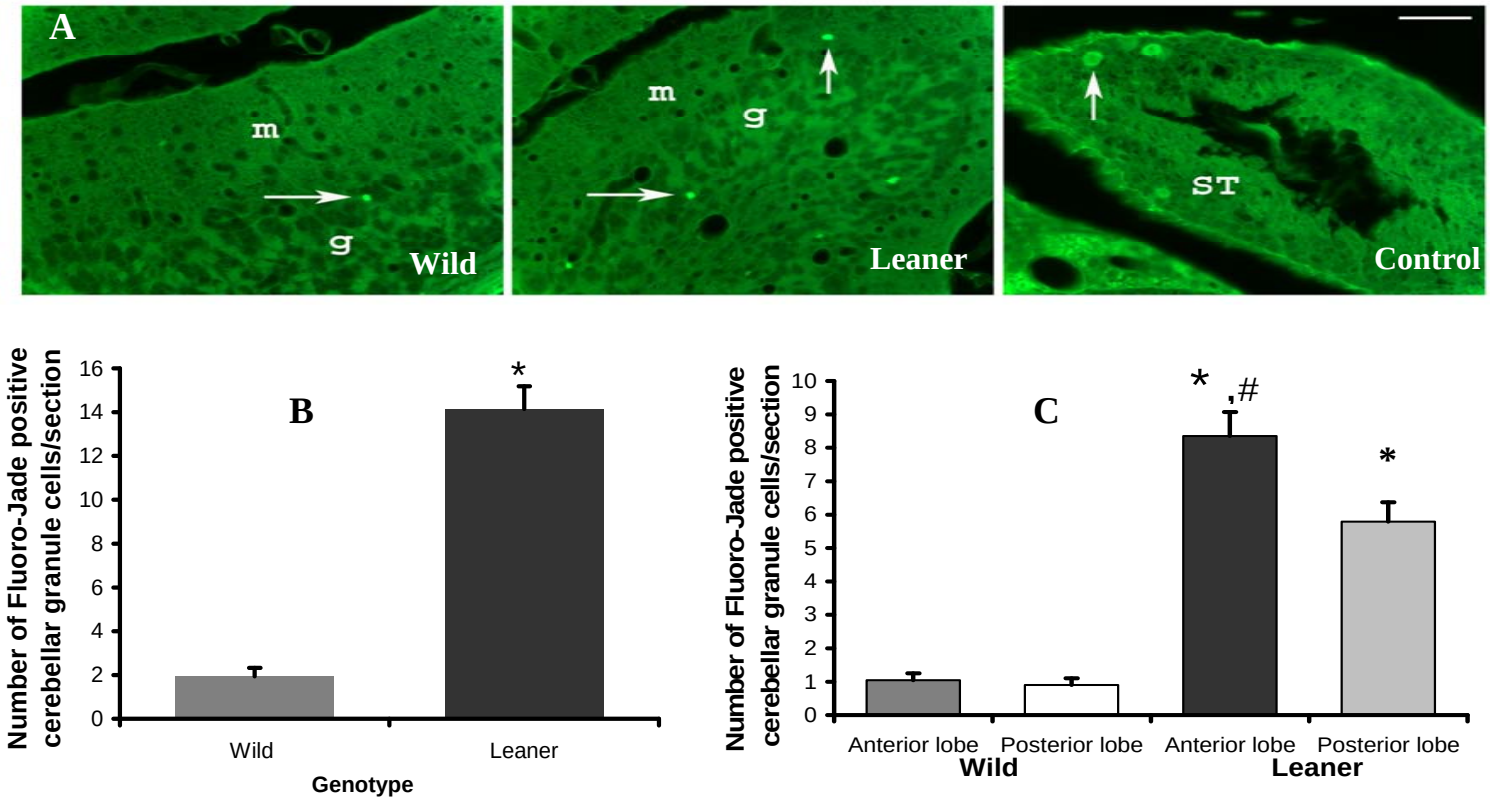

Figure II-1. Fluoro-Jade staining of cerebellar granule cells. "A" is showing representative photomicrographs of wild type, leaner and testes as positive control sections. Scale bar is 50 µm. White arrows indicate Fluoro-Jade positive cerebellar granule cells in wild type and leaner section and Fluoro-Jade positive spermatogonia and spermatocytes in control. g = granule cell layer, M = molecular cell layer, ST = seminiferous tubule. "B" is showing average number of Fluoro-Jade positive cerebellar granule cells/section from adult wild type (gray bar; wild) and homozygous leaner mice (black bar; leaner), where as "C" is average number of Fluoro-Jade positive cerebellar granule cells/section for different regions of homozygous leaner (leaner) and wild type (wild) cerebellum. Data are presented as mean ± SEM; where n = 4 for each genotype. The "*" indicates a significantly higher number of Fluoro-Jade positive cerebellar granule cells in leaner as compared to wild type and "#" indicates significantly higher number of Fluoro-Jade positive cerebellar granule cells in anterior lobe as compared to posterior lobe in leaner mice. A one-way ANOVA was significant at $\alpha = 0.05$.

We observed a small but significantly higher number of TUNEL positive CGCs in leaner cerebella compared to age-matched wild type mice (Fig. II-3A). As seen during Fluoro-Jade staining, higher numbers of apoptotic cells are present in the anterior lobe of the leaner cerebellum (Fig. II-3B). Both the Fluoro-Jade staining and the TUNEL assay were carried out only for wild type and leaner mice and not in tottering mice, as there has been no report of excessive granule cell death in tottering mice (Isaacs and Abbott, 1995).

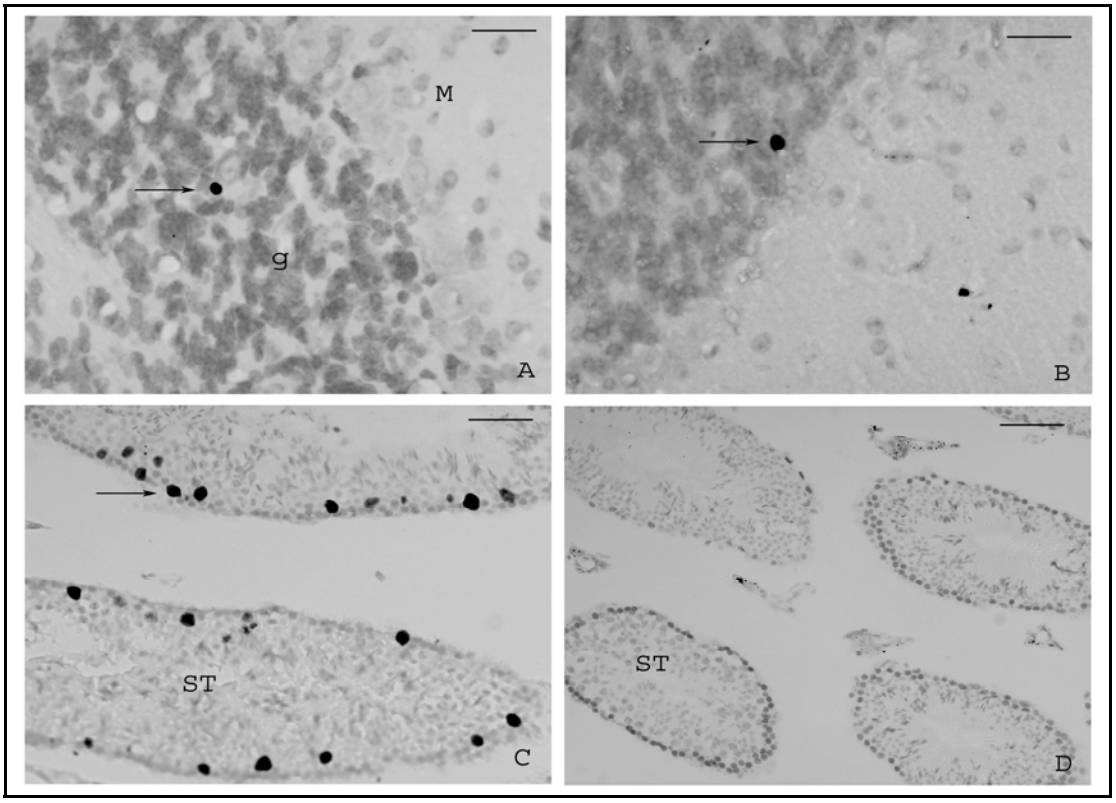

Figure II-2. Photomicrographs showing TUNEL staining of representative leaner (A), wild type (B), positive control (C) and negative control (D) testis sections. Scale bars in A and B are 50 µm, and in C and D are 100 µm and 200 µm, respectively. Black arrows indicate TUNEL positive cerebellar granule cells in image A, B and TUNEL positive spermatogonia and spermatocytes in C. g = granule cell layer, M = molecular cell layer, ST = seminiferous tubule.

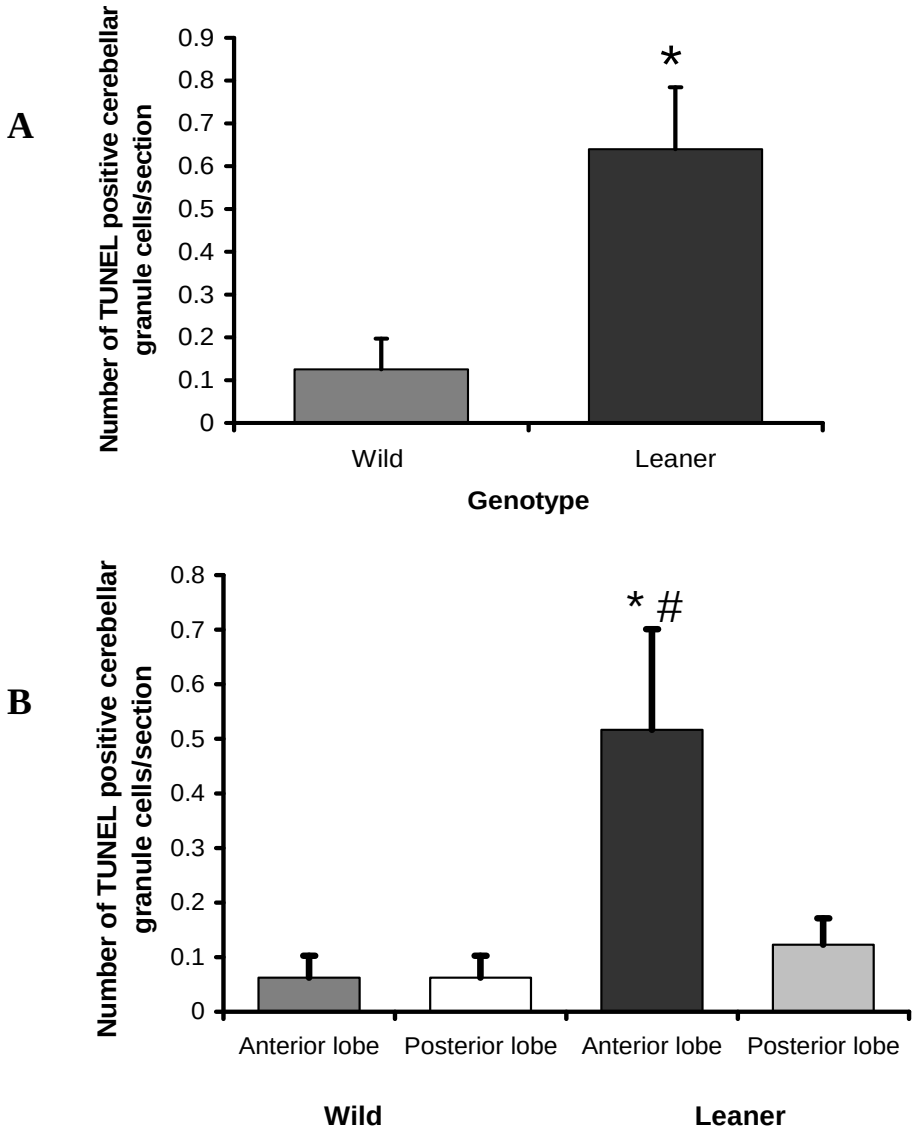

Figure II-3. Graphs showing overall average number and spatial distribution of TUNEL positive cerebellar granule cells. "A" is showing average number of TUNEL positive cerebellar granule cells/section from adult wild type (gray bar; wild) and homozygous leaner mice (black bar; leaner). "B" is showing average number of TUNEL positive cerebellar granule cells/section for different regions of homozygous leaner (leaner) and wild type (wild) cerebellum. Data are presented as mean ± SEM; where n = 4 for each genotype. The "*" indicates a significantly higher number of TUNEL positive cerebellar granule cells in leaner mice as compared to age matched wild type mice, where as "#" indicates significantly higher number of TUNEL positive cerebellar granule cells in anterior lobe as compared to posterior lobe in leaner mice.. A one-way ANOVA was significant at $\alpha = 0.05$.

Calcium ion homeostasis was measured as basal free intracellular calcium ($[Ca^{2+}]_i$) using the ratiometric dye, Fura-2 AM, which is one of the most widely used calcium indicators for ratiometric measurement. Although CGCs are by the far the most numerous cerebellar neuronal population we validated the acutely isolated cells as neurons by staining with NeuN, a specific neuronal nuclei marker and DAPI, a non specific marker of DNA to label all cell nuclei. NeuN is highly expressed by CGCs but not Purkinje cells (Mullen et al., 1992; Sarnat et al., 1998). Thus, NeuN is an excellent marker to identify CGCs in a mixed cell population from the cerebellum. CGCs also were identified on the basis of their size, as they are the smallest neurons in the cerebellum. Double fluorescence imaging showed that our isolation procedure yields many more granule cells then any other neuronal/cellular population (Fig. II-4).

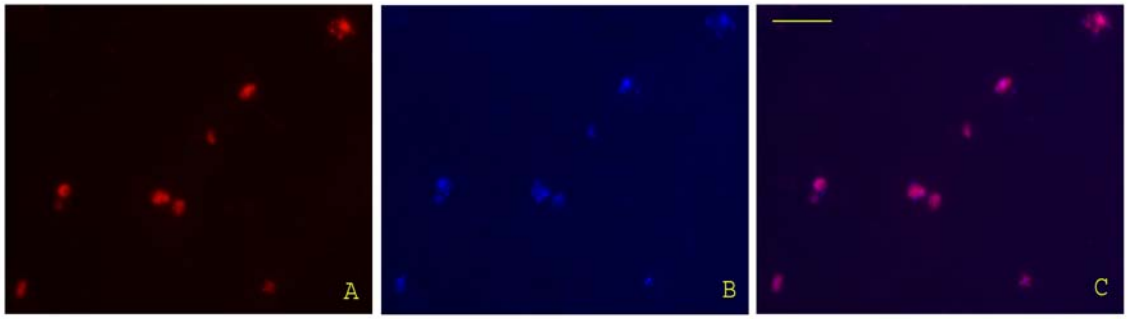

Figure II-4. Representative images of NeuN and DAPI double fluorescence imaging. Isolated granule cells were plated onto coverslips and double stained with the specific neuronal marker, NeuN, (A) and the specific double stranded DNA marker, DAPI (B). A and B are the same field of view captured under epi-fluorescence at excitation wavelengths of 560 nm (A) and 350 nm (B) wavelengths. Image C is the overlay of images A and B, revealing that the vast majority of cells were double labeled for NeuN and DAPI. Images were adjusted for brightness and contrast using Adobe Photoshop 7.0. Scale bar in C is 20 μm; the same scale applies to all photomicrographs.

Isolated CGCs were incubated with Fura-2 AM and exposed to dual excitation at 340 and 380 nm (Fig. II-5A) to measure $[Ca^{2+}]_i$. We found a significantly reduced $[Ca^{2+}]_i$ in both leaner and tottering CGCs compared to age-matched wild type CGCs (Fig. II-5B). Resting $[Ca^{2+}]_i$ levels were reduced by approximately 20% in leaner and tottering CGCs compared to wild type mice ($p < 0.001$). However, there was no significant difference in basal $[Ca^{2+}]_i$ between tottering and leaner CGCs. Our observation of basal intracellular calcium ion concentration suggested the existence of altered calcium ion homeostasis. Therefore, since leaner CGC die via apoptosis and we suspected an intrinsic apoptotic pathway involving mitochondria, we chose to examine mitochondrial function/dysfunction in CGCs.

Mitochondrial membrane potential (ψ_m) has often been used as a marker for mitochondrial activity and neuronal viability during the various cell death cascades (Nicholls and Ward, 2000). We examined mitochondrial membrane potential in individual CGCs from leaner, tottering and wild type mice, using tetramethyl rhodamine methyl ester (TMRM), which is a lipophilic cation dye that accumulates in mitochondria in proportion to the membrane potential of the mitochondria (Russell et al., 1999). Only CGCs showing a punctate pattern of staining (Fig. II-6A) were used for final analysis. Fluorescence intensity was measured from individual CGCs after thresholding and subtracting background fluorescence. GLM-Multivariate Analysis of Variance showed an overall significance ($p<0.001$) and the Tukey's HSD post hoc test indicated a reduced ψ_m in leaner CGCs compared to both age matched wild type and tottering CGC (Fig. II-

6B), indicating reduced mitochondrial activity in leaner CGC. However, no significant difference in ψ_m beween tottering and wild type CGCs was observed.

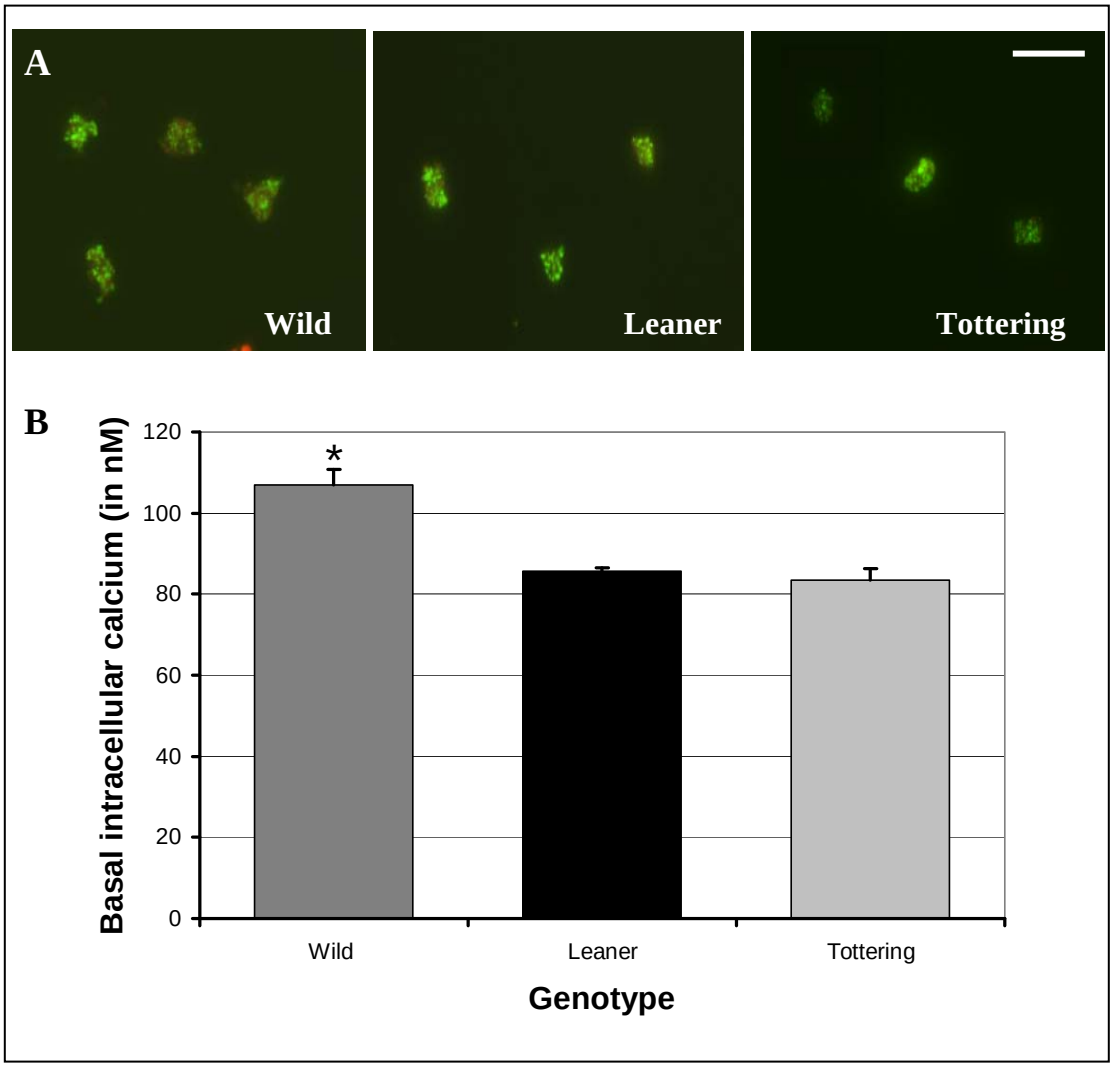

Figure II-5. Basal intracellular calcium in cerebellar granule cells stained with Fura-2AM. "A" is showing representative photomicrographs of adult wild type, leaner and tottering cerebellar granule cells stained with Fura-2AM. Scale bar is 10 µm. "B" is graph of mean basal $[Ca^{2+}]_i$ data from isolated cerebellar granule cells of adult wild type, leaner and tottering mice. A one-way ANOVA revealed a significantly lower basal $[Ca^{2+}]_i$ in cerebellar granule cells of leaner and tottering mice as compared to wild type mice ("*" = $p<0.001$; where n = 5 for each genotype).

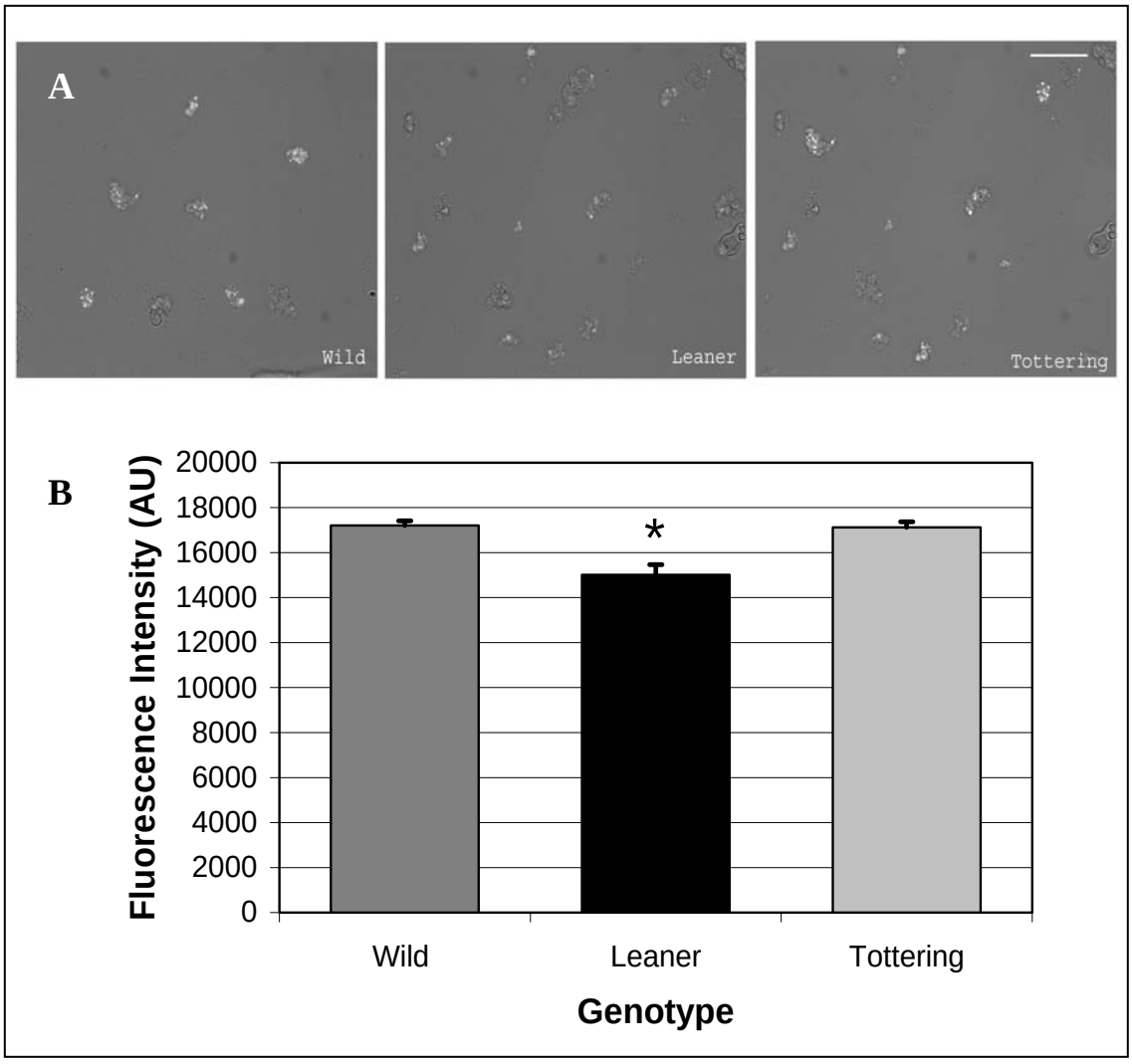

Figure II-6. Effects of genotype on mitochondrial membrane potential (MMP) of acutely isolated cerebellar granule cells from adult wild type, leaner and tottering mice. Photomicrographs in "A" show representative cerebellar granule cells stained with TMRM. Note that the fluorescence intensity of wild type and tottering CGCs is greater than leaner CGCs, demonstrating lower MMP in leaner CGCs. Scale bar = 10μm. The graph in B indicates the mean ± SEM fluorescence intensity in arbitrary units (AU) for all three genotypes; n = 5 for each genotype. One-way ANOVA revealed a significant reduction in fluorescence intensity in leaner cerebellar granule cells ("*" = $p < 0.05$. Images were adjusted for brightness and contrast using Adobe photoshop 7.0.

The observed decreased ψ_m in leaner and tottering CGCs could be due to a decrease in ψ_m of the overall CGC mitochondrial population or it could be due to a decrease in the mitochondrial mass of individual CGCs. To address this question we measured the mitochondrial mass of CGCs in leaner, tottering and wild type cerebella. We used two approaches to measure mitochondrial mass. The first method was an indirect approach that measured cytochrome C expression in whole cerebellum. Cytochrome C is a ubiquitous, heme-containing protein that normally resides in the space between the inner and outer mitochondrial membranes (Newmeyer and Ferguson-Miller 2003). Since granule cells are the major cell type within the cerebellum, measurement of whole cerebellar cytochrome C expression by Western blotting would primarily reflect CGC cytochrome C expression. Western blot analysis done on total cerebellar protein revealed a 15kDa band in all three genotypes (Fig. II-7B).

It was difficult to find an appropriate control 'housekeeping' protein, such as actin, to use for comparison between the mutant mice and control mice because many proteins utilize cytosolic calcium ion concentration to regulate expression, and calcium homeostasis is altered in these cerebella (Dove et al., 1998). Therefore, to ensure equal loading and transfer of protein, the gels and membrane were stained with Coomassie blue stain (Fig. II-7A). Densitometric analysis performed on the immunoreactive bands did not reveal any significant difference in optical density between the three genotypes (Fig. II-7C), suggesting no difference in whole cerebellar cytochrome C expression of leaner, tottering and wild type mice. Thie experiment was conducted in triplicate and similar results were observed each time.

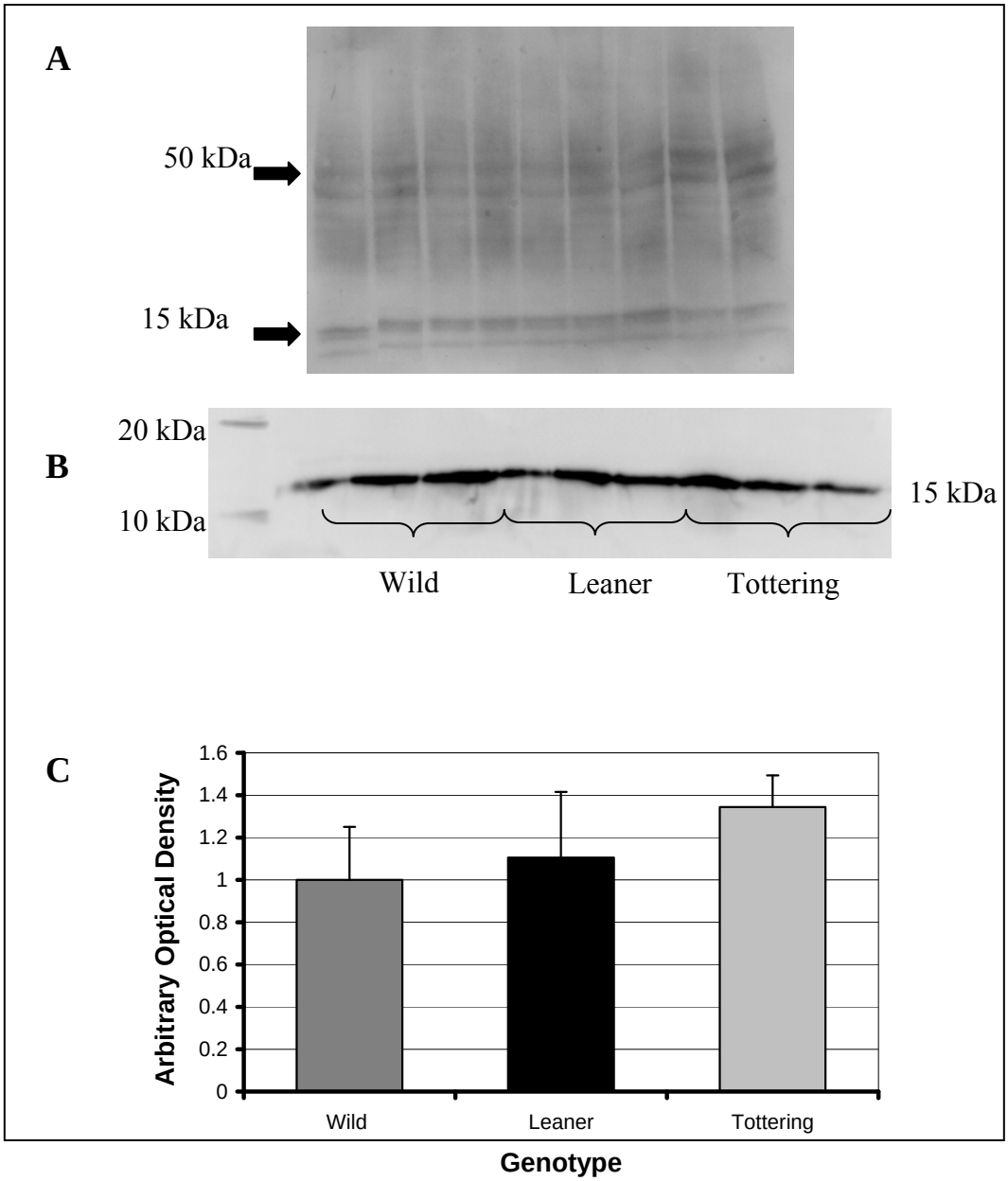

Figure II-7. Cytochrome C (Cyto C) protein expression in adult wild type, leaner and tottering whole cerebella. Panel A is the Coomassie-stained membrane following Western blotting. Panel B is a representative Western blot for Cyto C, which is a 15-kDa protein. Panel C is a graph of densitometry of the Cyto C bands from Western blotting of whole cerebella from each genotype. Densitometry was calculated by determining the integrated density value of Cyto C bands from Western blotting using AlphaEase FC software. Western blotting with densitometry was repeated 3 times with consistent results. ANOVA and Tukey's HSD post hoc test indicated that Cyto C was not significantly different between three genotypes. Error bars indicate standard error of the mean.

The second method used to measure mitochondrial mass was direct estimation of cardiolipin content of individual CGCs. Cardiolipin is a major phospholipid of mitochondrial membranes. Acutely isolated CGCs were incubated in 50 μm NAO and exposed to excitation of 488 nm (Fig. II-8A). One way Analysis of Variance indicated no overall significant difference of fluorescence intensity emitted by CGCs from leaner, tottering or wild type mice (Fig. II-8B), indicating no difference in the cardiolipin content of CGCs from all three genotypes.

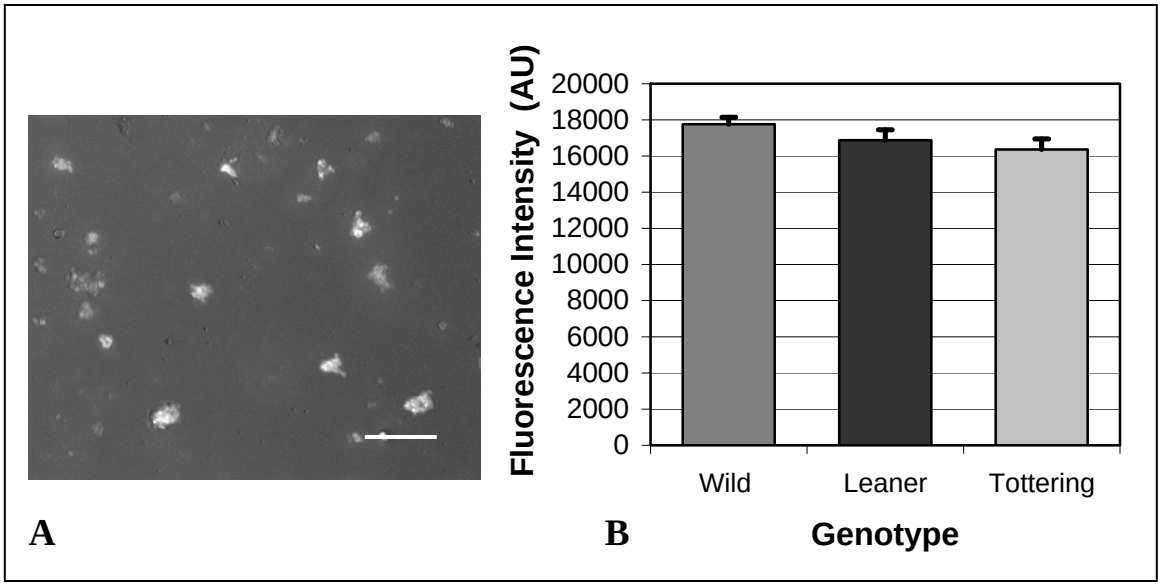

Figure II-8. Measurement of Cardiolipin content in cerebellar granule cells of adult wild type, leaner and tottering mice. Photomicrographs in "A" show representative cerebellar granule cells from wild type mice stained with 10-nonyl acridine orange. Scale bar = 10μm. The graph in B indicates the mean ± SEM fluorescence intensity in arbitrary units (AU) for all three genotypes; n = 4 for each genotype. One-way ANOVA revealed no significant reduction in fluorescence intensity in leaner cerebellar granule cells. Images were adjusted for brightness and contrast using Adobe photoshop 7.0.

Cell damage due to ROS formation has been associated in the pathophysiology of many neurologic disorders and mitochondrial dysfunction associated with loss of calcium ion homeostasis has been implicated in generation of superoxide radicals (Rego and Oliveira, 2003). The observed changes in basal intracellular calcium ion concentrations and mitochondrial activity led us to determine whether CGCs are under oxidative stress by looking at generation of ROS. Cerebellar granule cells were acutely isolated and the ROS levels in CGCs of all three genotypes were measured based on analysis of the intensity of fluorescence of CM-H_2DCFDA dye using sequential time course fluorescent image capture (Fig. II-9A). GLM-Repeated measures test and the Tukey's HSD post hoc test indicated no significant difference in fluorescent intensity of CM-H_2DCFDA dye in CGCs of leaner, tottering and wild type mice (n = 4; Fig. II-9B).

DISCUSSION

Granule cell death in the leaner cerebellum follows a temporospatial pattern, which peaks at postnatal day 20 (P20), and the anterior cerebellum shows more cell death (Lau et al., 2004). Although, Herrup and Wilczynski (1982) speculated that neuronal cell death was continuous throughout life in the leaner mouse, the proportion and pattern were not identified. We used Fluoro-Jade and TUNEL staining to demonstrate the proportion, pattern and mode of granule cell death in adult leaner cerebellum. Our results demonstrate a significantly higher number of Fluoro-Jade positive granule cells in adult leaner cerebellum as compared to age-matched wild type.

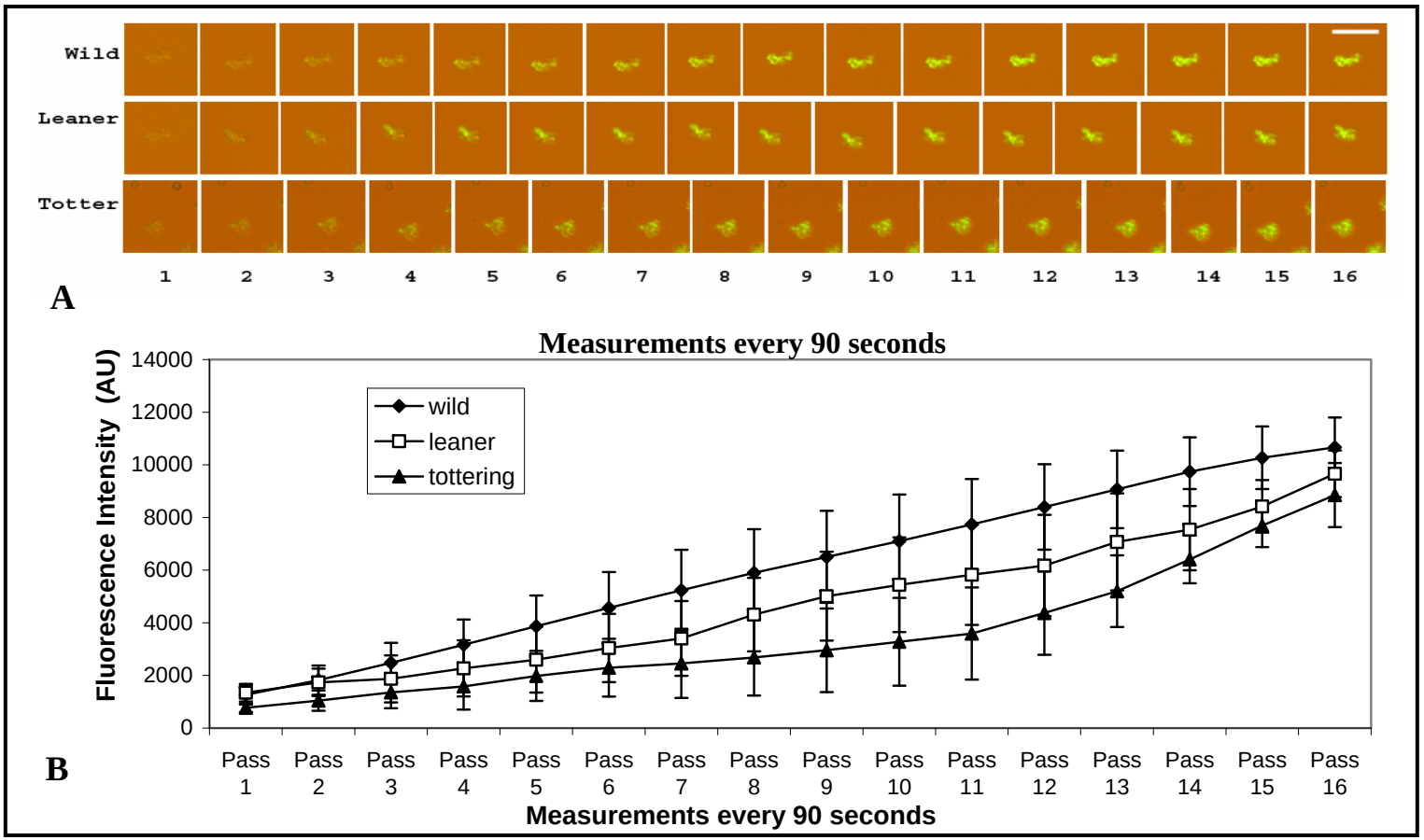

Figure II-9. Measurement of reactive oxygen species (ROS) using CM-H2DCFDA dye. Panel A shows photomicrographs of acutely isolated cerebellar granule cells from adult wild, leaner and tottering mice loaded with CM-H2DCFDA dye. Scale bar = 10 microns. Panel B shows relative mean total cellular ROS of granule cells from wild, leaner and tottering mice (n = 4). GLM-Repeated measure test indicated not change in total ROS production in cerebellar granule cells of three genotypes.

This observation was confirmed with TUNEL staining, which also indicated that cell death is due to apoptosis. The leaner mutation leads to decreased granule cell volume (Herrup and Wilczynski, 1982) with no change in granule cell density (Nahm et al., 2002), at least in 3-week-old leaner mice. We have reported CGC death in midsagittal sections without correcting for cell volume or area in the leaner cerebellum compared to age-matched wild type mice. Even without this correction, these results demonstrate higher numbers of dying CGC compared to wild type cerebellum, although the adult leaner cerebellar volume is significantly smaller than age-matched wild type mice.

Apoptosis is a process characterized by rapid progression once triggered, rapid elimination of apoptotic cells by macrophages and the death of only small number of cells at any one time (Wallig et al., 2002). The difference in magnitude of cell death observed in Fluoro-Jade staining compared to TUNEL staining is because TUNEL identifies a terminal biochemical stage of apoptosis; DNA fragmentation (Enari et al., 1998), whereas Fluoro-Jade identifies dead neurons regardless of cause of death. This study has not only confirmed that leaner CGC death continues into adulthood but, more importantly, the spatial pattern of granule cell death observed during postnatal development (Lau et al., 2004) also continues into adulthood.

Our lab has previously shown that the leaner mutation does not result in altered expression and/or localization of the mutated voltage-dependent Ca^{2+} channel $\alpha_1 2.1$ subunit mRNA or protein (Lau et al., 1998). However, intracellular Ca^{2+} homeostasis could be altered that may well directly and/or indirectly lead to leaner granule cell death,

since Ca^{2+} plays pivotal roles in neuronal survival and death (Missiaen et al., 2000). A large body of literature supports the idea that elevated neuronal $[Ca^{2+}]_i$, whether mediated by excitotoxicity or other mechanisms, can cause neuronal death (Stys et al., 1991; Sattler and Tymianski, 2001; Arundine and Tymianski, 2003; Canzoniero and Snider, 2005; Slemmer et al., 2005). The mechanism(s) of cell death most frequently invoked by increased Ca^{2+} result in subsequent generation of ROS (Boldyrev et al., 2004). Although less studied, equally compelling evidence exists that reduced basal $[Ca^{2+}]_i$ also is associated with neuronal cell death (Galli et al., 1995; Ichikawa et al., 1998; Tabuchi et al., 2003; Yoon et al., 2003).

We assessed basal $[Ca^{2+}]_i$ as an index to estimate Ca^{2+} homeostasis and observed decreased basal $[Ca^{2+}]_i$ in CGC of leaner and tottering mice as compared to age-matched wild type mice. The results obtained with CGC in this study are contrary to results obtained with leaner cerebellar Purkinje cells, where no change in basal $[Ca^{2+}]_i$ was reported (Dove et al., 2000). However, it is known that Purkinje cells have more extensive buffering and a greater storage capacity for Ca^{2+} than do the much smaller granule cells (Murchison et al., 2002), which would provide leaner Purkinje cells a greater capacity to maintain basal $[Ca^{2+}]_i$ in spite of the reduced function of Ca_v 2.1 voltage-gated channels in these mutant mice. Our results suggest that reduced basal $[Ca^{2+}]_i$ may not be directly related to CGC death as tottering CGC also showed reduced basal $[Ca^{2+}]_i$ but they do not exhibit excessive CGC death. On the other hand, resting $[Ca^{2+}]_i$ alone cannot be considered the sole index of determining Ca^{2+} homeostasis, which includes several homeostatic mechanisms to control the subcellular location of

Ca^{2+} and the level of $[Ca^{2+}]_i$. These mechanisms include Ca^{2+} influx through voltage-regulated and receptor-regulated channels, Ca^{2+} buffering by the plasma membrane and cytosolic proteins, Ca^{2+} storage in intracellular organelles including mitochondria, endoplasmic reticulum and nucleus and the Ca^{2+} efflux plasma membrane Ca^{2+}-ATPase and Na^+/Ca^{2+} exchanger (Miller, 1991; Weber, 2004). It would be interesting to identify how adult leaner CGC behave under depolarization, especially when we know that the leaner mutation results in decreased Ca^{2+} current through the Ca_v 2.1 channels (Dove et al., 1998; Dove et al., 2000; Lorenzon et al., 1998) and that there is reduced calretinin expression, the major calcium ion binding protein present in these cells (Nahm et al., 2002).

Mitochondria play an important role in maintaining Ca^{2+} homeostasis, which when disturbed, can lead to significant cellular pathophysiology and cell death. Mitochondria have large conductance pores called mitochondrial transition pores (MTP), whose opening is considered to be a key event during apoptosis (Ichas & Mazat, 1998). When MTP open, mitochondrial membrane potential (ψ_m) is decreased and in the process small, mitochondria-specific proteins such as cytochrome C, apoptosis inducing factor (AIF) and/or Smac/Diablo, are released into the cytosol (Adams and Cory, 1998). These proteins in turn can act alone to trigger apoptosis or activate caspase proteases that lead to apoptosis (Liu et al., 1996; Du et al., 2000). We observed decreased ψ_m in leaner CGC compared to both age matched tottering and wild type CGC. Decreased ψ_m could be due to decreased numbers of mitochondria or to decreased functional capacity of

mitochondria in leaner CGC. Two different methods were used to assess mitochondrial mass as a measure of mitochondria numbers. First we quantified the inner mitochondrial membrane protein, cytochrome C and second we estimated directly the amount of the mitochondrial phospholipid, cardiolipin, in acutely isolated, live CGC. Both experiments indicated no change in mitochondrial mass of CGC comparing leaner, tottering and wild type mice. These results substantiated our previous finding that CGC death in leaner mice occurs through apoptosis via activation of mitochondria-associated genes and caspase-2 and -3 (Nahm 2002; Lau et al., 2004). However, we have yet to elucidate additional molecules involved in this specific cell death cascade.

Oxidative stress is known to be involved in the pathogenetic mechanism of many neurodegenerative disorders including excitotoxicity, Alzheimer's disease and Parkinson's disease (Butterfield et al., 2002; Floyd and Hensley, 2002; Jenner, 2003; Facheris et al., 2004). We determined whether the mitochondrial stress demonstrated by loss of ψ_m leads to increased oxidative stress in leaner CGC. Total cellular ROS levels were determined in leaner, tottering and wild type CGC using CM-H_2DCFDA dye. Our results showed no change in generation of ROS in CGC of leaner mice compared to tottering and wild type CGC. ROS have complex chemical and physiological properties in normal mitochondrial and cell functioning. Schulz et al. (1996) demonstrated that ROS are essential mediators of K^+ deprivation-induced apoptosis of cerebellar granule neurons because neuronal death was blocked by superoxide dismutase. However, Boldyrev et al. (2004) showed that cell death in CGC acutely exposed to Amyloid-β was independent of ROS generation. Vergun et al. (2001) suggested that ROS accumulation

during toxic glutamate challenge in hippocampal neurons was not a prerequisite for altered Ca^{2+} homeostasis and/or the observed collapse of mitochondrial membrane potential. It also has been noted that polychlorinated biphenyls at doses that rapidly kill acutely isolated rat CGC do not cause increased ROS generation (Tan et al., 2004). Thus, it is the case that ROS exist in a state of dynamic equilibrium and excess ROS can result in fatal consequences for affected cells (Zorov et al., 2005) but cell death also can take place independent of excess ROS.

ROS functions are tightly linked to the function of another radical, nitric oxide (NO) (Zorov et al., 2005) and it has been suggested that NO may have a regulatory role in mitochondrial respiration (Cooper et al., 2003). It is interesting to note that neuronal NO synthase (n-NOS), and presumably also NO, is elevated in the tottering mouse cerebellum, but not in the leaner mouse cerebellum (Rhyu et al., 2003). While still speculative, it is possible that increased NO production in the tottering mouse cerebellum may stimulate mitochondrial respiration and be reflected by the normal ψ_m in tottering CGC. The lack of increased NO production in the leaner cerebellum would, on the other hand, be reflected in the reduced ψ_m in leaner CGC.

In conclusion, our results show that CGC death in leaner mice may be occurring via mitochondrial dysfunction and may not be directly related to decreased basal $[Ca^{2+}]_i$. However a, more detailed study is required to elucidate all the calcium ion homeostatic mechanisms and possible compensatory actions taking place in leaner CGC. It is possible that reduced Ca^{2+} influx and altered Ca^{2+} buffering lead to mitochondrial stress, which could be an underlying factor in neuronal cell death in these mice.

CHAPTER III

DETERMINATION OF THE ROLE OF THE LEANER CALCIUM CHANNEL MUTATION IN POSTNATAL DEVELOPMENT OF CEREBELLAR GRANULE CELLS

OVERVIEW

Cerebellar granule cells (CGC) of leaner mice start to show apoptotic cell death after postnatal (P) day 10 and cell death peaks at P20. Apoptosis is an energy dependent, highly regulated process, which can be associated with mitochondrial dysfunction. Since the mutation in leaner mice results in dysfunctional Ca_V 2.1 channels, we hypothesized that decreased mitochondrial activity and altered calcium homeostasis will coincide with peak granule cell death at P20. We assessed cellular changes related to mitochondrial function and calcium homeostasis during postnatal development in CGCs from leaner mice. To demonstrate altered calcium ion homeostasis we used the calcium indicator dye Fura -2 AM in acutely isolated CGCs. Reduced basal intracellular calcium was observed in CGCs from leaner mice after P10. Isolated CGCs loaded with Fura-2AM were then depolarized using potassium chloride (KCl) to demonstrate calcium transients. No differences in calcium ion transients were seen in leaner CGCs during postnatal development. Our results demonstrated a functional compensation for the defective Ca_V 2.1 channels by other voltage gated calcium channels (VGCC). Calcium influx through

Ca_V 2.1 channels was blocked by ω-Agatoxin IVA to confirm that Ca_V 2.1 channels were not contributing towards whole cell calcium current and other channels were in fact compensating for the defective Ca_V 2.1 channels.

Mitochondrial function was demonstrated using the mitochondrial indicator dye, tetramethyl rhodamine methylester (TMRM). Reduced mitochondrial activity was observed at P20 and P40; however no change was seen at P30. Reduced mitochondrial function could be either due to over all reduced cellular mitochondrial activity or reduced number of mitochondria. To investigate this, we measured mitochondrial mass by quantifying the mitochondrial protein, Cytochrome C and mitochondrial phospholipids, cardiolipin. Both experiments showed reduced mitochondrial activity and not a decrease in the number of mitochondria in CGCs of leaner mice. Although, mitochondrial activity was reduced, our results using generation of reactive oxygen species (ROS) indicator dye CMH_2DCFDA, showed no change in ROS production in CGC of leaner mice as compared to wild type mice. This suggested mitochondria-mediated but ROS independent cell death in CGCs of leaner mice.

INTRODUCTION

During early postnatal development CGC death begins at P10 in both wild type and leaner mice, however in wild type mice the rate of CGC death starts decreasing after P15 whereas in leaner mice the granule cell death accelerates and peaks at P20 (Lau, 1999). Previous work in our lab has shown that CGC in leaner mice die via apoptosis

during postnatal development (Lau et al., 2004). This degenerative profile of granule cells is observed only until after the cells have reached their adult position. This implies that the major developmental events that guide the cell types of the cerebellar cortex to their final position are intact in leaner mice (Herrup and Wilczynski 1982).

Neurons have evolved to have mechanisms to allow for rapid changes in intracellular calcium ions and these changes are involved in regulation of numerous cellular functions, including control of excitability, neurotransmitter release, cell differentiation, cell death and survival (Kirischuk et al., 1996). During neuronal signaling the increase in intracellular calcium ions ($[Ca^{2+}]_i$) is accomplished by both extracellular Ca^{2+} entry through various channels and Ca^{2+} mobilization from intracellular calcium stores. Calcium ions enter into neurons via voltage-gated calcium ion channels and ligand-gated calcium ion channels. Mitochondria play an important role in intracellular Ca^{2+} signaling pathways which, when disturbed, lead to significant cellular pathophysiology and cell death. Alteration of cellular calcium homeostasis can lead to disruption of mitochondrial activity, which can be determined by measuring mitochondrial membrane potential (ψ_m) (Nicholls and Ward, 2000).

The leaner mutation results in decreased Ca^{2+} current through Ca_V 2.1 Ca^{2+} channels in cerebellar Purkinje cells (Dove et al., 1998; Dove et al., 2000; Murchison et al., 2002) and changes in buffering capacities have been observed in both Purkinje and granule cells (Dove et al., 2000; Nahm et al., 2002). Also, the leaner mutation leads to altered expression of mitochondrial function related genes (Nahm, 2002). So, it is very likely that the leaner mutation leads to alteration of Ca^{2+} homeostasis in CGC, which

results in cell death through disrupted mitochondrial activity. The objective of this study was to elucidate the mitochondrial function and basal intracellular Ca^{2+} level in CGC of postnatally developing mice. We hypothesized that decreased ψ_m and altered Ca^{2+} homeostasis will coincide with peak CGC death, which is postnatal day (P) 20. We studied three age groups P10, P20 and P30. Any observed change in mitochondrial membrane potential could be due to overall change in mitochondrial activity or change in the mitochondrial mass. To investigate this question we estimated mitochondrial mass by quantifying the mitochondrial protein, Cytochrome C and also measured the mitochondrial phospholipid, cardiolipin.

According to Lorenzon et al. (1998) there is 65 % decrease in Ca^{2+} currents in leaner Purkinje cells and there is also threefold reduced probability of channel opening, reducing the frequency of opening and thus the amount of Ca^{2+} able to enter the cell following depolarization (Dove et al, 1998). P-type calcium channels contribute approximately 90% of whole Ca^{2+} cell current on the soma (Dove et al, 1998), whereas in granule cells $Ca_V2.1$ channels constitutes 46% of whole cell current (Randall and Tsien, 1995). The second objective of this study was to look for calcium transient currents when CGC are depolarized. Potassium chloride is very commonly used to depolarize neurons and induce Ca^{2+} influx through voltage gated Ca^{2+} channels (Hartmann et al., 1995; Savidge and Bristow, 1997; Ichikawa et al., 1998; Nogueron et al., 2001). In order to demonstrate the overall percentage of $Ca_V2.1$ type current in leaner CGC we used the specific $Ca_V2.1$ calcium channel blocker, ω-Agatoxin IVA.

MATERIALS AND METHODS

Animals

Wild type (+/+), homozygous leaner (tg^{la}/tg^{la} or Cacna1a$^{tg\text{-}la}$) and homozygous tottering (tg/tg or Cacna1a^{tg}) mice on an inbred C57BL/6J background were used. All mice were bred and housed at the Comparative medicine program facility at Texas A&M University. Homozygous leaner pups started to show ataxia around postnatal day 12 (P12). As a result of their neurological deficits, these mice have limited ability to move about the cage and adequately access food and water, which increases their mortality due to hypothermia and dehydration. To increase their survival rate all homozygous leaner mice were supplemented with moistened rodent chow starting at P17-18. Additionally, since homozygous leaner females do not nurture their pups well, homozygous leaner pups were fostered to lactating Swiss White Webster mice at the age of P0 to P1. Male and female wild type and homozygous leaner mice at four postnatal age (P) groups (P10, P20, P30 and P40) were used, whereas the comparison with homozygous tottering was done only at P20 and P30. Animals were maintained under a 12hr light/dark photoperiod with a constant room temperature (21-22^{o}C) and provided with access to food and water *ad libitum*. Procedures for animal use were approved by the Texas A&M University Laboratory Animal Use Committee and carried out in accordance with the National Institutes of Health Guide for the Care and Use of Laboratory Animals (National Institutes of Health Publication No. 85-23, revised 1996).

Acute isolation of cerebellar granule cells

Cerebellar granule cells (CGC) were acutely isolated as described in Current Protocols in Toxicology (Oberdoerster, 2001) with some modifications. Briefly, at the specified ages mice were anesthetized using isoflurane and killed by decapitation. The brain was removed and the cerebellum isolated. The meninges were removed and the cerebellum was chopped in 6-8 pieces and transferred to a chilled 50 ml falcon tube containing minimum essential medium with Earle's salts (MEM; Life Technologies inc., Rockville, MD). The pieces of cerebellum were transferred to dissociation medium made of MEM and 1.5 U/ml protease (Sigma, St. Louis, MO, USA) and stirred. During the stirring 0.2% DNase (Sigma) was added to digest genomic DNA released by damaged cells. After the final stirring the media containing cells was centrifuged at 1000g for 10 min and resuspended in MEM.

To confirm isolation of CGCs, isolated cells were plated onto coverslips coated with 500 μg/ml of poly-D-lysine (Sigma, St. Louis, MO, USA) and fixed using 4% paraformaldehyde for 15 min at room temperature (RT). CGCs were permeabilized with 0.3% Triton X-100 and then blocked with 5% normal goat serum (NGS). The cells were incubated with a specific neuronal nuclei marker, mouse anti-neuronal nuclei (NeuN, 0.1 μg/ml, Chemicon) overnight at 4^{o}C, diluted to 1:2,000 in sterile PBS containing 2% NGS, followed by a 2 hr RT incubation in 1:1,000 diluted secondary antibody (Goat-Anti-mouse, Alexa fluor 568, Molecular Probes Inc. Eugene, OR). Then CGCs were incubated for 2 min at RT with DAPI (Molecular Probes Inc. Eugene, OR) to label all cell nuclei. Coverslips were then mounted onto slides using Prolong antifade (Molecular

Probes Inc.). The cells were evaluated using epi-fluorescence at excitation wavelengths of 560 nm and 350 nm wavelengths. Digital images were captured using a Zeiss Axioplot 2 Research Microscope (Carl Zeiss, Inc., Thornwood, NY, USA) and a three-chip Hamamatsu video camera.

Basal intracellular calcium ion levels

For basal intracellular calcium ion ($[Ca^{2+}]_i$) measurements, CGCs were acutely dissociated as described previously from wild type, leaner and tottering male and female mice (n=5 per age group for leaner all the genotypes). Isolated CGC were plated onto chambered slides (VWR, West Chester, PA, USA) and incubated at 37^{o}C for 20 min using 95% O_2 and 5% CO_2. Cells were loaded with 5 μM Fura-2 AM made in 20% pluronic acid (Sigma) and further incubated at 37^{o}C for 30 min. De-esterification of the dye was done by washing the cells with fresh MEM media and incubating at 37^{o}C for an additional 30 min. Fura-2AM changes fluorescence intensity differentially at excitation wavelengths of 340 and 380 nm upon binding Ca^{2+}. The cells were exposed to dual excitation at 340 and 380 nm and fluorescence was monitored at 510 nm. Fluorescent images were acquired using 40X UV objectives on an Olympus 1X-70 microscope and a Hamamatsu ORCA-ER cooled charge-coupled device camera. Image capturing and R-values were calculated using Simple PCI Version 5.0.0.1503 Compix Inc. and Imaging System (Cranberry Township, PA). $[Ca^{2+}]_i$ was determined by the equation

$$[Ca^{2+}]_i = K_D\,(F_{min}/F_{max})\,[(R - R_{min})/(R_{max} - R)],$$

where, R is the observed 340:380 fluorescence ratio and the dissociation constant (K_D) value used was 224 (Grynkiewicz et al 1985). F_{min} and F_{max} indicate fluorescence intensity at 380nm in the absence of Ca^{2+} and high Ca^{2+}, respectively. R_{min} and R_{max} represent the ratio of F340/380 in the absence of Ca^{2+} and high Ca^{2+}, respectively. The values used for F_{min}/F_{max}, R_{min} and R_{max} were 8.36, 0.2 and 8.47, respectively. The calibrations were done using a calcium calibration kit (Molecular Probes Inc.).

Quantification of the depolarization induced calcium transients

After measuring resting free intracellular calcium as an index of calcium homeostasis, the next obvious step was to ascertain how these $Ca_V2.1$ calcium channels in leaner mice behave when depolarized. Ca^{2+} transients were evoked by KCl-induced depolarization and imaged using Fura-2AM. Control experiments were carried to ensure that observed change in fluorescence intensity is due to change in $[Ca^{2+}]_i$. We examined the effect of KCl induced depolarization by loading acutely isolated cerebellar granule cells with Fura -2AM dye both in the presence and absence of extracellular calcium to validate our experimental system. Five wild type and 5 leaner mice were used for all the above mentioned age groups. After measuring basal intracellular calcium as mentioned above, the extracellular KCl was increased to 40mM by superfusing granule cells with 20 μl of 1mM KCl. K^+ induced calcium influx was measured for 10 mins and the data point demonstrating peak increase of $[Ca^{2+}]_i$ was used for comparison with the initial basal levels. Data are expressed as the peak increase of $[Ca^{2+}]_i$ over initial basal levels. A minimum of 12 cells were analyzed for each age group and genotype.

To demonstrate the overall percentage of $Ca_V2.1$ current in leaner granule cells we used a specific $Ca_V2.1$ channel blocker, ω-Agatoxin IVA (Peptide International, Louisvelle, KY). Acutely isolated granule cells from 20 day old wild type and leaner mice were loaded with Fura-2AM. The cells were later incubated in 200nM of ω-Agatoxin IVA for 20mins at room temperature and then depolarized with KCl. Peak $[Ca^{2+}]_i$ was recorded and data are presented as peak increase of $[Ca^{2+}]_i$ over initial basal levels.

Mitochondria membrane potential (MMP) measurement

Cerebellar granule cells were isolated as described previously from wild type, leaner and tottering male and female mice (n=6 per genotype). Dissociated CGCs were plated onto coverslips coated with poly-D-lysine (Sigma) and incubated in MEM in 95% O_2 and 5% CO_2 at 37^{o}C for 25 min. Then CGCs were loaded with tetramethyl rhodamine methyl ester (TMRM, Molecular Probes) at 150 nM made in 100% dimethyl sulfoxide (Sigma) and incubated at 37^{o}C for 15 min. Fluorescent images were acquired using a 40X oil objective on an Olympus 1X-70 microscope and a Hamamatsu ORCA-ER cooled charge-coupled device camera at excitation and emission of 555nm and 600nm, respectively. CGCs were illuminated minimally to reduce the photo bleaching. All images were corrected for background fluorescence. Image analysis was carried out to determine mitochondrial membrane potential using the Simple PCI Imaging System (Compix).

Mitochondrial mass measurement

Two different methods were used to estimate mitochondrial mass in cerebellar granule cells of 20 and 30 day old wild type and leaner mice. First, we measured cytochrome C protein expression in protein extracted from whole cerebella using Western blotting. Second, we estimated the inner mitochondrial membrane phospholipid, cardiolipin contents in mitochondria of CGC.

Cytochrome C expression: Three mice of each genotype, wild type, leaner and tottering mice, were anesthetized with isoflurane and killed by decapitation. The brains were rapidly removed and immediately frozen with powdered dry ice, then stored at -70 °C until used. Total protein from each cerebellum was extracted by sonication in 0.5ml of protein extraction reagent (M-PER; Pierce, Rockford, IL, USA) and one tablet of Complete, Mini, EDTA-free protease inhibitor cocktail (Roche Diagnostics Corp, Indianapolis, IN, USA) per 10 mL of M-PER. At the time of analysis, 30 µg of protein sample was denatured and loaded into a 4-20% gradient polyacrylamide gel. Protein was then transferred onto PVDF blotting membrane (BioRad, Hercules, CA, USA) using a Mini Trans-Blot Electrophoretic Transfer Cell system (BioRad). Membranes were blocked with 5% skim milk in phosphate-buffered saline containing 0.1% Tween-20 for 2 hours at room temperature (RT) then incubated with monoclonal mouse cytochrome C antibody (1 µg/ml, BD Pharmingen, San Diego, CA, USA) overnight at 4ºC, followed by peroxidase labeled secondary antibody (1:20,000, Anti-Mouse IgG, Cell Signaling Technology, Danvers, MA) for 2 hours at RT. The immunoreactive bands were visualized by enhanced chemiluminescence substrate (Pierce, Rockford, IL, USA). The

chemiluminescence signal was obtained by capturing images using the FluorChem 8800 Imaging System (Alpha Innotech, San Leandro, CA, USA). After detecting immunoreactive bands, the gels and membranes were stained with Coomassie blue using GelCode blue stain (Pierce) to ensure equal protein loading and transfer. Densitometric analysis was performed using AlphaEaseFC^{TM} Imaging system (Alpha Innotech) to determine the optical density of the immunoreactive bands. Gels were repeated at least three times and the integrated density value obtained was used as percent control for statistical analysis.

Cardiolipin: Cellular cardiolipin content was estimated by visualization of CGCs stained with 10-*N*-Nonly acridine orange (NAO, Molecular Probes), a dye that binds with high affinity to cardiolipin (Petit et al., 1992, 1994). CGCs were isolated from 4 mice of each genotype (wild type, leaner and tottering mice) as described previously, plated onto chambered slides (VWR) and incubated at 37^{o}C for 25 min at 95% O_2 and 5% CO_2. Cells were loaded with of 10 µl of 50 µM NAO made in 100% ETOH to reach a final concentration of 500 nM and further incubated at RT for 25 min. Fluorescent images were acquired using a 20X objective on an Olympus 1X-70 microscope and a Hamamatsu ORCA-ER cooled charge-coupled device camera at excitation and emission of 488 nm and 520nm, respectively. CGCs were illuminated minimally to reduce photo bleaching. Image analysis was carried out to determine the fluorescent emitted by CGCs as an index of cardiolipin content potential using the Simple PCI Imaging System (Compix).

Reactive oxygen species (ROS) measurement

For determination of ROS we used Chloromethyl-dihydrodichlorofluorescein diacetate (CM-H_2DCFDA) (Molecular Probes Inc), which is a redox-sensitive dye. It is membrane permeable and gets trapped in cells by binding of the chloromethyl group to cellular thiols. Subsequently the dye becomes fluorescent when oxidized by H_2O_2 and/or downstream free radical products of H_2O_2. CGCs were acutely dissociated as described above, plated onto chambered slides (VWR International, Inc.) and incubated in 95% O_2 and 5% CO_2 at 37^{o}C for 25 min. The cells were loaded with CM-H_2DCFDA at a concentration of 500 nmol and incubated in 95% O_2 and 5% CO_2 at 37°C for 8 min. Sequential time course fluorescent image capturing was performed for 22.5 minutes using a 90 second interval with a 20X objective on an Olympus 1X-70 microscope and a Hamamatsu ORCA-ER cooled charge-coupled device camera at excitation and emission of 490 nm and 520 nm, respectively. Image capturing and ROS levels were analyzed using Simple PCI Version 5.0.0.1503 Compix Inc. and Imaging.

Statistics

Data are presented as means ± standard error of mean. All data were analyzed using statistical software SPSS Version 12.0.1 for windows. General Linear Model (GLM) - Univariate Analysis of Variance (ANOVA) at $\alpha = 0.05$ was used to analyze all data except ROS, which was analyzed using GLM - repeated measures analysis. Significant differences among genotypes were interpreted using the Tukey's honest significant difference (HSD) post hoc test.

RESULTS

Studies done on cerebellar Purkinje cells of leaner mice have showed a reduced P-type calcium channel current however, the resting intracellular free calcium ($[Ca^{2+}]_i$) is not significantly different in leaner Purkinje cells compared to wild type Purkinje cells (Dove et al., 1998; Dove et al., 2000). The levels of intracellular free calcium have not been examined previously in leaner cerebellar granule cells (CGC). Since the cerebellar granule cells death and the behavioral symptoms shown by leaner mice coincide, we were interested in dissecting out cellular changes observed in leaner CGC during postnatal development. We measured basal intracellular calcium in acutely isolated CGC as an index of calcium homeostasis. To validate our procedure, acutely isolated CGCs were stained with NeuN, a specific neuronal nuclei marker and DAPI, a non specific marker of DNA to label all cell nuclei. Since NeuN is highly expressed by CGC, and not by Purkinje cells (Mullen et al., 1992; Sarnat et al., 1998), it is an excellent marker to identify CGCs in a mixed cell population from the cerebellum. CGCs also were identified on the basis of their size, as they are the smallest neurons in the cerebellum. Double fluorescence imaging showed that our isolation procedure yields many more granule cells then any other neuronal/cellular population (Fig. II-4).

Mean basal $[Ca^{2+}]_i$ data in cerebellar granule cells during postnatal development is showed in Figure III-1. A GLM-univariate analysis of Variance indicated an overall significant difference between genotypes and postnatal days ($P<0.001$). No significant difference in basal $[Ca^{2+}]_i$ was observed between wild type and leaner CGC at P10.

Starting from P20 there was reduced basal $[Ca^{2+}]_i$ in CGC of leaner mice as compared to age matched wild type ($P < 0.001$).

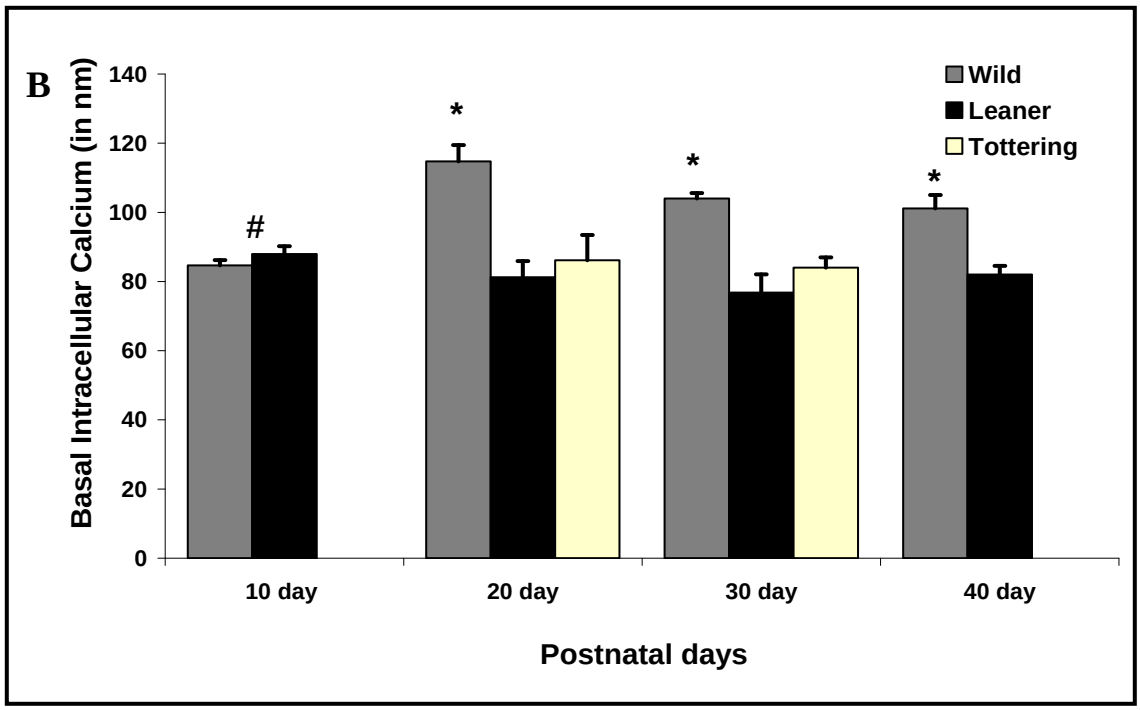

Figure III-1. Mean basal intracellular calcium in cerebellar granule cells during postnatal development. Graph shows mean basal $[Ca^{2+}]_i$ data from isolated cerebellar granule cells of wild type, leaner and tottering mice. The basal intracellular calcium level in wild type granule cells was significantly higher than observed in leaner and tottering granule cells at P20 and P30 ($P < 0.001$). There was also significant differences between wild type and leaner basal $[Ca^{2+}]_i$ at P40 ($P < 0.001$). However, we did not observe any significant difference in basal $[Ca^{2+}]_i$ between wild type and leaner granule cells at P10. "*" indicates significant differences between wild type and other genotypes and "#" indicates significant differences within the wild type mouse groups. Data was analyzed using GLM-Univariate Analysis of Variance at $\alpha = 0.05$.

Results using tottering mice at P20 and P30 showed significantly reduced basal $[Ca^{2+}]_i$ in tottering mice CGC as compared to wild type ($P < 0.001$). However, no difference was seen in tottering and leaner CGC ($P = 0.376$). Basal $[Ca^{2+}]_i$ in CGC of

wild type at P10 was significantly reduced when compared to P20, P30 and P40 wild type CGC, however, no significant difference within genotype was observed in CGC of leaner and tottering mice.

After observing basal $[Ca^{2+}]_i$ in CGC of mutant mice, we looked at depolarization induced calcium transient in CGCs from leaner and wild type mice. KCl induced depolarization is very commonly used to observe calcium influx in CGCs (Nogueron et al., 2001; Ichikawa et al., 1998; Savidge and Bristow, 1997; Hartmann et al., 1995). We ran a control experiment to see if the observed changes in fluorescent intensity are due to intracellular calcium influx. Isolated CGCs were loaded with Fura-2AM and depolarized using KCl both in the presence and absence of calcium in the media (Fig. III-2).

Statistical analysis using one way ANOVA shows a significant increase in $[Ca^{2+}]_i$ in granule cells from both wild type and leaner mice depolarized with KCl in the presence of extracellular calcium ($p<0.001$, $n=20$). There was no significant increase in intracellular calcium in granule cells depolarized in the calcium free media ($p=0.999$, $n=12$). The time course of change $[Ca^{2+}]_i$ in following depolarization of CGC with KCl exhibits two phases (Nogueron et al., 2001). The first phase is a transient peak, which represents a combination of Ca^{2+} entry into the cells via a Ca^{2+} channels and intracellular Ca^{2+} release (Pocock et al., 1993). During the second phase i:e $[Ca^{2+}]_i$ plateau, reaches an equilibrium as a result of continued depolarization and continuous buffering (Werth and Thayer, 1994).

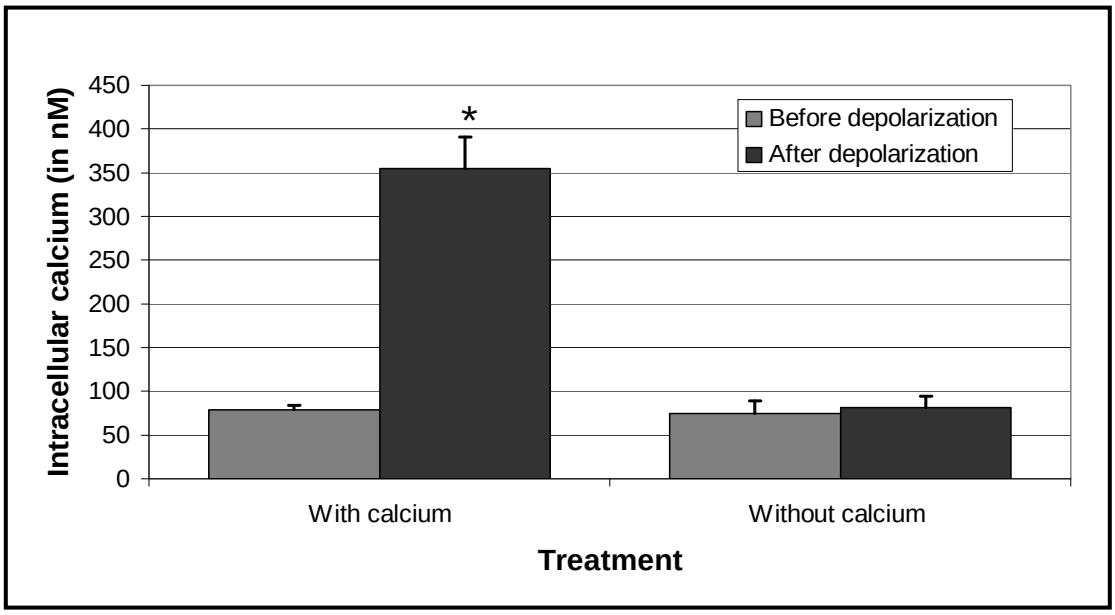

Figure III-2. Mean intracellular Ca^{2+} in CGCs loaded with Fura -2AM and depolarized with KCl both in the presence and absence of extracellular Ca^{2+}. A one way ANOVA shows significant increase in $[Ca^{2+}]_i$ after depolarizing the granule cells from both wild type and leaner mice in the presence of extracellular Ca^{2+} ($P<0.001$), However, there was no significant increase in Ca^{2+} transients after depolarizing granule cells in calcium free media. "*" indicates significant difference

Our experimental setup also showed two phases of Ca^{2+} depolarization (Fig III-3). We were interested only in the first phase, i:e. the calcium transient, when there is peak Ca^{2+} influx to understand the effect of leaner mutation on whole cell calcium currents in CGC. Figure III-4A shows representative photomicrographs of CGC from 20 day old wild type mice before and after depolarization. Only CGCs which showed both the initial peak and then plateau were used for data analysis. A GLM-univariate analysis showed no difference between genotypes at all the age groups. There was significant

difference in Ca^{2+} transients in CGC of 10 day old wild type as compared to CGC from 20, 30 and 40 day old wild type (Fig III-4B). Similarly, there were also significantly reduced calcium transients in CGC of 10 day old leaner mouse as compared to CGC from 30 and 40 day old leaner mice.

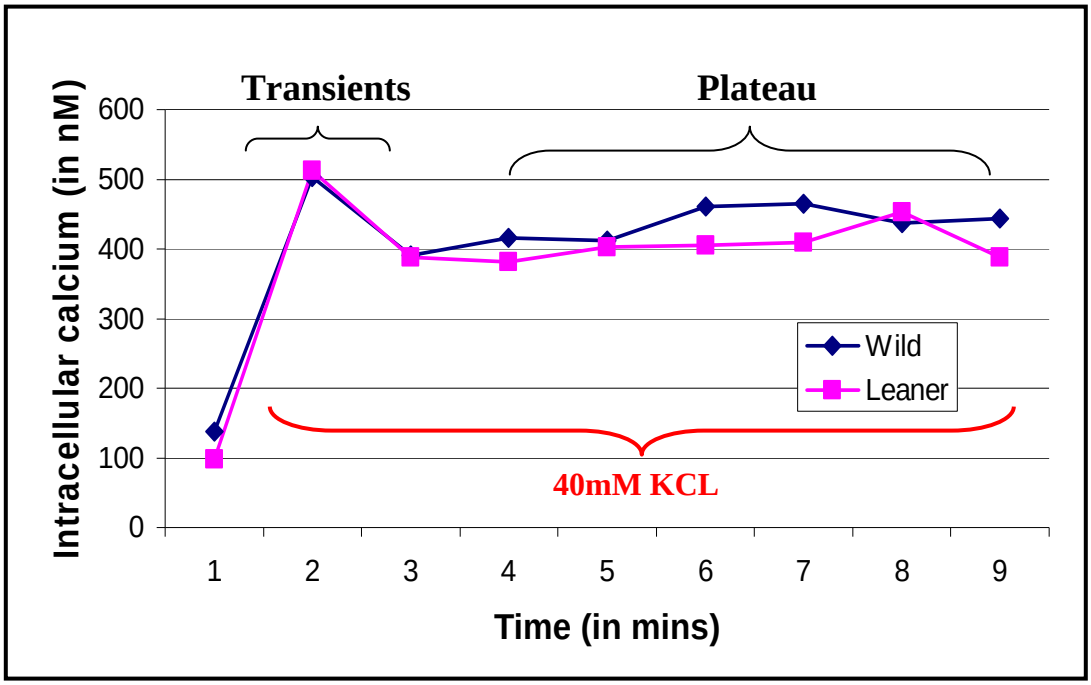

Figure III-3. The time course of change in calcium current following depolarization of granule cells with KCl has two phases. The first phase is a transient peak where there is combination of Ca^{2+} entry into the cell and intracellular calcium release and second phase is called the plateau, where Ca^{2+} reaches equilibrium due to continued depolarization. The time of KCl addition is indicated by the arrow (n=10 for leaner and 14 for wild type).

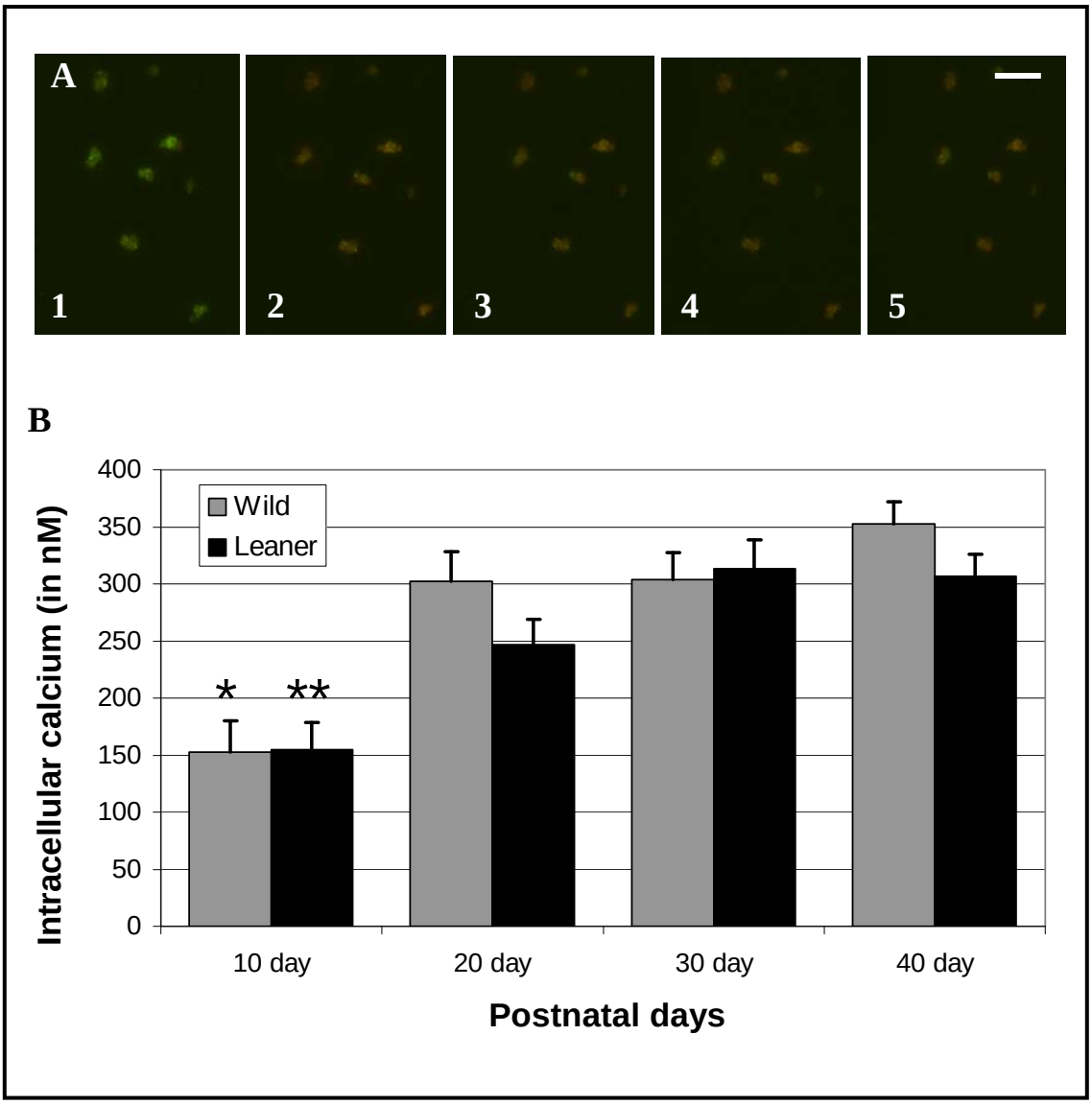

Figure III-4. Mean calcium transients in cerebellar granule cells of wild type and leaner mice during postnatal development. Panel A contains photomicrographs showing representative cerebellar granule cells at P20 from wild type mice before depolarization with KCl (1), and 0 minute (2), one minute (3), two minute (4) and three minute (5) after adding KCl. Scale bar in A is 10 µm. Panel B is a graph showing mean calcium transient data in leaner and wild type cerebellar granule cells after they were depolarized using 40mM KCl. There were no significant differences between wild type and leaner CGCs at all the age groups observed. However, Ca^{2+} transient in CGC from P10 wild type was different from the entire wild type group ("*", $P<0.05$) and Ca^{2+} transient in CGC from P10 leaner was different from P30 and P40 ("**", $P<0.05$).

Our results suggest that even though leaner CGCs have dysfunctional $Ca_V2.1$ calcium channels still there is no change in overall Ca^{2+} transients. This suggests that $Ca_V2.1$ calcium channels are not contributing a major portion of the whole cell calcium current in granule cells of leaner mice. To confirm this, we depolarized the CGCs in the presence and absence of specific $Ca_V2.1$ channel blocker, ω-Agatoxin IV A, which is known to block both the P- and Q- type of calcium current on the basis of different inactivation kinetics and sensitivity (Randall and Tsien, 1995).

Results using $Ca_V2.1$ channel specific blocker, ω-Agatoxin IV-A, showed a significant reduction in depolarization induced Ca^{2+} transients in CGC of 20 day old wild type mice. There was almost 40% reduction in Ca^{2+} transients in CGC of wild type mouse. ω-Agatoxin IV-A was not able to significant reduce depolarization induced Ca^{2+} transients in CGC of leaner mice (Fig III-5). Although, there was 17% reduction in agatoxin treated whole cell Ca^{2+} transients in CGC of leaner mice, this decrease was not significantly different from non agatoxin treated Ca^{2+} transients.

In the previous chapter we demonstrated reduced mitochondrial function in CGC of adult leaner mice as compared to age matched wild type and tottering mice. To continue that study during postnatal development, we assessed mitochondrial membrane potential (ψ_m) in CGCs of leaner and wild type mice during four age groups (P10, P20, P30 and P40). We have also compared our results with ψ_m data obtained from CGCs of tottering mice at P20 and P30. Figure II-6A shows representative photomicrographs of wild, leaner and tottering CGCs stained with TMRM. A GLM univariate analysis of variance along with Tukey's HSD post hoc analysis was conducted.

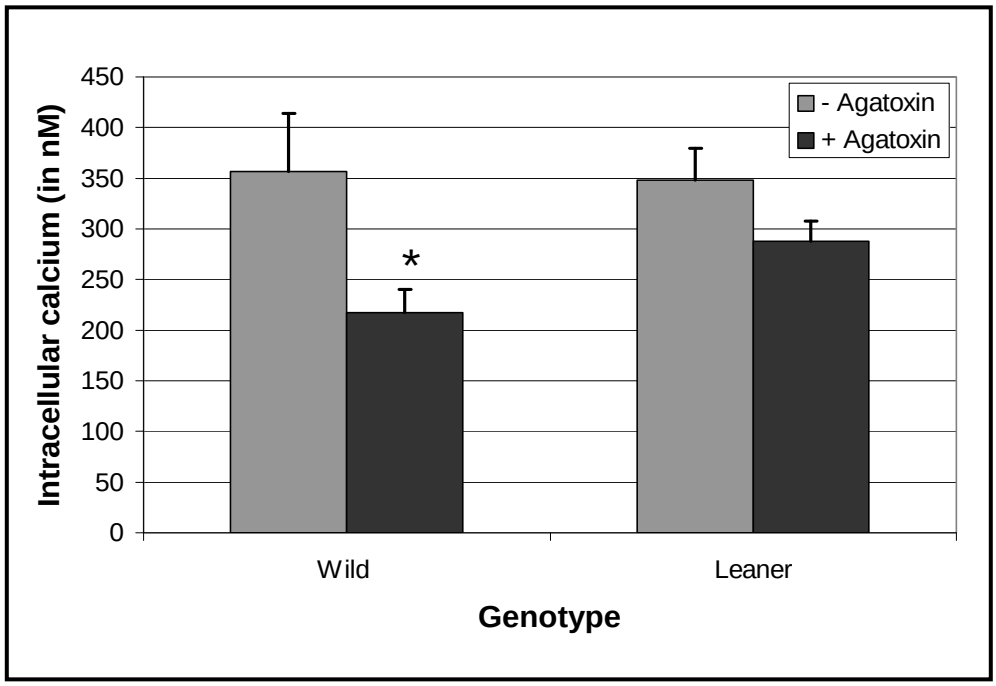

Figure III-5. Mean calcium transients data in leaner and wild type cerebellar granule cells after they were incubated in the presence and absence of ω-Agatoxin IV-A and depolarized with KCl. A GLM-univariate analysis of variance showed reduced calcium transients in only wild type but not leaner cerebellar granule cells after incubating with $Ca_V2.1$ channel specific blocker ω-Agatoxin IV A ($P<0.05$; n=30).

Starting from P10 we observed no difference in ψ_m in CGCs of leaner mice as compared to wild type mice (Fig. III-6). At P20 leaner mice showed reduced fluorescence intensity in TMRM stained CGCs as compared to age matched wild type and tottering mice, suggesting reduced ψ_m ($P<0.001$). Similarly, at P40 leaner CGCs showed reduced ψ_m as compared to wild type ($P<0.001$). However, at P30 there was no change in fluorescence intensity in leaner CGCs as compared to wild type and tottering

mice. Rather, the fluorescence intensity at P30 was significantly greater then observed at P20 and P40 in leaner mice (P<0.001).

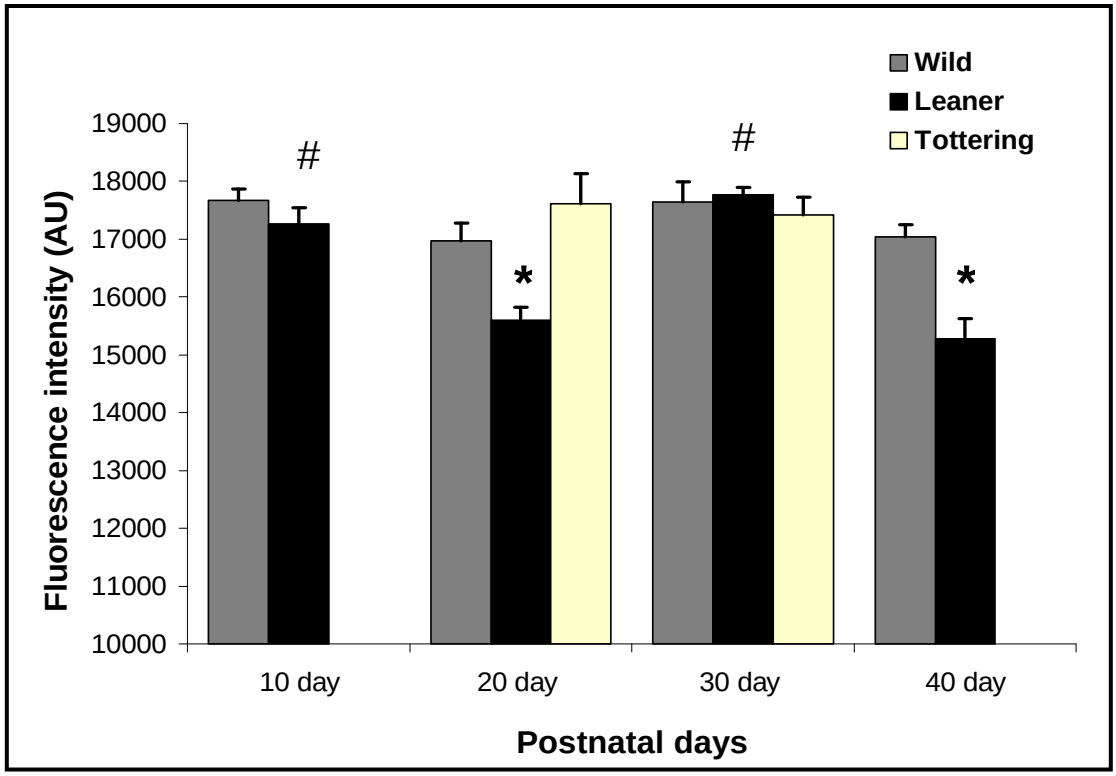

Figure III-6. Average mitochondrial membrane potential of CGCs during postnatal development. The graph indicates the mean ± SEM fluorescence intensity (FI) in arbitrary units (AU) for all three genotypes; n = 6 for each genotype. A GLM univariate ANOVA with post hoc test revealed no significant reduction in FI in CGCs from leaner mice at P10 as compared to wild type. Reduced FI was observed in CGCs from P20 as compared to both wild type and tottering mice (P<0.001). FI in leaner CGCs at P40 was also different from age matched wild type (P<0.001). Interestingly, P30 leaner mice were not significantly different from other two genotypes but they were different from P20 and P40 leaner mice (p<0.001). "*" indicate significant difference between genotypes and "#" shows significant different within genotype.

As mentioned previously, a reduced mitochondrial function could be due to either reduced overall cellular mitochondrial activity or reduced mitochondrial mass. To address this question we measured mitochondrial mass in leaner and wild type CGCs at P20. Mitochondrial membrane potential data demonstrated increased ψ_m at P30 as compared to P20 in leaner mice. This suggests that either the mitochondrial activity or mass is increasing at this age group. To understand this further we carried out mitochondrial mass measurements on CGCs from P30 leaner and wild type mice.

The mitochondrial mass was first assessed indirectly by quantifying cytochrome C expression whole cerebellum from P20 and P30 wild type and leaner mice. Cytochrome C is a ubiquitous, heme-containing protein that normally resides in the space between the inner and outer mitochondrial membranes (Newmeyer and Ferguson-Miller 2003). Since granule cells are the major cell type within the cerebellum, measurement of whole cerebellar cytochrome C expression by Western blotting would primarily reflect CGC cytochrome C expression. Western blot analysis done on total cerebellar protein revealed a 15kDa band (Fig. III-7B).

It was difficult to find an appropriate control 'housekeeping' protein, such as actin, to use for comparison between the mutant mice and control mice because many proteins utilize cytosolic Ca^{2+} ion concentration to regulate expression, and Ca^{2+} homeostasis is altered in cerebellar neurons of these mutant mice (Dove et al., 1998). Therefore, to ensure equal loading and transfer of protein, the gels and membrane were stained with Coomassie blue stain (Fig. III-7A).

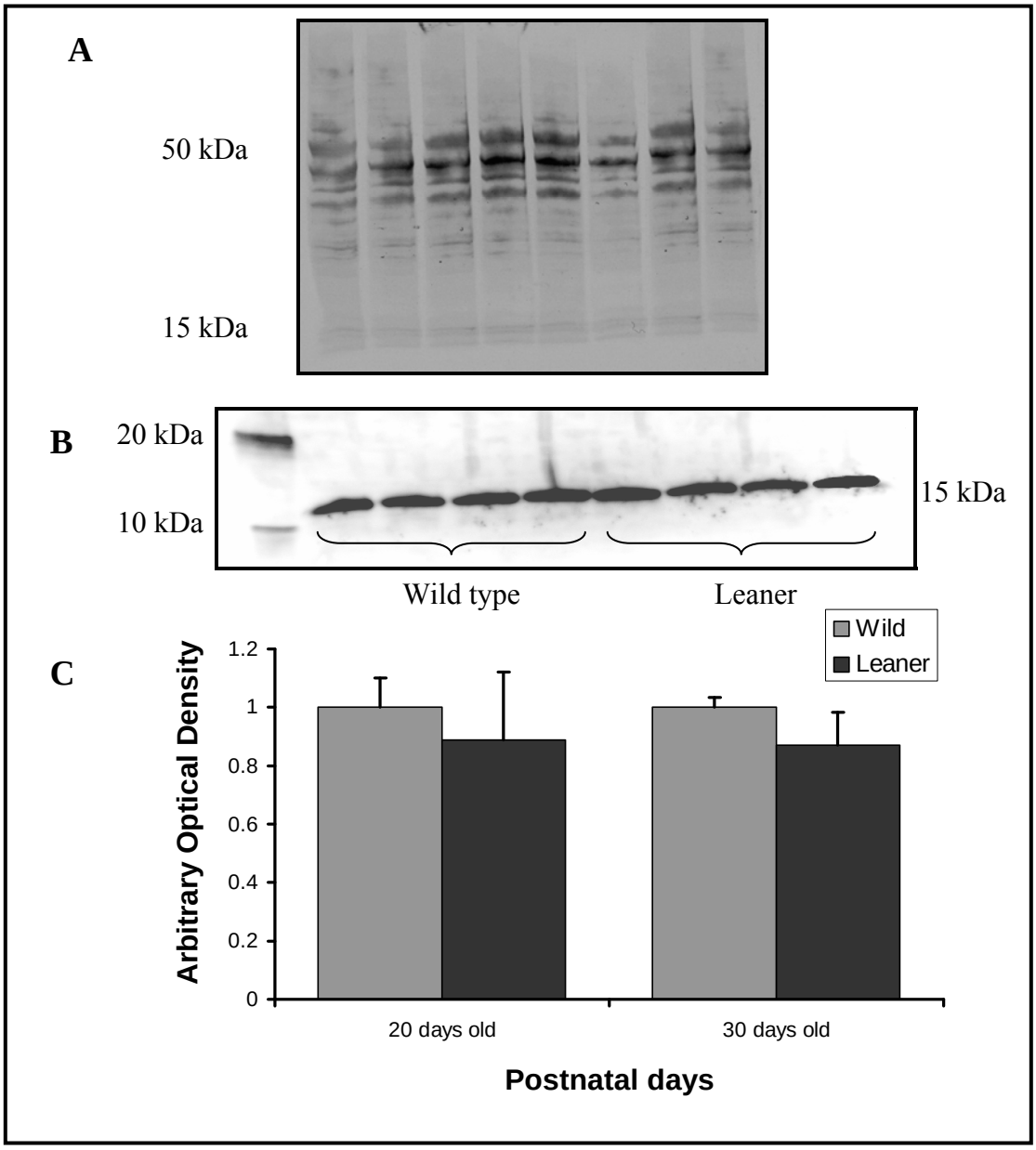

Figure III-7. Postnatal cytochrome C (Cyto C) protein expression in wild type and leaner whole cerebella. Panel A is the Coomassie-stained membrane following Western blotting. Panel B is a representative Western blot for Cyto C, which is a 15-kDa protein. Panel C is a graph of densitometry of the Cyto C bands from Western blotting of whole cerebella. Densitometry was calculated by determining the integrated density value of Cyto C bands from Western blotting using AlphaEase FC software. Western blotting with densitometry was repeated three times with consistent results. A GLM-univariate analysis of variance showed no significant difference in Cyto C expression between genotypes and age. Error bars indicate standard error of the mean.

Densitometric analysis performed on the immunoreactive bands did not reveal any significant difference in optical density between the three genotypes (Fig. III-7C), suggesting no difference in whole cerebellar cytochrome C expression of leaner, tottering and wild type mice. This experiment was conducted in triplicate and similar results were for each replica.

The second method used to measure mitochondrial mass was the direct estimation of cardiolipin content of individual CGCs at P20 and P30 in both leaner and wild type mice. Cardiolipin is a major phospholipid of mitochondrial membranes. Acutely isolated CGCs were incubated in 50 μm NAO and exposed to excitation of 488 nm. A GLM univariate analysis of Variance indicated no significant difference of fluorescence intensity emitted by CGCs between genotypes and postnatal days (Fig. III-8), indicates no difference in the cardiolipin content.

The above data suggest a reduced mitochondrial function in leaner CGCs, which coincides with peak cell death observed in these mice. Generation of reactive oxygen species (ROS), through the electron transport chain attached to the inner mitochondrial membrane, is a part of normal cellular function. However, mitochondrial dysfunction may lead to increased generation of ROS and subsequent ROS mediated cell death. Cell damage due to ROS formation has been associated in the pathophysiology of many neurologic disorders and mitochondrial dysfunction associated with loss of calcium ion homeostasis has been implicated in generation of superoxide radicals (Rego and Oliveira, 2003). To understand this further we looked for generation of ROS in CGC of wild type and leaner mice at P20 and P30. CGCs were acutely isolated and the ROS

levels were measured based on analysis of the intensity of fluorescence of CM-H_2DCFDA dye using sequential time course fluorescent image capture (Fig. III-9A). A GLM-univariate analysis of variance revealed no significant difference in fluorescent intensity of CM-H_2DCFDA dye in CGCs from two genotype and two age groups studied. A GLM Repeated measures test and the Tukey's HSD post hoc test indicated no significant difference in fluorescent intensity with regard to time course sequential analysis (n=4; Fig. III-9B).

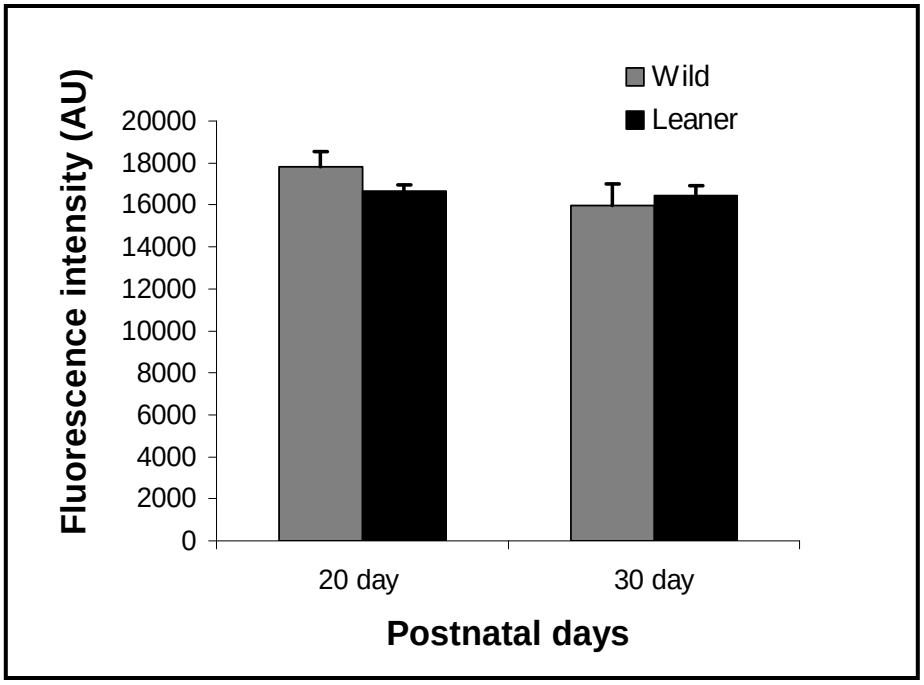

Figure III-8. Mitochondrial phospholipids, cardiolipin content in cerebellar granule cells of wild type and leaner mice. The graph indicates the mean ± SEM fluorescence intensity in arbitrary units (AU) for all three genotypes; n = 4 for each genotype. A GLM-univariate analysis of variance showed no significant difference in cardiolipin content between genotypes and age. Error bars indicate standard error of the mean. Images were adjusted for brightness and contrast using Adobe photoshop 7.0.

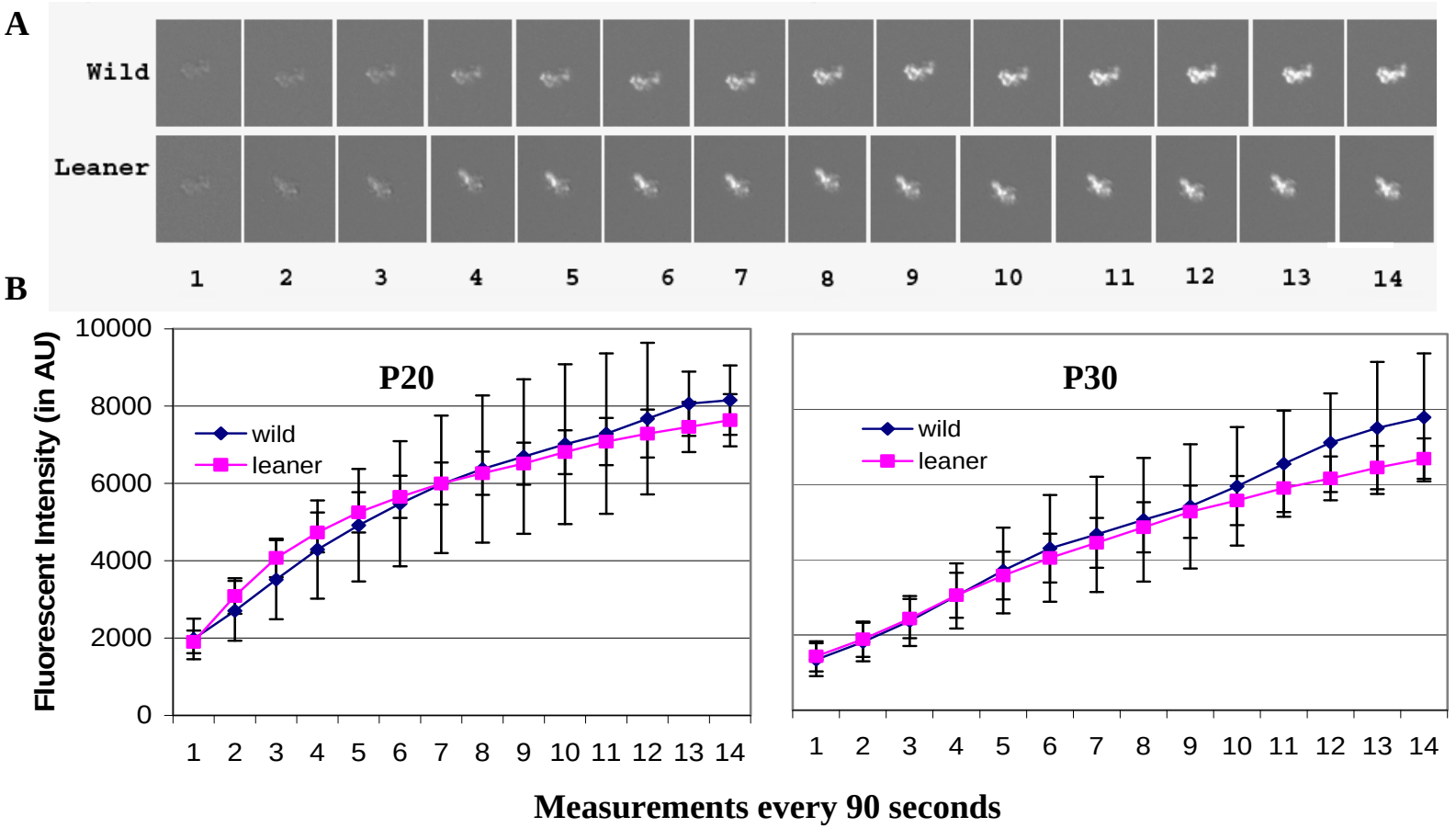

FIGURE III-9. Reactive oxygen species (ROS) measurement in cerebellar granule cells during postnatal development. Panel A contains photomicrographs showing acutely isolated cerebellar granule cells loaded with CM-H_2DCFDA dye. Images were adjusted for brightness and contrast using Adobe photoshop 7.0. Scale bar is 10 μm. Panel B shows the total cellular ROS levels in cerebellar granule cells from 20 and 30 day old wild type and leaner mice. GLM – repeated measure analysis and Tukey's post hoc test indicated no significant difference in generation of ROS in CGC of wild type and leaner mice at P20 and P30.

DISCUSSION

The developing leaner cerebellum undergoes excessive granule cell death that peaks at P20 and apoptosis is the primary mechanism of cell death (Lau et al., 2004). It has been shown previously that CCG death in leaner mice is apparently not due to altered expression and/or localization of the mutated voltage-dependent Ca^{2+} channel $\alpha_1$2.1 subunit mRNA or protein (Lau et al., 1998). However, mutations in Ca_V2.1 channels can lead to alterations in intracellular Ca^{2+} homeostasis, which could be the primary reason for leaner granule cell death. Also, according to the gene expression profile done on leaner mice at the peak cell death stage, there is altered expression of apoptosis and mitochondrial function related genes (Nahm, 2002).

It is also known that alteration in Ca^{2+} homeostasis can lead to mitochondrial mediated cell death (Nicholls and Ward, 2000). We have looked at the basal $[Ca^{2+}]_i$ as an index of Ca^{2+} homeostasis and mitochondrial functional activity in CGCs of leaner mice during postnatal development. At postnatal day (P) 10 no difference was observed in basal $[Ca^{2+}]_i$ between wild type and leaner CGCs. However, the basal $[Ca^{2+}]_i$ was significantly lower in P10 wild type CGCs as compared to other age groups of wild type (Fig. III-2B). This could be due to the developmental expression of various voltage gated calcium channels and their subunits. Although, the α_{1A} subunit is expressed in CGCs of P7 rat cerebellum, it is most evident at P14 (Tanaka et al., 1995). Similarly, the expression of the β4 Ca^{2+} channel subunit in CGCs of rat cerebellum is most evident between P7-P14 (Tanaka et al., 1995). Coexpression of α_{1A} and β subunits increases the

magnitude of whole-cell barium current and shifts the voltage-dependent properties of the currents (Stea et al., 1994). It is likely that the reduced basal $[Ca^{2+}]_i$ observed in P10 wild type CGCs is a developmental pattern, since the expression of α and β subunits of $Ca_V2.1$ Ca^{2+} channel is most evident after P10 and their coexpression is required for proper channel functionality.

Starting from P20 onwards CGCs from leaner mice exhibited a reduced basal $[Ca^{2+}]_i$ as compared to age matched wild type mice. In contrast, the basal $[Ca^{2+}]_i$ levels in leaner Purkinje cells are not different from age-matched wild type Purkinje cells (Dove et al., 1998). However, CGCs of tottering mice also showed reduced basal $[Ca^{2+}]_i$ levels as compared to wild type CGCs, while the level was not different from leaner CGCs. Since the CGCs from tottering mice do not show any excessive neuronal cell death (Isaacs and Abbott, 1995), this is suggestive that reduced basal $[Ca^{2+}]_i$ alone can not be directly responsible for neuronal cell death in leaner CGCs. Therefore, we looked at depolarization induced Ca^{2+} transients in CGCs during postnatal development. We found no difference in KCl induced Ca^{2+} transients in CGCs of leaner and wild type mice at all the age groups observed (Fig III-5B).

A reduced Ca^{2+} transient was observed in CGCs of P10 wild type as compared to the rest of the age groups. The developmental changes observed in Ca^{2+} current are relevant to the processes of granule cell maturation and excitability. Our result is in line with large body of evidence suggesting Ca^{2+} currents are lower in immature granule cells (Cull-Candy et al., 1989; Rossi et al., 1994; Randall & Tsien, 1995; D'Angelo et al., 1997). At P10, CGCs from leaner mice showed the same pattern as CGCs from wild

type mice except, unlike wild type CGCs, leaner CGCs showed no difference in Ca^{2+} transients between P10 and P20 (Fig. III-5B). This suggests either delayed maturation of CGCs or developmental defects due to $Ca_V2.1$-type channel mutation in leaner mice.

No significant differences were noted in Ca^{2+} transients between leaner and wild type CGCs following KCl induced depolarization. This suggests that either there is a possible functional compensation by other VGCCs for dysfunctional $Ca_V2.1$ channels or reduced Ca^{2+} buffering in CGCs such that the Ca^{2+} influx that does take place in leaner CGCs is not buffered efficiently, leading to increased Ca^{2+} transients. Another possibility is the presence of both of the above mentioned mechanisms. We have observed decreased calretinin expression, the major Ca^{2+} binding protein, in leaner CGCs as compared to age-matched wild type granule cells (Nahm et al., 2002) and this reduction in calretinin expression in leaner granule cells may exaggerate the response to K^+-induced $[Ca^{2+}]_i$ increase due to lower Ca^{2+} buffering capacity.

To understand if there is compensation for the defective $Ca_V2.1$ channels by other VGCCs in leaner mice, we used specific $Ca_V2.1$ channel blocker, ω-Agatoxin IVA. There was a significant reduction (40%) in Ca^{2+} transients in wild type CGCs, but not in leaner CGCs. Our data are in agreement with a previous report that approximately 45% of the Ca^{2+} current in cerebellar granule cells can be accounted for by $Ca_V2.1$ VGCCs (Randall and Tsien, 1995). Although, a 17% reduction in Ca^{2+} transients was observed in leaner CGCs after blocking with ω-Agatoxin IVA, this difference was not statistically significant. This suggests that there is a functional compensation for $Ca_V2.1$ calcium channels by other VGCCs. The types of channels that are compensating for

dysfunctional $Ca_V2.1$ channels in leaner CGCs are not known. However, Etheredge et al. (2007) recently reported functional upregulation of Ca_V1 channels to compensate for reduced $Ca_V2.1$ channel function in basal forebrain neurons from leaner mice. Like CGCs and unlike Purkinje cells, basal forebrain neurons possess the full complement of Ca^{2+} channel subtypes (Griffith et al., 1994). Similarly, $Ca_V2.2$ (N-type) channels have been shown to compensate for reduced P-type function in tottering mice (Leenders et al., 2002; Matsushita et al., 2002; Zhou et al., 2003).

T-type calcium channel α1G subunit is shown to be differently regulated in leaner cerebellar Purkinje and granule cells (Nahm et al., 2004). While cerebellar Purkinje cells show increased α1G subunit expression, the granule cell layer shows decreased α1G subunit expression (Nahm et al., 2004). $Ca_V2.1$ Ca^{2+} calcium channel null mutant mice also showed increased calcium influx thru Ca_V1 and $Ca_V2.2$ Ca^{2+}channel in cerebellar Purkinje cells but not in granule cells (Jun et al., 1999). Thus, it seems that the genetic alteration in $Ca_V2.1$ Ca^{2+} channels is causing different consequences in calcium channel expression and functions of cerebellar Purkinje and granule cells.

Mitochondria play an important role in maintaining Ca^{2+} homeostasis, which when disturbed, can lead to significant cellular pathophysiology and cell death. At the time of peak CGC death in leaner mice we observed reduced mitochondrial membrane potential ($\psi_{m)}$, which was significantly reduced as compared to wild type and tottering CGCs. This substantiates previous findings from our lab which demonstrated increased

expression of apoptosis and mitochondria associated genes at peak cell death in CGCs of leaner mice (Nahm, 2002). Although a reduced ψ_m was observed at P40, we noticed no change in ψ_m at P30 in CGCs from leaner mice as compared to age matched wild type mice. Althougth the reason for increased ψ_m after peak cell death is not known, it could be compensatory mechanism to regulate cellular energy level.

We further investigated to see if this decreased and increased ψ_m observed at P20 and P30 respectively is due to change in cellular mitochondrial activity or mass. The first method employed Western blotting to quantify expression of the inner mitochondrial membrane protein, cytochrome C. The second method was direct estimation of the mitochondrial phospholipid, cardiolipin, in acutely isolated, live CGCs. Both experiments indicated no change in mitochondrial mass of CGCs from P20 and P30 wild type and leaner mice. However, we have yet to elucidate additional molecules involved in this specific cell death cascade.

Oxidative stress is known to be involved in the pathogenetic mechanism of many neurodegenerative disorders including excitotoxicity, Alzheimer's disease and Parkinson’s disease (Butterfield et al., 2002; Floyd and Hensley, 2002; Jenner 2003; Facheris et al., 2004). We determined whether the mitochondrial stress demonstrated by loss of ψ_m leads to increased oxidative stress in leaner CGCs. Total cellular ROS levels were determined in P20 and P30 leaner and wild type CGCs using CM-H_2DCFDA dye. Our results showed no change in generation of ROS in CGCs of leaner mice compared to wild type CGCs at both P20 and P30. Our experiments suggest a mitochondrial

mediated but ROS independent cell death in CGCs of leaner mice. ROS have complex chemical and physiological properties in normal mitochondrial and cell functioning. Schulz et al. (1996) demonstrated that ROS are essential mediators of K^+ deprivation-induced apoptosis of cerebellar granule neurons because neuronal death was blocked by superoxide dismutase. However, Boldyrev et al (2004) showed that cell death in CGCs acutely exposed to Amyloid-β was independent of ROS generation. Vergun et al. (2001) suggested that accumulation of ROS during toxic glutamate challenge in hippocampal neurons was not a prerequisite for altered Ca^{2+} homeostasis and/or the observed collapse of mitochondrial membrane potential. It also has been noted that polychlorinated biphenyls at doses that rapidly kill acutely isolated rat CGCs do not cause increased ROS generation (Tan et al., 2004). Thus, it is the case that ROS exist in a state of dynamic equilibrium and excess ROS can result in fatal consequences for affected cells (Zorov et al., 2005) but cell death also can take place independent of excess ROS.

In conclusion the early development in leaner CGCs is normal as no differences were observed in mitochondrial activity and intracellular calcium concentration at P10. Our results have substantiated previous experiments in our lab which suggest a mitochondrial mediated cell death in leaner mice. We have now shown that mitochondrial activity is compromised in leaner CGCs but at the same time there is no generation of ROS. Even though the CGCs from leaner mice have dysfunctional $Ca_V2.1$ channels, no change in calcium transients were observed. This suggests functional compensation for $Ca_V2.1$ channel by other VGCCs. This observation was further supported by using a specific $Ca_V2.1$ channel blocker. Thus, elucidating mechanism

responsible for compensating $Ca_V2.1$ channel dysfunction in the leaner mouse will be important.

CHAPTER IV

ASSESSMENT WHETHER INCREASED CALCIUM INFLUX IN CULTURED GRANULE CELLS CAN ELIMINATE OR REDUCE THE CELL DEATH

OVERVIEW

A sustained level of cytosolic calcium is crucial for neuronal survival. The leaner mutation results in reduced calcium transients through Ca_V 2.1 channels. Reduced calcium transients through Ca_V 2.1 channels are compensated in cerebellar granule cells (CGC) by increased influx through other voltage gated calcium channels. Also, the leaner mutation results in truncation of the carboxy terminal of Ca_V 2.1 voltage gated calcium channel (VGCC), which can regulate gene expression. Neurodegeneration in leaner mice seems to be occurring either due to decreased intracellular calcium transients or due to the defective Ca_V2.1 channel protein, which results in an altered protein-protein interaction at the C-terminus triggering a lethal cascade of altered gene expression. In this study we have assessed whether increased calcium influx in cultured CGCs can eliminate or reduce cell death. Cerebellar slices from 10 day old wild type and leaner mice were cultured under conditions of both physiological and increased extracellular calcium. After 10 days *in vitro*, cerebellar slices were fixed and granule cell death was quantified using Fluoro-Jade staining. Under the condition of physiological levels of extracellular calcium, CGCs from wild type and leaner mice showed no

significant difference in neuronal cell death. Thus, we were not able to replicate the *in vivo* cell death difference between wild type and leaner CGCs in our *in vitro* explant culture. In the presence of increased extracellular calcium we observed a significantly reduced CGC death in both wild type and leaner cerebellar slice. This finding supports other studies, which showed a reduced cell death in mouse CGCs cultured in increased extracellular calcium.

INTRODUCTION

Neuronal survival has been correlated with a sustained level of cytosolic calcium in several neuronal models such as rat sympathetic neurons (Koike et al., 1989), chick ciliary ganglia (Collins et al., 1991), dorsal root ganglion neurons (Eichler et al., 1992) and developing cerebellar granule cells (CGC) (Gallo et al., 1987; Pearson et al., 1992b). It has been established that CGC when cultured chronically under physiological concentrations of potassium (5mM) for more than 5 days in vitro, die, exhibiting biochemical and morphological features of apoptosis (Moran and Rivera-Gaxiola, 1992; D`Mello et at., 1993). Therefore, CGC are typically cultured with high concentrations of potassium leading to chronic depolarization of CGC. Since entry of Ca^{2+} into neurons through voltage gated calcium channels is the principal means by which changes in membrane potential can influence intracellular events, the most likely mechanism by which chronic depolarization exerts its effect on neuronal survival is by activating Ca^{2+} channels. Gallo et al. (1987) demonstrated that high concentrations of potassium

depolarizes CGCs leading to opening of voltage gated calcium channels and hence increased resting $[Ca^{2+}]_i$. Several pieces of evidence suggest that chronic depolarization caused by elevated concentrations of potassium, rather than potassium ions per se, is responsible for survival promoting effects, as other depolarizing agents have also been successfully used to promote survival of CGC (Gallo et al., 1987; Pearson et al., 1992a).

Increased Ca^{2+} after depolarization mimics some of the signaling events such as proliferation, migration, maturation and activation of downstream molecules like Ca^{2+}/calmodulin dependent calcineurin phosphatase (Sato et al., 2005). Calcineurin is a serine/threonine phosphatase whose activation requires increased availability of intracellular calcium and leads to dephosphorylation of various transcription factors, which alter the gene expression (Rusnak and Mertz, 2000). Decreased calcium influx may lead to decreased activation of calcineurin resulting in altered development and synaptic organization of granule cells during postnatal period. Similarly, other signaling molecules that are dependent on intracellular calcium including Ca^{2+}/calmodulin-dependent protein kinase type IV, which is highly enriched in the nucleus and thought to be critical for improved survival (Tremper-Wells and Vallano, 2005).

The leaner mouse carries an autosomal recessive mutation at $\alpha_1$2.1 gene, which encodes the pore forming subunit of Ca_V 2.1 or P/Q-type VGCCs (Westenbroek et al., 1995; Dove et al., 1998; Wakamori et al., 1998; Lorenzon et al., 1998). The main effect of the mutation is alteration in Ca_V2.1 channel activity as shown by Purkinje neurons in the form of reduced Ca^{2+} currents. It is shown that the open probability of Ca_V2.1 type calcium channels is reduced threefold and therefore decreasing the amount of overall

Ca^{2+} entering leaner Purkinje cells (Dove et al., 1998; Lorenzon et al., 1998; Wakamori et al., 1998). However, in chapter III we showed no difference in depolarization induced calcium influx in CGCs of leaner mice as compared to age matched wild type CGCs. This suggests that other voltage gated calcium channels (VGCC) are compensating for dysfunctional Ca_V 2.1 channels atleast in CGC, which was also confirmed using ω-Agatoxin IVA, a specific Ca_V 2.1 channel blocker.

The leaner mutation results in truncation of the carboxy terminal of the α_1 2.1 protein giving rise to two $\alpha_1$2.1 splice variants (Fletcher et al., 1996). The $\alpha_1$2.1 C-terminus participates in a number of protein–protein interactions and plays a prominent role in modulating channel activity (Walker and De Waard, 1998). The C-terminus of Ca_V 2.1 VGCC has regulatory sites which are modulated by G-protein coupled receptor Gβγ subunits (Hille, 1994; Herlitze, et al., 1996; Qin et al., 1997; Ikeda and Dunlap, 1999) and a site for Ca^{2+}- calmodulin binding (Lee et al., 1999). Recently, it was shown that the C-terminus of the $\alpha_1$2.1 subunit of the Ca_V2.1 VGCC is cleaved from the full-length protein and translocated to the Purkinje cell nucleus (Kordasiewicz et al., 2006). It is speculated that this C-terminus may be required for survivability and its alteration in leaner mice may be the reason for cell death (Kordasiewicz et al., 2006). It seems that either the decreased intracellular calcium or calcium influx is directly leading to neurodegeneration or the defective Ca_V2.1 channel protein is causing an altered protein-protein interaction at the C-terminus triggering a lethal cascade of altered gene expression.

Nevertheless, if decreased calcium currents are indeed responsible for neurodegeneration, than culturing CGCs along with chronic depolarization should be able to rescue CGCs from cell death in leaner cerebellum. To answer this question we have cultured cerebellar slices in a high potassium environment to achieve chronic depolarization. After culturing cerebellar slices for 10 days, Fluoro-Jade staining was used to quantify the cell death in granule cells.

MATERIALS AND METHODS

Animals

Wild type (+/+) and homozygous leaner (tg^{la}/tg^{la} or $Cacna1a^{tg\text{-}la}$) mice on an inbred C57BL/6J background were used. All mice were bred and housed at the Comnparative medicine program facility at Texas A&M University. Homozygous leaner pups started to show ataxia around postnatal day 12 (P12). As a result of their neurological deficits, these mice have limited ability to move about the cage and adequately access food and water, which increases their mortality due to hypothermia and dehydration. To increase their survival rate all homozygous leaner mice were supplemented with moistened rodent chow starting at P17-18. Additionally, since homozygous leaner females do not nurture their pups well, homozygous leaner pups were fostered to lactating Swiss White Webster mice at the age of P0 to P1. Male and female wild type and homozygous leaner mice at postnatal day 10 were used for the experiment. Animals were maintained under a 12hr light/dark photoperiod with a

constant room temperature (21-22^{o}C) and provided with access to food and water *ad libitum*. Procedures for animal use were approved by the Texas A&M University Laboratory Animal Use Committee and carried out in accordance with the National Institutes of Health Guide for the Care and Use of Laboratory Animals (National Institutes of Health Publication No. 85-23, revised 1996).

Organotypic slice culture

For cultured cerebellar slices, P10 mice were anesthetized with isoflurane and exsanguinated by cutting the heart. The brains were then removed using sterile surgical technique (Miranda et al., 1996; McAlhany et al., 1997; Cheema et al., 2000) and the cerebella were sectioned coronally at 350 μm in ice cold dissection media containing 36mM glucose, 10mM MgCl2·6H2O in Gey's balanced salt solution (Sigma-Aldrich, St. Louis, MO, USA) on an Electron Microscopy Sciences (EMS) tissue slicer (OTS-4000, Hatfield, PA, USA). The whole cerebellum of each mouse was sectioned and cultured.

The cerebella were placed on Millicell organotypic inserts (PICM ORG 50, Millipore, Bedford, MA, USA) in sterile six well plates (Falcon, BD Biosciences, Franklin Lakes, NJ, USA). Culture media containing 50% Basal Media Eagle with Earle salts (Gibco, Carlsbad, CA, USA), 22.5% Hank's balanced salts (Gibco, Carlsbad, CA, USA), 25% heat inactivated horse serum (Sigma-Aldrich, St. Louis, MO, USA), 36mM glucose (Sigma), 1 mM glutamine (Sigma) and 50 μg/mL vitamin C (Sigma) was changed every 3 days for the duration of the culture. Additionally, slices which were

cultured under chronic depolarization were exposed to 25mM of KCl through out the culture period. Slices were kept in a humid incubator at 37°C and 5% CO2 for 10 days, the equivalent of approximately P20 *in vivo*.

Fluoro-Jade staining

Slices from 6 wild type and 6 homozygous leaner mice were cultured either in the presence of or absence of chronic depolarization. After 10 days of culturing, slices were fixed in 4% paraformaldehyde in 0.12 M phosphate buffer (pH 7.4) overnight in the refrigerator, and then washed in 0.1 M phosphate buffered saline. The membrane of Millicell organotypic inserts having cerebellar slices was cut and laid upside down on the microscopic slides. The slides were left overnight in incubator at 37^{o}C. Membranes were peeled off while the slices remain adherent to the slides. The Fluoro-Jade staining procedure is same as described in chapter I with certain modifications. The slices were immersed in distilled water for 1 min and transferred to a 0.06% potassium permanganate solution for 15 minutes on a rotating platform. Slides were then washed in deionized water for 1 minute and incubated in 0.001% Fluoro-Jade (Histo-chem Inc., Jefferson, AR, USA) in deionized water with 0.1% acetic acid for 30 minutes on a rotating platform.

After staining with Fluoro-Jade, slices were rinsed with three 1-minute changes of deionized water, dried thoroughly in a hot-air stream, immersed in xylene and coverslipped using DPX mounting media (EMS, Fort Washington, PA, USA). Paraffin embedded testes sections were used as positive control. Sections were examined under

epifluorescence microscope using FITC filter. Fluorescent images were acquired using a Zeiss Axioplot 2 research microscope (Carl Zeiss, Inc., Thornwood, NY, USA) equipped with a three-chip Hamamatsu video camera.

Cell counting

The slides were evaluated both under bright field and fluorescence (using a fluorescein filter). The bright field images were captured using Nikon digital camera DXM1200 attached to Nikon E400 microscope. Area measurement on bright field images was carried out using Image J (1.36b) (NIH, USA) software by researcher unknown to the genotype. Only areas that were definitively identified as granule cell layers were used for data analysis. Fluoro-Jade positive CGCs were counted on images acquired using Zeiss Axioplot 2 research microscope, using fluorescein filter, without knowing the genotype of the mouse from which the images were obtained. Fluorescence images of same area were taken using bright field images as reference. Only the CGC area marked in bright field images were used for counting Fluoro-Jade positive cells and statistical analysis. The number of Fluoro-Jade positive CGCs per unit area was calculated for each genotype and treatment.

Statistics

Data are presented as means ± standard error of mean. All data were analyzed using statistical software SPSS Version 12.0.1 for windows. General Linear Model (GLM) - Univariate Analysis of Variance (ANOVA) at $\alpha = 0.05$ was used to analyze

data. After identifying an overall significant difference in model the genotype and treatment differences were interpreted using the Tukey's honest significant difference (HSD) post hoc test.

RESULTS

The leaner mutation in $\alpha_1 2.1$ gene, which encodes the pore forming subunit of Ca_V 2.1 channel, leads to alteration in channel activity in the form of reduced Ca^{2+} currents (Westenbroek et al., 1995; Dove et al., 1998; Wakamori et al., 1998; Lorenzon et al., 1998). If reduced Ca^{2+} currents were directly responsible for neurodegeneration observed in leaner cerebellum then long term increased calcium influx should reduce or rescue the cell death in leaner cerebellum.

To investigate this further, *in vitro* organotypic cerebellar culture were used to determine the dependence of leaner cerebellar granule cell death on reduced Ca^{2+} currents. Wild type and leaner organotypic cerebellar slices cultures were established at P10 and maintained for 10 days both in the presence and absence of KCl induced calcium influx, until the peak of leaner granule cell death, equivalent of approximately P20 *in vivo*. Cell death was quantified using Fluoro-Jade staining. The number of dead cells per unit area was established by measuring area in bright field and then counting Fluoro-Jade positive cells in the same area under fluorescein, fluorescence (Fig. IV-1).

GLM - Univariate Analysis of Variance ($\alpha = 0.05$) showed no difference in Fluoro-Jade positive cerebellar granule cells per unit area in leaner cerebellar slices

cultured as compared to wild type. However, cerebellar slices cultured in increased extracellular KCl showed reduced cell death in both wild type and leaner cerebellar slices (Fig. IV-2).

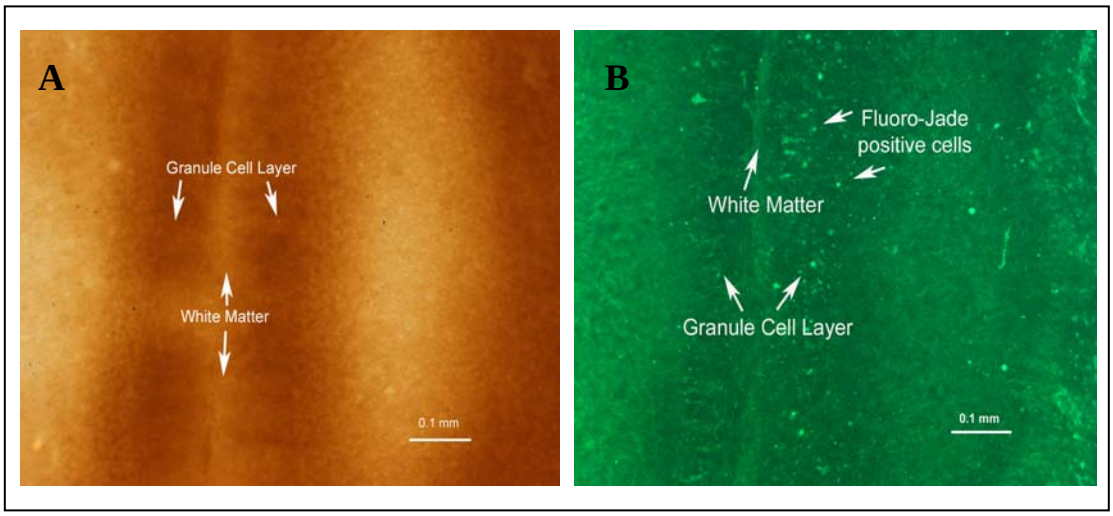

Figure IV-1. Photomicrographs of cerebellar slices after 10 days in culture. A and B are the same field of view captured under different light sources, bright field (A) and FITC fluorescence for Fluoro-Jade (B). Scale bar is 0.1 mm (Images taken by Christine McCoy)

DISCUSSION

Developing cerebellar granule cells require sustained levels of cytosolic calcium for its survival (Gallo et al., 1987; Pearson et al., 1992b). In chapter III we showed that unlike leaner cerebellar Purkinje cells (Dove et al., 1998; Lorenzon et al., 1998; Wakamori et al., 1998) leaner cerebellar granule cells (CGC) did not show reduced cellular calcium currents. We also showed that there is functional compensation of Ca_V

2.1 channels by other voltage gated calcium channels (VGCC). These experiments suggested that reduced calcium influx cannot be directly related to CGC in leaner mice. However, to substantiate our results we cultured cerebellar slices for 10 days with increased calcium influx and looked at CGC death. We hypothesized that if reduced calcium influx is leading to cell death then culturing cerebellar slices with increased calcium influx will reduce or rescue cell death.

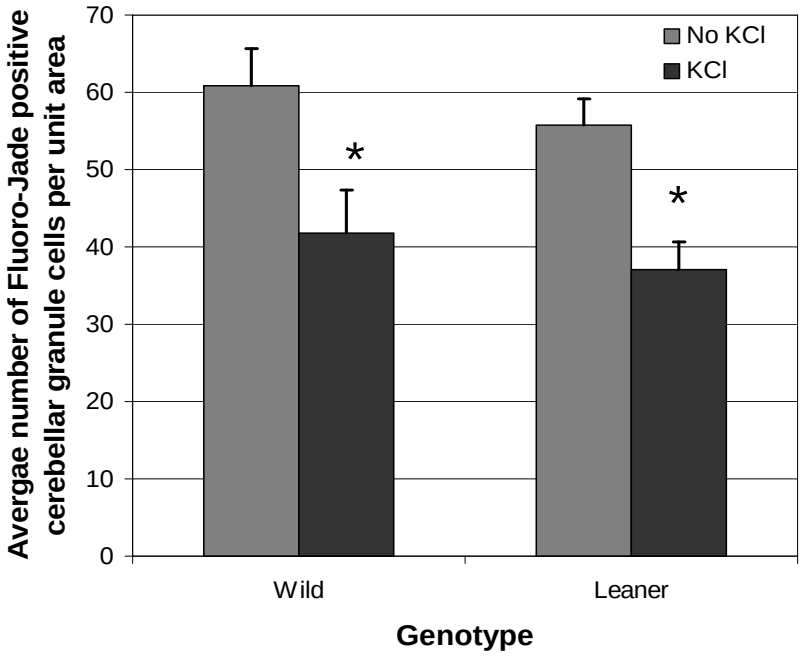

Figure IV-2. Cell death observed in wild type and leaner cerebellar slices after 10 days *in vitro.* Graph representing average number of Fluoro-Jade positive cerebellar granule cells in leaner and wild type cerebellar slices after 10 days of culture. A GLM univariate analysis of variance showed no significant difference in cerebellar granule cell death in leaner and wild type after 10 days *in vitro.* However, culturing cerebellar slices in increased extracellular KCl was able to significantly reduce cerebellar granule cell death in both wild type and leaner cerebellar slices ("*", $P<0.05$).

We used KCl to induce chronic depolarization. It has been shown previously that high concentrations of potassium depolarize CGCs and results in calcium influx via opening of voltage gated calcium channels (Galo et al., 1987; Franklin and Johnson, 1992).

We expected the *in vivo* CGC death pattern to be replicated in our *in vitro* explant cerebellar slices. However, our results showed no difference in granule cell death in leaner cerebellar slices as compared to age matched wild type cerebellar slices. This suggests that leaner CGC death in culture condition is occurring via a mechanism different from that observed *in vivo*. However, a plethora of evidence suggests that CCG death in culture is mainly due to apoptosis (Didier et al., 1989; Yan et al., 1994; Galli et al., 1995; Schulz et al., 1996; Ichikawa et al., 1998; Tabuchi et al., 2000) and we also know that CGC death in the leaner cerebellum during postnatal development also occurs via apoptosis (Fletcher et al., 1996; Lau et al., 2004). Therefore, we do not believe that a different cell death mechanism is taking place *in vitro*. Moreover, we used Fluoro-Jade to identify granule cell death, which marks degenerating neurons irrespective of the type of cell death (Schmued et al., 1997; Frank et al., 2003), which makes it difficult for us to identify the mechanism of cell death. We think that the CGC death in culture conditions, in the absence of chronic depolarization, is so massive that it completely masks the difference observed between wild type and leaner CGC death *in vivo*.

However, cerebellar slices from both wild type and leaner mice showed significantly reduced cell death when cultured under chronic depolarization. It is well established that cultured cerebellar granule neurons from neonatal rats require chronic

depolarization for their survival (Gallo et al., 1987; Segal et al., 1992; Kohara et al., 1998). However, Mogensen et al. (1994) reported that the situation was different in mouse cerebellar granule neurons which survived without addition of KCl. Fujikawa et al. (2000) reported that the requirement for depolarization for the survival of mouse cerebellar granule neuron was strain dependent. They further reported that cerebellar granule neurons from Balb/C mouse could survive without KCl addition, whereas cerebellar granule neurons from C57Bl/6 mouse could not. Our results from cerebellar slices, obtained from C57Bl/6 mouse background, are in accordance and support their study.

This study demonstrates and supports previous findings that cerebellar granule cells obtained from C57Bl/6 mouse when cultured in high KCl show reduced cell death. However, we were not able to replicate the *in vivo* cell death difference observed between wild type and leaner CGCs in our *in vitro* explant culture. We have shown here that the leaner mouse is not a very good model for *in vitro* study of cerebellar granule cells.

CHAPTER V

CONCLUSIONS

SUMMARY

The leaner mouse is a neurologic mutant mouse that carries a mutation in the pore forming (α1A) subunit of $Ca_V2.1$ voltage-gated calcium channels (VGCC) (Fletcher et al., 1996; Doyle et al., 1997). Phenotypically the leaner mouse exhibit a severe cerebellar ataxia, absence seizures and paroxysmal dyskinesia (Sidman et al., 1965). $Ca_V2.1$ VGCCs are highly expressed in the cerebellum (Stea et al., 1994) and as a result of its dysfunction, due to mutation; many behavioral and morphological abnormalities associated with cerebellar function are produced. Leaner mice provide a great opportunity to learn about inherited human neurological disorders like familial hemiplegic migraine, episodic ataxia type 2 and spinocerebellar ataxia type 6, which are caused by mutations in the homologous gene of the leaner mouse.

Neurodegeneration in the leaner cerebellum is extensive, about 50% of cerebellar granule cells and Purkinje cells die by the time animals attain maturity (Herrup and Wilczynski, 1982). The cerebellar granule cell (CGC) death begins shortly after P10 and peaks at P20 (Lau et al., 2004). However, CGC death, while decreased at P30 and P40 compared to P20, is still significantly greater than seen in age-matched wild type mice (Lau et al., 2004). In the present investigation we expanded on previous work by Herrup

and Wilczynski (1982) by precisely identifying the pattern and mode of CGC death in adult leaner mouse. By using mechanism independent Fluoro-Jade and apoptosis specific TUNEL staining, we showed that leaner CGC death continues into adulthood and the spatial pattern of granule cell death observed during postnatal development (Lau et al., 2004) also continues into adulthood.

The primary effect of the leaner mutation is decreased calcium current through $Ca_V2.1$ VGCCs (Dove et al., 1998; Lorenzon et al., 1998; Wakamori et al., 1998). In cerebellar Purkinje cells, $Ca_V2.1$ channel contribute 90% of the whole cell Ca^{2+} currents. As a result there is a 65 % decrease in Ca^{2+} currents in leaner Purkinje cells, which is accompanied by compensatory responses including decreased concentrations of calcium binding proteins and altered calcium buffering at the ER and mitochondria that allow leaner Purkinje cells to maintain normal resting Ca^{2+} concentrations (Dove et al., 2000; Murchison et al., 2002). In cerebellar granule cells 46% of the whole cell Ca^{2+} current is due to $Ca_V2.1$ channels (Randall and Tsien, 1995). The present investigation showed a reduced resting intracellular calcium ($[Ca^{2+}]_i$) in CGC from leaner mice as compared to age matched wild type mice. Using tottering mice as our second control we showed that reduced resting $[Ca^{2+}]_i$ cannot be directly responsible for CGC death as these mice also showed reduced resting $[Ca^{2+}]_i$ but without cell death.

Our results also showed that even though CGCs from leaner mice have dysfunctional $Ca_V2.1$ channels, there is no change in depolarization induced Ca^{2+} influx. This suggests that either there is a possible functional compensation by other VGCCs for dysfunctional $Ca_V2.1$ channels or reduced Ca^{2+} buffering in CGCs such that the Ca^{2+}

influx that does take place in leaner CGCs is not buffered efficiently, leading to increased Ca^{2+} transients. Using $Ca_V2.1$ channel blocker, ω-Agatoxin IVA, there was no decrease in depolarization induced Ca^{2+} transients in leaner CGCs, which suggests that there is a functional compensation for the defective $Ca_V2.1$ calcium channels by other VGCCs.

Mitochondria play an important role in maintaining Ca^{2+} homeostasis, which when disturbed, can lead to significant cellular pathophysiology and cell death. The present investigation showed a reduced mitochondrial membrane potential ($\psi_{m)}$ at the time of peak CGC death in leaner mice as compared to wild type and tottering CGCs. We further discovered that this decreased ψ_m in CGCs of leaner mice is due to change in cellular mitochondrial activity and not the mitochondrial mass. Oxidative stress is known to be involved in the pathogenetic mechanism of many neurodegenerative disorders. However; our experiments suggest a mitochondrial mediated but reactive oxygen species independent cell death in CGCs of leaner mice.

The mechanism of neuronal death in the leaner cerebellum under the environment of reduced calcium influx has been poorly understood. If reduced calcium influx is leading to cell death then culturing cerebellar slices with increased calcium influx should reduce or rescue cell death. In the present investigation we were not able to replicate the *in vivo* cell death difference observed between wild type and leaner CGCs in our *in vitro* explant culture suggesting that leaner mouse is not a very good model for *in vitro* of cerebellar granule cells.

FUTURE STUDIES

As discussed in chapter III, the depolarization induced calcium transients in leaner cerebellar granule cells are not different from age matched wild type granule cells. This means that other voltage gated calcium channels are compensating for the dysfunctional $Ca_V2.1$ channels. Further experiments need to be done to elucidate the channel subtypes that might be carrying out this compensation. This can be established by investigating the pharmacological profile of calcium currents in leaner and wild type CGCs by applying nifedipine, ω-conotoxin GVIA and ω-CTX-MVIIC, antagonists of Ca_V1 (L-type), $Ca_V2.2$ (N-type), and both $Ca_V2.1$ and $Ca_V2.2$ (P/Q- and N-type) calcium channels, respectively (Aosaki and Kasai, 1989; Bean,1989; Hillyard et al., 1992). If a change in the fraction of whole cell Ca^{2+} current carried by other voltage gated Ca^{2+} channels is increased in leaner mice, we can substantiate this finding by looking at the increase in levels of the channel transcript. We can use semi-quantitative RT-PCR to measure the mRNA levels of each of the Ca^{2+} channels subtypes from cerebellar granule cells of wild type and leaner mouse.

We also showed a loss of mitochondrial membrane potential (MMP) in CGCs from leaner mice at peak cell stage (P20), however we were unable to explain the temporary increase in MMP at P30. Loss of MMP is usually accompanied by depletion of intracellular ATP levels. We speculate that the increase in MMP at P30 could be a compensatory mechanism to regulate cellular energy levels. To validate this hypothesis, ATP measurements can be performed in acutely isolated cerebellar granule cells (as

described previously) using a bioluminescence assay kit HSII as described by Gatti et al., (2004)

In the present investigation we were not able to replicate the *in vivo* cell death difference observed between wild type and leaner CGCs in our *in vitro* explant culture. We used the mechanism independent stain, Fluoro-Jade to quantify cell death. It would be interesting to identify the exact mechanism of cell death. Cerebellar slices cultured for 10 days *in vitro* can be stained with apoptosis specific TUNEL staining.

The leaner mutation results in truncation of the carboxy terminal of the α_1 2.1 proteins, which leads to reduced calcium currents through dysfunctional $Ca_V2.1$ channels. It seems that either the decreased intracellular calcium influx is directly leading to neurodegeneration or the defective $Ca_V2.1$ channel protein is causing an altered protein-protein interaction at the C-terminus triggering a lethal cascade of altered gene expression. The present investigation suggests that reduced calcium influx is not directly linked to cell death. Recently, it was shown that the C-terminus of the $\alpha_1$2.1 subunit of the $Ca_V2.1$ VGCC is cleaved from the full-length protein and translocated to the Purkinje cell nucleus (Kordasiewicz et al., 2006). The author speculated that this C-terminus may be required for survivability and its alteration in leaner mice may be the reason for Purkinje cell death. Cerebellar granule cells can be isolated as mentioned previously. Cerebellar granule cells fractionation can be performed with NE-PER Nuclear and cytoplasmic extraction reagent kit (Pierce). Nuclear and cytoplasmic protein separated on SDS page gel can be transferred to membrane. By using custom designed antibodies against C-terminus of the $\alpha_1$2.1 subunit of $Ca_V2.1$ VGCC we can identify the

translocation of C-terminus to nucleus in cerebellar granule cells. Future work in cerebellar granule cell death of leaner mice should be concentrated on identifying the proteins interacting with C-terminus of $Ca_V2.1$ VGCC.

A great deal of research is still required in this area to further elucidate the mechanisms of cerebellar granule cell death in leaner mouse. Once we have complete understanding of the underlying molecular pathways only then we will be able to apply that knowledge to investigate potential therapies aimed at preserving neuronal survival and cerebellar function.

REFERENCES

Abbott LC, Jacobowitz DM (1995) Development of calretinin-immunoreactive unipolar brush-like cells and an afferent pathway to the embryonic and early postnatal mouse cerebellum. Anat Embryol (Berl) 191:541-559.

Abbott LC, Jacobowitz DM (1999) Developmental expression of calretinin-immunoreactivity in the thalamic eminence of the fetal mouse. Int J Dev Neurosci 17:331-345.

Abbott LC, Bump M, Brandl A, De Laune S (2000) Investigation of the role of the cerebellum in the myoclonic-like movement disorder exhibited by tottering mice. Mov Disord 15 Suppl 1:53-59.

Adams JM, Cory S (1998) The Bcl-2 protein family: arbiters of cell survival. Science 281:1322-1326.

Alonso MT, Villalobos C, Chamero P, Alvarez J, Garcia-Sancho J (2006) Calcium microdomains in mitochondria and nucleus. Cell Calcium 40:513-525.

Altman J (1972) Postnatal development of the cerebellar cortex in the rat. II. Phases in the maturation of Purkinje cells and of the molecular layer. J Comp Neurol 145:399-463.

Altman J, Bayer SA (1997a) Basic cellular organization and circuitry of the cerebellar cortex. In: Development of the cerebellar system (Altman J, Bayer SA, eds), pp 26-43. Boca Raton, FL: CRC Press.

Altman J, Bayer SA (1997b) Comparative anatomy of cerebellum: An evolutionary perspective In: Development of the cerebellar system (Altman J, Bayer SA, eds), pp 2-25. Boca Raton, FL: CRC Press.

Altman J, Bayer SA (1997c) Postnatal development of Purkinje cells In: Development of the cerebellar system (Altman J, Bayer SA, eds), pp 378-411. Boca Raton, FL: CRC Press.

Altman J, Bayer SA (1997d) The generation, movements and settling of cerebellar granule cells and the formation of parallel fibers In: Development of the cerebellar system (Altman J, Bayer SA, eds), pp 334-361. Boca Raton, FL: CRC Press.

Altman J, Bayer SA (1997e) An overview of the postnatal development of the rat cerebellum In: Development of the cerebellar system (Altman J, Bayer SA, eds), pp 324-333. Boca Raton, FL: CRC Press.

Ambudkar IS (2006) Ca^{2+} signaling microdomains: platforms for the assembly and regulation of TRPC channels. Trends in Pharmacological Sciences 27:25-32.

Andre P, Pompeiano O, White SR (1993) Activation of muscarinic receptors induces a long-lasting enhancement of Purkinje cell responses to glutamate. Brain Res 617:28-36.

Andressen C, Blumcke I, Celio MR (1993) Calcium-binding proteins: selective markers of nerve cells. Cell Tissue Res 271:181-208.

Aosaki T, Kasai H (1989) Characterization of two kinds of high-voltage-activated Ca-channel currents in chick sensory neurons. Differential sensitivity to dihydropyridines and omega-conotoxin GVIA. Pflugers Arch 414:150-156.

Arundine M, Tymianski M (2003) Molecular mechanisms of calcium-dependent neurodegeneration in excitotoxicity. Cell Calcium 34:325-337.

Austin MC, Schultzberg M, Abbott LC, Montpied P, Evers JR, Paul SM, Crawley JN (1992) Expression of tyrosine hydroxylase in cerebellar Purkinje neurons of the mutant tottering and leaner mouse. Brain Res Mol Brain Res 15:227-240.

Ayata C, Shimizu-Sasamata M, Lo EH, Noebels JL, Moskowitz MA (2000) Impaired neurotransmitter release and elevated threshold for cortical spreading depression in mice with mutations in the alpha1A subunit of P/Q type calcium channels. Neuroscience 95:639-645.

Baimbridge KG, Celio MR, Rogers JH (1992) Calcium-binding proteins in the nervous system. Trends Neurosci 15:303-308.

Barclay J, Rees M (1999) Mouse models of spike-wave epilepsy. Epilepsia 40 Suppl 3:17-22.

Barili P, Bronzetti E, Ricci A, Zaccheo D, Amenta F (2000) Microanatomical localization of dopamine receptor protein immunoreactivity in the rat cerebellar cortex. Brain Res 854:130-138.

Barmack NH, Baughman RW, Eckenstein FP (1992a) Cholinergic innervation of the cerebellum of rat, rabbit, cat, and monkey as revealed by choline acetyltransferase activity and immunohistochemistry. J Comp Neurol 317:233-249.

Barmack NH, Baughman RW, Eckenstein FP, Shojaku H (1992b) Secondary vestibular cholinergic projection to the cerebellum of rabbit and rat as revealed by choline acetyltransferase immunohistochemistry, retrograde and orthograde tracers. J Comp Neurol 317:250-270.

Bastianelli E (2003) Distribution of calcium-binding proteins in the cerebellum. Cerebellum 2:242-262.

Bean BP (1989) Classes of calcium channels in vertebrate cells. Annu Rev Physiol 51:367-384.

Bear MF, Connors BW, Paradiso MA (2001) The action potential In: Neuroscience: Exploring the brain (Bear MF, Connors BW, Paradiso MA, eds), pp 74-98. Baltimore, MD: Lippincott Williams & Wilkins.

Benn SC, Woolf CJ (2004) Adult neuron survival strategies--slamming on the brakes. Nat Rev Neurosci 5:686-700.

Berggren PO, Yang SN, Murakami M, Efanov AM, Uhles S, Kohler M, Moede T, Fernstrom A, Appelskog IB, Aspinwall CA, Zaitsev SV, Larsson O, de Vargas LM, Fecher-Trost C, Weissgerber P, Ludwig A, Leibiger B, Juntti-Berggren L, Barker CJ, Gromada J, Freichel M, Leibiger IB, Flockerzi V (2004) Removal of Ca^{2+} channel beta3 subunit enhances Ca2+ oscillation frequency and insulin exocytosis. Cell 119:273-284.

Bernardi P, Scorrano L, Colonna R, Petronilli V, Di Lisa F (1999) Mitochondria and cell death. Mechanistic aspects and methodological issues. Eur J Biochem 264:687-701.

Berridge MJ (1998) Neuronal calcium signaling. Neuron 21:13-26.

Berridge MJ, Lipp P, Bootman MD (2000) The versatility and universality of calcium signalling. Nat Rev Mol Cell Biol 1:11-21.

Berridge MJ, Bootman MD, Roderick HL (2003) Calcium signalling: dynamics, homeostasis and remodelling. Nat Rev Mol Cell Biol 4:517-529.

Bezanilla F (2005) Voltage-gated ion channels. IEEE Trans Nanobioscience 4:34-48.

Bezin S, Charpentier G, Fossier P, Cancela J-M (2006) The Ca^{2+}-releasing messenger NAADP, a new player in the nervous system. Journal of Physiology, Paris 99:111-118.

Bidaud I, Mezghrani A, Swayne LA, Monteil A, Lory P (2006) Voltage-gated calcium channels in genetic diseases. Biochim Biophys Acta 1763:1169-1174.

Billups D, Liu Y-B, Birnstiel S, Slater NT (2002) NMDA receptor-mediated currents in rat cerebellar granule and unipolar brush cells. Journal of Neurophysiology 87:1948-1959.

Black JL, 3rd (2003) The voltage-gated calcium channel gamma subunits: a review of the literature. J Bioenerg Biomembr 35:649-660.

Blackstone C, Sheng M (2002) Postsynaptic calcium signaling microdomains in neurons. Front Biosci 7:d872-885.

Blakeley J, Jankovic J (2002) Secondary paroxysmal dyskinesias. Mov Disord 17:726-734.

Blanchard KT, Allard EK, Boekelheide K (1996) Fate of germ cells in 2,5-hexanedione-induced testicular injury. I. Apoptosis is the mechanism of germ cell death. Toxicology & Applied Pharmacology 137:141-148.

Boatright KM, Renatus M, Scott FL, Sperandio S, Shin H, Pedersen IM, Ricci JE, Edris WA, Sutherlin DP, Green DR, Salvesen GS (2003) A unified model for apical caspase activation. Mol Cell 11:529-541.

Boldyrev A, Koudinov A, Berezov T, Carpenter DO (2004) Amyloid-beta induced cell death is independent of free radicals. Journal of Alzheimer's Disease 6:633-638; discussion 673-681.

Bourinet E, Soong TW, Sutton K, Slaymaker S, Mathews E, Monteil A, Zamponi GW, Nargeot J, Snutch TP (1999) Splicing of alpha 1A subunit gene generates phenotypic variants of P- and Q-type calcium channels. Nat Neurosci 2:407-415.

Budd SL, Nicholls DG (1996) A reevaluation of the role of mitochondria in neuronal Ca^{2+} homeostasis. Journal of Neurochemistry 66:403-411.

Bursch W (2001) The autophagosomal-lysosomal compartment in programmed cell death. Cell Death Differ 8:569-581.

Butterfield DA, Castegna A, Drake J, Scapagnini G, Calabrese V (2002) Vitamin E and neurodegenerative disorders associated with oxidative stress. Nutritional Neuroscience 5:229-239.

Cajal S (1888a) Estructura de los centros nerviosos de las aves. Rev Trim Histol Normal Patol 1:pp. 1–10. .

Cajal S (1888b) Sobre las fibras nerviosas de la capa molecular del cerebelo. Rev Trim Histol Normal Patol 1:pp. 33–49.

Cajal S (1911) Histologie du Système Nerveux de l'Homme et des Vertébrés. vol. II. A. Maloine, Paris.

Campbell DB, Hess EJ (1998) Cerebellar circuitry is activated during convulsive episodes in the tottering (tg/tg) mutant mouse. Neuroscience 85:773-783.

Campbell DB, Hess EJ (1999) L-type calcium channels contribute to the tottering mouse dystonic episodes. Mol Pharmacol 55:23-31.

Canzoniero LMT, Snider BJ (2005) Calcium in Alzheimer's disease pathogenesis: too much, too little or in the wrong place? Journal of Alzheimer's Disease 8:147-154; discussion 209-115.

Carafoli E, Tiozzo R, Lugli G, Crovetti F, Kratzing C (1974) The release of calcium from heart mitochondria by sodium. Journal of Molecular & Cellular Cardiology 6:361-371.

Carafoli E (2002) Calcium signaling: a tale for all seasons. Proc Natl Acad Sci USA 99:1115-1122.

Carafoli E (2004) Calcium-mediated cellular signals: a story of failures. Trends Biochem Sci 29:371-379.

Carrera P, Stenirri S, Ferrari M, Battistini S (2001) Familial hemiplegic migraine: a ion channel disorder. Brain Res Bull 56:239-241.

Catterall WA (2000) Structure and regulation of voltage-gated Ca^{2+} channels. Annu Rev Cell Dev Biol 16:521-555.

Catterall WA, Perez-Reyes E, Snutch TP, Striessnig J (2005) International Union of Pharmacology. XLVIII. Nomenclature and structure-function relationships of voltage-gated calcium channels. Pharmacol Rev 57:411-425.

Chan DC (2006) Mitochondrial fusion and fission in mammals. Annu Rev Cell Dev Biol 22:79-99.

Chan-Palay V, Palay SL, Brown JT, Van Itallie C (1977) Sagittal organization of olivocerebellar and reticulocerebellar projections: autoradiographic studies with 35S-methionine. Exp Brain Res 30:561-576.

Cheema ZF, West JR, Miranda RC (2000) Ethanol induces Fas/Apo [apoptosis]-1 mRNA and cell suicide in the developing cerebral cortex. Alcohol Clin Exp Res 24:535-543.

Chen H, Chan DC (2005) Emerging functions of mammalian mitochondrial fusion and fission. Hum Mol Genet 14 Spec No. 2:R283-289.

Clapham DE (2003) TRP channels as cellular sensors. Nature 426:517-524.

Collins F, Schmidt MF, Guthrie PB, Kater SB (1991) Sustained increase in intracellular calcium promotes neuronal survival. J Neurosci 11:2582-2587.

Cooper CE, Davies NA, Psychoulis M, Canevari L, Bates TE, Dobbie MS, Casley CS, Sharpe MA (2003) Nitric oxide and peroxynitrite cause irreversible increases in the K(m) for oxygen of mitochondrial cytochrome oxidase: in vitro and in vivo studies. Biochimica et Biophysica Acta 1607:27-34.

Cory S, Adams JM (2002) The Bcl2 family: regulators of the cellular life-or-death switch. Nat Rev Cancer 2:647-656.

Crepel F, Jaillard D (1990) Protein kinases, nitric oxide and long-term depression of synapses in the cerebellum. Neuroreport 1:133-136.

Crompton M, Costi A (1990) A heart mitochondrial Ca2(+)-dependent pore of possible relevance to re-perfusion-induced injury. Evidence that ADP facilitates pore interconversion between the closed and open states. Biochem J 266:33-39.

Crompton M (1999) The mitochondrial permeability transition pore and its role in cell death. Biochem J 341 (Pt 2):233-249.

Cull-Candy SG, Marshall CG, Ogden D (1989) Voltage-activated membrane currents in rat cerebellar granule neurones. J Physiol 414:179-199.

D'Angelo E, De Filippi G, Rossi P, Taglietti V (1997) Synaptic activation of Ca^{2+} action potentials in immature rat cerebellar granule cells in situ. J Neurophysiol 78:1631-1642.

Das J (2006) The role of mitochondrial respiration in physiological and evolutionary adaptation. Bioessays 28:890-901.

Davidson AM, Halestrap AP (1990) Partial inhibition by cyclosporin A of the swelling of liver mitochondria in vivo and in vitro induced by sub-micromolar [Ca^{2+}], but not by butyrate. Evidence for two distinct swelling mechanisms. Biochem J 268:147-152.

Didier M, Roux P, Piechaczyk M, Verrier B, Bockaert J, Pin JP (1989) Cerebellar granule cell survival and maturation induced by K+ and NMDA correlate with c-fos proto-oncogene expression. Neurosci Lett 107:55-62.

Dino MR, Schuerger RJ, Liu Y, Slater NT, Mugnaini E (2000) Unipolar brush cell: a potential feedforward excitatory interneuron of the cerebellum. Neuroscience 98:625-636.

D'Mello SR, Galli C, Ciotti T, Calissano P (1993) Induction of apoptosis in cerebellar granule neurons by low potassium: inhibition of death by insulin-like growth factor I and cAMP. Proc Natl Acad Sci USA 90:10989-10993.

Dove LS, Abbott LC, Griffith WH (1998) Whole-cell and single-channel analysis of P-type calcium currents in cerebellar Purkinje cells of leaner mutant mice. J Neurosci 18:7687-7699.

Dove LS, Nahm SS, Murchison D, Abbott LC, Griffith WH (2000) Altered calcium homeostasis in cerebellar Purkinje cells of leaner mutant mice. J Neurophysiol 84:513-524.

Doyle J, Ren X, Lennon G, Stubbs L (1997) Mutations in the Cacnl1a4 calcium channel gene are associated with seizures, cerebellar degeneration, and ataxia in tottering and leaner mutant mice. Mamm Genome 8:113-120.

Du C, Fang M, Li Y, Li L, Wang X (2000) Smac, a mitochondrial protein that promotes cytochrome c-dependent caspase activation by eliminating IAP inhibition. Cell 102:33-42.

Duchen MR (2004) Mitochondria in health and disease: perspectives on a new mitochondrial biology. Mol Aspects Med 25:365-451.

Ducros A, Denier C, Joutel A, Vahedi K, Michel A, Darcel F, Madigand M, Guerouaou D, Tison F, Julien J, Hirsch E, Chedru F, Bisgard C, Lucotte G, Despres P, Billard C, Barthez MA, Ponsot G, Bousser MG, Tournier-Lasserve E (1999) Recurrence of the T666M calcium channel CACNA1A gene mutation in familial hemiplegic migraine with progressive cerebellar ataxia. Am J Hum Genet 64:89-98.

Duguez S, Feasson L, Denis C, Freyssenet D (2002) Mitochondrial biogenesis during skeletal muscle regeneration. Am J Physiol Endocrinol Metab 282:E802-809.

Earnshaw WC, Martins LM, Kaufmann SH (1999) Mammalian caspases: structure, activation, substrates, and functions during apoptosis. Annu Rev Biochem 68:383-424.

Eccles JC, Sasaki K, Strata P (1967) A comparison of the inhibitory actions of Golgi cells and of basket cells. Exp Brain Res 3:81-94.

Eichler ME, Dubinsky JM, Rich KM (1992) Relationship of intracellular calcium to dependence on nerve growth factor in dorsal root ganglion neurons in cell culture. J Neurochem 58:263-269.

Enari M, Sakahira H, Yokoyama H, Okawa K, Iwamatsu A, Nagata S (1998) A caspase-activated DNase that degrades DNA during apoptosis, and its inhibitor ICAD.[erratum appears in Nature 1998 May 28;393(6683):396]. Nature 391:43-50.

Ertel EA, Campbell KP, Harpold MM, Hofmann F, Mori Y, Perez-Reyes E, Schwartz A, Snutch TP, Tanabe T, Birnbaumer L, Tsien RW, Catterall WA (2000) Nomenclature of voltage-gated calcium channels. Neuron 25:533-535.

Etheredge JA, Murchison D, Abbott LC, Griffith WH (2007) Functional compensation by other voltage-gated Ca2+ channels in mouse basal forebrain neurons with Ca(V)2.1 mutations. Brain Res 1140:105-119.

Facheris M, Beretta S, Ferrarese C (2004) Peripheral markers of oxidative stress and excitotoxicity in neurodegenerative disorders: tools for diagnosis and therapy? Journal of Alzheimer's Disease 6:177-184.

Fletcher CF, Lutz CM, O'Sullivan TN, Shaughnessy JD, Jr., Hawkes R, Frankel WN, Copeland NG, Jenkins NA (1996) Absence epilepsy in tottering mutant mice is associated with calcium channel defects. Cell 87:607-617.

Fletcher CF, Tottene A, Lennon VA, Wilson SM, Dubel SJ, Paylor R, Hosford DA, Tessarollo L, McEnery MW, Pietrobon D, Copeland NG, Jenkins NA (2001) Dystonia and cerebellar atrophy in Cacna1a null mice lacking P/Q calcium channel activity. Faseb J 15:1288-1290.

Floyd RA, Hensley K (2002) Oxidative stress in brain aging. Implications for therapeutics of neurodegenerative diseases. Neurobiology of Aging 23:795-807.

Frank TC, Nunley MC, Sons HD, Ramon R, Abbott LC (2003) Fluoro-jade identification of cerebellar granule cell and purkinje cell death in the alpha1A calcium ion channel mutant mouse, leaner. Neuroscience 118:667-680.

Franklin JL, Johnson EM, Jr. (1992) Suppression of programmed neuronal death by sustained elevation of cytoplasmic calcium. Trends Neurosci 15:501-508.

Freund TF, Katona I, Piomelli D (2003) Role of endogenous cannabinoids in synaptic signaling. Physiol Rev 83:1017-1066.

Fride E (2005) Endocannabinoids in the central nervous system: from neuronal networks to behavior. Curr Drug Targets CNS Neurol Disord 4:633-642.

Fujikawa N, Tominaga-Yoshino K, Okabe M, Ogura A (2000) Depolarization-dependent survival of cultured mouse cerebellar granule neurons is strain-restrained. Eur J Neurosci 12:1838-1842.

Fujita S, Shimada M, Nakamura T (1966) H3-thymidine autoradiographic studies on the cell proliferation and differentiation in the external and the internal granular layers of the mouse cerebellum. J Comp Neurol 128:191-208.

Fureman BE, Jinnah HA, Hess EJ (2002) Triggers of paroxysmal dyskinesia in the calcium channel mouse mutant tottering. Pharmacol Biochem Behav 73:631-637.

Galione A, Churchill GC (2002) Interactions between calcium release pathways: multiple messengers and multiple stores. Cell Calcium 32:343-354.

Galione A, Ruas M (2005) NAADP receptors. Cell Calcium 38:273-280.

Galli C, Meucci O, Scorziello A, Werge TM, Calissano P, Schettini G (1995) Apoptosis in cerebellar granule cells is blocked by high KCl, forskolin, and IGF-1 through distinct mechanisms of action: the involvement of intracellular calcium and RNA synthesis. Journal of Neuroscience 15:1172-1179.

Gallo V, Kingsbury A, Balazs R, Jorgensen OS (1987) The role of depolarization in the survival and differentiation of cerebellar granule cells in culture. J Neurosci 7:2203-2213.

Gatti R, Belletti S, Uggeri J, Vettori MV, Mutti A, Scandroglio R, Orlandini G (2004) Methylmercury cytotoxicity in PC12 cells is mediated by primary glutathione depletion independent of excess reactive oxygen species generation. Toxicology 204:175-185.

Gerschenson LE, Rotello RJ (1992) Apoptosis: a different type of cell death. Faseb J 6:2450-2455.

Ghez C, Thach W (2000) The cerebellum In: Principles of neural science (Kandel ER, Schwartz JH, Jessell TM, eds), pp 823-852. New York, NY: McGraw-Hill.

Gilbert PF (2001) An outline of brain function. Brain Res Cogn Brain Res 12:61-74.

Goldowitz D (1989) The weaver granuloprival phenotype is due to intrinsic action of the mutant locus in granule cells: evidence from homozygous weaver chimeras. Neuron 2:1565-1575.

Goldowitz D, Hamre K (1998) The cells and molecules that make a cerebellum. Trends Neurosci 21:375-382.

Gomes DA, Leite MF, Bennett AM, Nathanson MH (2006) Calcium signaling in the nucleus. Can J Physiol Pharmacol 84:325-332.

Good CH (2007) Endocannabinoid-dependent regulation of feedforward inhibition in cerebellar Purkinje cells. J Neurosci 27:1-3.

Gozuacik D, Kimchi A (2007) Autophagy and cell death. Curr Top Dev Biol 78:217-245.

Green MC, Sidman RL (1962) Tottering-a neuromusclar mutation in the mouse and its linkage with oligosyndacylism. J Hered 53:233-237.

Griffith WH, Taylor L, Davis MJ (1994) Whole-cell and single-channel calcium currents in guinea pig basal forebrain neurons. J Neurophysiol 71:2359-2376.

Griparic L, van der Bliek AM (2001) The many shapes of mitochondrial membranes. Traffic 2:235-244.

Grynkiewicz G, Poenie M, Tsien RY (1985). A new generation of Ca^{2+} indicators with greatly improved fluorescence properties. J Biol Chem. 260(6):3440-50.

Guerrini R (2001) Idiopathic epilepsy and paroxysmal dyskinesia. Epilepsia 42 Suppl 3:36-41.

Gunter TE, Buntinas L, Sparagna G, Eliseev R, Gunter K (2000) Mitochondrial calcium transport: mechanisms and functions. Cell Calcium 28:285-296.

Hamre KM, Goldowitz D (1997) meander tail acts intrinsic to granule cell precursors to disrupt cerebellar development: analysis of meander tail chimeric mice. Development 124:4201-4212.

Hartmann H, Velbinger K, Eckert A, Muller WE (1996) Region-specific downregulation of free intracellular calcium in the aged rat brain. Neurobiology of Aging 17:557-563.

Hasel KW, Sutcliffe JG (1990) Nucleotide sequence of a cDNA coding for mouse cyclophilin. Nucleic Acids Res 18:4019.

Hatten ME, Alder J, Zimmerman K, Heintz N (1997) Genes involved in cerebellar cell specification and differentiation. Curr Opin Neurobiol 7:40-47.

Herlitze S, Garcia DE, Mackie K, Hille B, Scheuer T, Catterall WA (1996) Modulation of Ca2+ channels by G-protein beta gamma subunits. Nature 380:258-262
.
Herrup K, Wilczynski SL (1982) Cerebellar cell degeneration in the leaner mutant mouse. Neuroscience 7:2185-2196.

Herrup K, Kuemerle B (1997) The compartmentalization of the cerebellum. Annual Review of Neuroscience 20:61-90.

Hess EJ, Wilson MC (1991) Tottering and leaner mutations perturb transient developmental expression of tyrosine hydroxylase in embryologically distinct Purkinje cells. Neuron 6:123-132.

Hibino H, Pironkova R, Onwumere O, Rousset M, Charnet P, Hudspeth AJ, Lesage F (2003) Direct interaction with a nuclear protein and regulation of gene silencing by a variant of the Ca^{2+}-channel beta 4 subunit. Proc Natl Acad Sci U S A 100:307-312.

Hille B (1994) Modulation of ion-channel function by G-protein-coupled receptors. Trends Neurosci 17:531-536.

Hillyard DR, Monje VD, Mintz IM, Bean BP, Nadasdi L, Ramachandran J, Miljanich G, Azimi-Zoonooz A, McIntosh JM, Cruz LJ (1992) A new Conus peptide ligand for mammalian presynaptic Ca^{2+} channels. Neuron 9:69-77.

Hofmann F, Biel M, Flockerzi V (1994) Molecular basis for Ca2+ channel diversity. Annu Rev Neurosci 17:399-418.

Horn R (2000) A new twist in the saga of charge movement in voltage-dependent ion channels. Neuron 25:511-514.

Ichas F, Jouaville LS, Sidash SS, Mazat JP, Holmuhamedov EL (1994) Mitochondrial calcium spiking: a transduction mechanism based on calcium-induced permeability transition involved in cell calcium signalling. FEBS Lett 348:211-215.

Ichas F, Mazat JP (1998) From calcium signaling to cell death: two conformations for the mitochondrial permeability transition pore. Switching from low- to high-conductance state. Biochim Biophys Acta 1366:33-50.

Ichikawa D, Tabuchi A, Taoka A, Tsuchiya T, Tsuda M (1998) Attenuation of cell death mediated by membrane depolarization different from that by exogenous BDNF in cultured mouse cerebellar granule cells. Brain Res Mol Brain Res 56:218-226.

Ikai Y, Takada M, Shinonaga Y, Mizuno N (1992) Dopaminergic and non-dopaminergic neurons in the ventral tegmental area of the rat project, respectively, to the cerebellar cortex and deep cerebellar nuclei. Neuroscience 51:719-728.

Ikeda SR, Dunlap K (1999) Voltage-dependent modulation of N-type calcium channels: role of G protein subunits. Adv Second Messenger Phosphoprotein Res 33:131-151.

Imbrici P, Jaffe SL, Eunson LH, Davies NP, Herd C, Robertson R, Kullmann DM, Hanna MG (2004) Dysfunction of the brain calcium channel CaV2.1 in absence epilepsy and episodic ataxia. Brain 127:2682-2692.

Isaacs KR, Abbott LC (1995) Cerebellar volume decreases in the tottering mouse are specific to the molecular layer. Brain Res Bull 36: 309-14.

Ito M (1984a) General introduction In: The cerebellum and neural control (Ito M, ed), pp 1-10. New York, NY: Raven Press.

Ito M (1984b) Purkinje cells: Morphology and development In: The cerebellum and neural control (Ito M, ed), pp 21-39. New York, NY: Raven Press.

Ito M (1984c) Granule cells. Morphology and development In: The cerebellum and neural control (Ito M, ed), pp 74-85. New York, NY: Raven Press.

Ito M (2006) Cerebellar circuitry as a neuronal machine. Prog Neurobiol 78:272-303.

Jaarsma D, Ruigrok TJ, Caffe R, Cozzari C, Levey AI, Mugnaini E, Voogd J (1997) Cholinergic innervation and receptors in the cerebellum. Prog Brain Res 114:67-96.

Jenner P (2003) Oxidative stress in Parkinson's disease. Annals of Neurology 53 Suppl 3:S26-36; discussion S36-28.

Jouvenceau A, Eunson LH, Spauschus A, Ramesh V, Zuberi SM, Kullmann DM, Hanna MG (2001) Human epilepsy associated with dysfunction of the brain P/Q-type calcium channel. Lancet 358:801-807.

Joza N, Susin SA, Daugas E, Stanford WL, Cho SK, Li CY, Sasaki T, Elia AJ, Cheng HY, Ravagnan L, Ferri KF, Zamzami N, Wakeham A, Hakem R, Yoshida H, Kong YY, Mak TW, Zuniga-Pflucker JC, Kroemer G, Penninger JM (2001) Essential role of the mitochondrial apoptosis-inducing factor in programmed cell death. Nature 410:549-554.

Jun K, Piedras-Renteria ES, Smith SM, Wheeler DB, Lee SB, Lee TG, Chin H, Adams ME, Scheller RH, Tsien RW, Shin HS (1999) Ablation of P/Q-type Ca(2+) channel currents, altered synaptic transmission, and progressive ataxia in mice lacking the alpha(1A)-subunit. Proc Natl Acad Sci USA 96:15245-15250.

Kajta M (2004) Apoptosis in the central nervous system: mechanisms and protective strategies. Pol J Pharmacol 56:689-700.

Kandel ER, Siegelbaum SA (2000) Synaptic integration In: Principles of neural science (Kandel ER, Schwartz JH, Jessell TM, eds), pp 207-228. New York, NY: McGraw-Hill.

Kirischuk S, Voitenko N, Kostyuk P, Verkhratsky A (1996) Calcium signalling in granule neurones studied in cerebellar slices. Cell Calcium 19:59-71.

Kirkland RA, Franklin JL (2003) Bax, reactive oxygen, and cytochrome c release in neuronal apoptosis. Antioxidants & Redox Signaling 5:589-596.

Klockgether T, Evert B (1998) Genes involved in hereditary ataxias. Trends Neurosci 21:413-418.

Koester J, Siegelbaum SA (2000) Propagated signaling: The action potential In: Principles of neural science (Kandel ER, Schwartz JH, Jessell TM, eds), pp. 150-174. New York, NY: McGraw-Hill.

Kohara K, Ono T, Tominaga-Yoshino K, Shimonaga T, Kawashima S, Ogura A (1998) Activity-dependent survival and enhanced turnover of calcium in cultured rat cerebellar granule neurons. Brain Res 809:231-237.

Koike T, Martin DP, Johnson EM, Jr. (1989) Role of Ca^{2+} channels in the ability of membrane depolarization to prevent neuronal death induced by trophic-factor deprivation: evidence that levels of internal Ca^{2+} determine nerve growth factor dependence of sympathetic ganglion cells. Proc Natl Acad Sci USA 86:6421-6425.

Kordasiewicz HB, Thompson RM, Clark HB, Gomez CM (2006) C-termini of P/Q-type Ca^{2+} channel alpha1A subunits translocate to nuclei and promote polyglutamine-mediated toxicity. Hum Mol Genet 15:1587-1599.

Kreitzer AC, Carter AG, Regehr WG (2002) Inhibition of interneuron firing extends the spread of endocannabinoid signaling in the cerebellum. Neuron 34:787-796.

Larramendi EM, Victor T (1967) Synapses on the Purkinje cell spines in the mouse. An electronmicroscopic study. Brain Res 5:15-30.

Lau FC, Abbott LC, Rhyu IJ, Kim DS, Chin H (1998) Expression of calcium channel alpha1A mRNA and protein in the leaner mouse (tgla/tgla) cerebellum. Brain Res Mol Brain Res 59:93-99.

Lau, FC (1999) Apoptosis, reduced intracellular free calcium level and altered gene expression in the cerebellum of the leaner mutant mouse. Dissertation. College Station, TX: Texas A&M University.

Lau FC, Frank TC, Nahm S-S, Stoica G, Abbott LC (2004) Postnatal apoptosis in cerebellar granule cells of homozygous leaner (tg1a/tg1a) mice. Neurotoxicity Research 6:267-280.

Laube G, Seidenbecher CI, Richter K, Dieterich DC, Hoffmann B, Landwehr M, Smalla KH, Winter C, Bockers TM, Wolf G, Gundelfinger ED, Kreutz MR (2002) The neuron-specific Ca^{2+}-binding protein caldendrin: gene structure, splice isoforms, and expression in the rat central nervous system. Mol Cell Neurosci 19:459-475.

Lee A, Wong ST, Gallagher D, Li B, Storm DR, Scheuer T, Catterall WA (1999) Ca^{2+}/calmodulin binds to and modulates P/Q-type calcium channels. Nature 399:155-159.

Leenders AG, van den Maagdenberg AM, Lopes da Silva FH, Sheng ZH, Molenaar PC, Ghijsen WE (2002) Neurotransmitter release from tottering mice nerve terminals with reduced expression of mutated P- and Q-type Ca^{2+}-channels. Eur J Neurosci 15:13-18.

Leite MF, Thrower EC, Echevarria W, Koulen P, Hirata K, Bennett AM, Ehrlich BE, Nathanson MH (2003) Nuclear and cytosolic calcium are regulated independently. Proc Natl Acad Sci U S A 100:2975-2980.

Li D, Wang F, Lai M, Chen Y, Zhang JF (2005) A protein phosphatase 2calpha-Ca2+ channel complex for dephosphorylation of neuronal Ca^{2+} channels phosphorylated by protein kinase C. J Neurosci 25:1914-1923.

Li P, Nijhawan D, Budihardjo I, Srinivasula SM, Ahmad M, Alnemri ES, Wang X (1997) Cytochrome c and dATP-dependent formation of Apaf-1/caspase-9 complex initiates an apoptotic protease cascade. Cell 91:479-489.

Li WC, Tang XH, Li HZ, Wang JJ (1999) Histamine excites rat cerebellar granule cells in vitro through H1 and H2 receptors. J Physiol Paris 93:239-244.

Liu X, Kim CN, Yang J, Jemmerson R, Wang X (1996) Induction of apoptotic program in cell-free extracts: requirement for dATP and cytochrome c. Cell 86:147-157.

Llinas RR, Sugimori M, Cherksey B (1989) Voltage-dependent calcium conductances in mammalian neurons. The P channel. Ann N Y Acad Sci 560:103-111.

Lorenzon NM, Lutz CM, Frankel WN, Beam KG (1998) Altered calcium channel currents in Purkinje cells of the neurological mutant mouse leaner. J Neurosci 18:4482-4489.

Lory P, Ophoff RA, Nahmias J (1997) Towards a unified nomenclature describing voltage-gated calcium channel genes. Hum Genet 100:149-150.

Magistretti PJ, Pellerin L, Rothman DL, Shulman RG (1999) Energy on demand. Science 283:496-497.

Mallet J, Huchet M, Pougeois R, Changeux JP (1976) Anatomical, physiological and biochemical studies on the cerebellum from mutant mice. III. Protein differences associated with the weaver, staggerer and nervous mutations. Brain Research 103:291-312
.
Malviya AN, Klein C (2006) Mechanism regulating nuclear calcium signaling. Can J Physiol Pharmacol 84:403-422.

Marani E, Voogd J (1979) The morphology of the mouse cerebellum. Acta Morphol Neerl Scand 17:33-52.

Mariani J, Crepel F, Mikoshiba K, Changeux JP, Sotelo C (1977) Anatomical, physiological and biochemical studies of the cerebellum from Reeler mutant mouse. Philosophical Transactions of the Royal Society of London - Series B: Biological Sciences 281:1-28.

Martin JH (1996) The cerebellum In: Neuroanatomy (Martin JH, ed), pp 291-322. Stamford, CT: Appleton & Lange.

Martinon F, Tschopp J (2004) Inflammatory caspases: linking an intracellular innate immune system to autoinflammatory diseases. Cell 117:561-574.

Matsushita K, Wakamori M, Rhyu IJ, Arii T, Oda S, Mori Y, Imoto K (2002) Bidirectional alterations in cerebellar synaptic transmission of tottering and rolling Ca2+ channel mutant mice. J Neurosci 22:4388-4398.

Mattson MP (2006) Neuronal life-and-death signaling, apoptosis, and neurodegenerative disorders. Antioxid Redox Signal 8:1997-2006.

McAlhany RE, Jr., West JR, Miranda RC (1997) Glial-derived neurotrophic factor rescues calbindin-D28k-immunoreactive neurons in alcohol-treated cerebellar explant cultures. J Neurobiol 33:835-847.

McBride HM, Neuspiel M, Wasiak S (2006) Mitochondria: more than just a powerhouse. Curr Biol 16:R551-560.

McMahon AP, Bradley A (1990) The Wnt-1 (int-1) proto-oncogene is required for development of a large region of the mouse brain. Cell 62:1073-1085.

Meier P, Finch A, Evan G (2000) Apoptosis in development. Nature 407:796-801.

Meldolesi J, Pozzan T (1998) The endoplasmic reticulum Ca^{2+} store: a view from the lumen. Trends Biochem Sci 23:10-14.

Meldolesi J (2001) Rapidly exchanging Ca^{2+} stores in neurons: molecular, structural and functional properties. Prog Neurobiol 65:309-338.

Miale IL, Sidman RL (1961) An autoradiographic analysis of histogenesis in the mouse cerebellum. Exp Neurol 4:277-296.

Middleton FA, Strick PL (1998) The cerebellum: an overview. Trends Neurosci 21:367-369.

Migheli A, Cavalla P, Marino S, Schiffer D (1994) A study of apoptosis in normal and pathologic nervous tissue after in situ end-labeling of DNA strand breaks. J Neuropathol Exp Neurol 53:606-616.

Mikhaylova M, Sharma Y, Reissner C, Nagel F, Aravind P, Rajini B, Smalla KH, Gundelfinger ED, Kreutz MR (2006) Neuronal Ca^{2+} signaling via caldendrin and calneurons. Biochim Biophys Acta 1763:1229-1237.

Miller RJ (1991) The control of neuronal Ca^{2+} homeostasis. Progress in Neurobiology 37:255-285.

Minke B (2006) TRP channels and Ca^{2+} signaling. Cell Calcium 40:261-275.

Mintz IM, Adams ME, Bean BP (1992) P-type calcium channels in rat central and peripheral neurons. Neuron 9:85-95.

Miranda R, Sohrabji F, Singh M, Toran-Allerand D (1996) Nerve growth factor (NGF) regulation of estrogen receptors in explant cultures of the developing forebrain. J Neurobiol 31:77-87.

Missiaen L, Robberecht W, van den Bosch L, Callewaert G, Parys JB, Wuytack F, Raeymaekers L, Nilius B, Eggermont J, De Smedt H (2000) Abnormal intracellular ca(2+)homeostasis and disease. Cell Calcium 28:1-21.

Mogensen HS, Hack N, Balazs R, Jorgensen OS (1994) The survival of cultured mouse cerebellar granule cells is not dependent on elevated potassium-ion concentration. Int J Dev Neurosci 12:451-460.

Montell C (2004) Exciting trips for TRPs. Nat Cell Biol 6:690-692.

Montell C (2005) The latest waves in calcium signaling. Cell 122:157-163.

Moran J, Rivera-Gaxiola M (1992) Effect of potassium and N-methyl-D-aspartate on the aspartate aminotransferase activity in cultured cerebellar granule cells. J Neurosci Res 33:239-247.

Morin F, Dino MR, Mugnaini E (2001) Postnatal differentiation of unipolar brush cells and mossy fiber-unipolar brush cell synapses in rat cerebellum. Neuroscience 104:1127-1139.

Mugnaini E, Floris A (1994) The unipolar brush cell: a neglected neuron of the mammalian cerebellar cortex. Journal of Comparative Neurology 339:174-180.

Mullen RJ, Buck CR, Smith AM (1992) NeuN, a neuronal specific nuclear protein in vertebrates. Development 116:201-211.

Murchison D, Griffith WH (1998) Increased calcium buffering in basal forebrain neurons during aging. Journal of Neurophysiology 80:350-364.

Murchison D, Dove LS, Abbott LC, Griffith WH (2002) Homeostatic compensation maintains Ca^{2+} signaling functions in Purkinje neurons in the leaner mutant mouse. Cerebellum 1:119-127.

Nahm SS, Tomlinson DJ, Abbott LC (2002) Decreased calretinin expression in cerebellar granule cells in the leaner mouse. J Neurobiol 51:313-322.

Nahm SS (2002) Analysis of gene and protein expression related to cerebellar neurodegeneration in the calcium channel mutant mouse, leaner. Dissertation. College Station, TX: Texas A&M University.

Nahm SS, Jung KY, Enger MK, Griffith WH, Abbott LC (2005) Differential expression of T-type calcium channels in P/Q-type calcium channel mutant mice with ataxia and absence epilepsy. J Neurobiol 62:352-360.

Nakai M, Takeda A, Cleary ML, Endo T (1993) The bcl-2 protein is inserted into the outer membrane but not into the inner membrane of rat liver mitochondria in vitro. Biochem Biophys Res Commun 196:233-239.

Narboux-Neme N, Louvi A, Alexandre P, Wassef M (2005) Regionalization of the isthmic and cerebellar primordia. Progress in Brain Research 148:29-36
.
Newmeyer DD, Ferguson-Miller S (2003) Mitochondria: releasing power for life and unleashing the machineries of death.[erratum appears in Cell. 2003 Mar 21;(112)6:873]. Cell 112:481-490.

Nicholls DG, Scott ID (1980) The regulation of brain mitochondrial calcium-ion transport. The role of ATP in the discrimination between kinetic and membrane-potential-dependent calcium-ion efflux mechanisms. Biochem J 186:833-839.

Nicholls DG, Ward MW (2000) Mitochondrial membrane potential and neuronal glutamate excitotoxicity: mortality and millivolts. Trend Neurosci 23(4):166-74.

Noebels JL (1984) Isolating single genes of the inherited epilepsies. Ann Neurol 16 Suppl:S18-21.

Nogueron MI, Porgilsson B, Schneider WE, Stucky CL, Hillard CJ (2001) Cannabinoid receptor agonists inhibit depolarization-induced calcium influx in cerebellar granule neurons. J Neurochem 79:371-381.

Nolte J (1999) The human brain: An introductions to its functional anatomy (Nolte J, ed), pp 469-493. New York, NY: Mosby.

Oberdoerster J (2001) Isolation of cerebellar granule cells from Neonatal rats In: Current protocols in toxicology (Maines MD, Costa LG, Hodgson E, Reed DJ, Sipes IG., eds), pp 12.7.1-12.7.10. Hoboken, NJ: John Wiley and Sons, Inc.

Oda S (1981) A new allele of the tottering locus, rolling mouse Nagoya, on chromosome no. 8 in the mouse. Jpn J Genet 56: 295-299.

Ogasawara M, Kurihara T, Hu Q, Tanabe T (2001) Characterization of acute somatosensory pain transmission in P/Q-type Ca(2+) channel mutant mice, leaner. FEBS Lett 508:181-186.

O'Leary JL, Smith JM, Inukai J, O'Leary M (1970) The inferior olive as a source of climbing fibers in the rat. Bibl Psychiatr 143:128-137.

Olschowka JA, Vijayan VK (1980) Postnatal development of cholinergic neurotransmitter enzymes in the mouse cerebellum. Biochemical, light microscopic and electron microscopic cytochemical investigations. J Comp Neurol 191:77-101.

Ophoff RA, Terwindt GM, Vergouwe MN, van Eijk R, Oefner PJ, Hoffman SM, Lamerdin JE, Mohrenweiser HW, Bulman DE, Ferrari M, Haan J, Lindhout D, van Ommen GJ, Hofker MH, Ferrari MD, Frants RR (1996) Familial hemiplegic migraine and episodic ataxia type-2 are caused by mutations in the Ca^{2+} channel gene CACNL1A4. Cell 87:543-552.

Palkovits M, Magyar P, Szentagothai J (1971) Quantitative histological analysis of the cerebellar cortex in the cat. 3. Structural organization of the molecular layer. Brain Res 34:1-18.

Panula P, Takagi H, Inagaki N, Yamatodani A, Tohyama M, Wada H, Kotilainen E (1993) Histamine-containing nerve fibers innervate human cerebellum. Neurosci Lett 160:53-56.

Parent A (1996) Cerebellum In: Human neuroanatomy (Parent A, ed), pp 583-604. Philadelphia, PA: Williams and Wilkins Inc.

Pearson H, Graham ME, Burgoyne RD (1992a) N-methyl-D-aspartate responses in rat cerebellar granule cells are modified by chronic depolarisation in culture. Neurosci Lett 142:27-30.

Pearson H, Graham ME, Burgoyne RD (1992b) Relationship between intracellular free calcium concentration and NMDA-induced cerebellar granule cell survival i*n vitro*. Eur J Neurosci 4:1369-1375.

Perkins GA, Renken CW, Frey TG, Ellisman MH (2001) Membrane architecture of mitochondria in neurons of the central nervous system. J Neurosci Res 66:857-865.

Petit JM, Maftah A, Ratinaud MH, Julien R (1992) 10N-nonyl acridine orange interacts with cardiolipin and allows the quantification of this phospholipid in isolated mitochondria. European Journal of Biochemistry 209:267-273.

Petit JM, Huet O, Gallet PF, Maftah A, Ratinaud MH, Julien R (1994) Direct analysis and significance of cardiolipin transverse distribution in mitochondrial inner membranes. European Journal of Biochemistry 220:871-879.

Pietrobon D (2002) Calcium channels and channelopathies of the central nervous system. Mol Neurobiol 25:31-50.

Pietrobon D, Striessnig J (2003) Neurobiology of migraine. Nat Rev Neurosci 4:386-398.

Pietrobon D (2005) Function and dysfunction of synaptic calcium channels: insights from mouse models. Curr Opin Neurobiol 15:257-265.

Pinton P, Pozzan T, Rizzuto R (1998) The Golgi apparatus is an inositol 1,4,5-trisphosphate-sensitive Ca^{2+} store, with functional properties distinct from those of the endoplasmic reticulum. EMBO Journal 17:5298-5308.

Pocock JM, Cousin MA, Nicholls DG (1993) The calcium channel coupled to the exocytosis of L-glutamate from cerebellar granule cells is inhibited by the spider toxin, Aga-GI. Neuropharmacology 32:1185-1194.

Polster BM, Fiskum G (2004) Mitochondrial mechanisms of neural cell apoptosis. J Neurochem 90:1281-1289.

Prunell GF, Arboleda VA, Troy CM (2005) Caspase function in neuronal death: delineation of the role of caspases in ischemia. Curr Drug Targets CNS Neurol Disord 4:51-61.

Putcha GV, Deshmukh M, Johnson EM, Jr. (1999) BAX translocation is a critical event in neuronal apoptosis: regulation by neuroprotectants, BCL-2, and caspases. J Neurosci 19:7476-7485.

Qin N, Platano D, Olcese R, Stefani E, Birnbaumer L (1997) Direct interaction of gbetagamma with a C-terminal gbetagamma-binding domain of the Ca^{2+} channel alpha1 subunit is responsible for channel inhibition by G protein-coupled receptors. Proc Natl Acad Sci USA 94:8866-8871.

Randall A, Tsien RW (1995) Pharmacological dissection of multiple types of Ca^{2+} channel currents in rat cerebellar granule neurons. J Neurosci 15:2995-3012.

Randall A, Benham CD (1999) Recent advances in the molecular understanding of voltage-gated Ca^{2+} channels. Mol Cell Neurosci 14:255-272.

Rego AC, Oliveira CR (2003) Mitochondrial dysfunction and reactive oxygen species in excitotoxicity and apoptosis: implications for the pathogenesis of neurodegenerative diseases. Neurochem Res 28:1563-1574.

Rhyu IJ, Oda S, Uhm CS, Kim H, Suh YS, Abbott LC (1999a) Morphologic investigation of rolling mouse Nagoya (tg(rol)/tg(rol)) cerebellar Purkinje cells: an ataxic mutant, revisited. Neurosci Lett 266:49-52.

Rhyu IJ, Abbott LC, Walker DB, Sotelo C (1999b) An ultrastructural study of granule cell/Purkinje cell synapses in tottering (tg/tg), leaner (tg(la)/tg(la)) and compound heterozygous tottering/leaner (tg/tg(la)) mice. Neuroscience 90:717-728.

Rhyu IJ, Nahm S-S, Hwang SJ, Kim H, Suh Y-S, Oda S-I, Frank TC, Abbott LC (2003) Altered neuronal nitric oxide synthase expression in the cerebellum of calcium channel mutant mice. Brain Research 977:129-140.

Rossi P, D'Angelo E, Magistretti J, Toselli M, Taglietti V (1994) Age-dependent expression of high-voltage activated calcium currents during cerebellar granule cell development in situ. Pflugers Arch 429:107-116.

Rousset M, Cens T, Charnet P (2005) Alone at last! New functions for Ca^{2+} channel beta subunits? Sci STKE 2005:pe11.

Rusnak F, Mertz P (2000) Calcineurin: form and function. Physiol Rev 80:1483-1521.

Russell JW, Sullivan KA, Windebank AJ, Herrmann DN, Feldman EL (1999) Neurons undergo apoptosis in animal and cell culture models of diabetes. Neurobiology of Disease 6:347-363.

Santella L, Bolsover S (1999) Calcium in the nucleus In: Calcium as a cellular regulator (Carafoli E, Klee C, eds), pp 487-511. New York, NY: Oxford University Press.

Sarnat HB, Nochlin D, Born DE (1998) Neuronal nuclear antigen (NeuN): a marker of neuronal maturation in early human fetal nervous system. Brain & Development 20:88-94.

Sastry PS, Rao KS (2000) Apoptosis and the nervous system. J Neurochem 74:1-20.

Sato M, Suzuki K, Yamazaki H, Nakanishi S (2005) A pivotal role of calcineurin signaling in development and maturation of postnatal cerebellar granule cells. Proc Natl Acad Sci USA 102:5874-5879.

Sattler R, Tymianski M (2001) Molecular mechanisms of glutamate receptor-mediated excitotoxic neuronal cell death. Molecular Neurobiology 24:107-129.

Savidge JR, Bristow DR (1997) Routes of NMDA- and K(+)-stimulated calcium entry in rat cerebellar granule cells. Neuroscience Letters 229:109-112.

Savill J, Fadok V, Henson P, Haslett C (1993) Phagocyte recognition of cells undergoing apoptosis. Immunol Today 14:131-136.

Savitz SI, Rosenbaum DM (1998) Apoptosis in neurological disease. Neurosurgery 42:555-572; discussion 573-554.

Scarlett JL, Murphy MP (1997) Release of apoptogenic proteins from the mitochondrial intermembrane space during the mitochondrial permeability transition. FEBS Lett 418:282-286.

Schmued LC, Albertson C, Slikker W, Jr. (1997) Fluoro-Jade: a novel fluorochrome for the sensitive and reliable histochemical localization of neuronal degeneration. Brain Res 751:37-46.

Schmued, LC, Hopkins, KJ (2000) Fluoro-Jade B: a high affinity fluorescent marker for the localization of neuronal degeneration. Brain Res 874: 123-130.

Schulz JB, Weller M, Klockgether T (1996) Potassium deprivation-induced apoptosis of cerebellar granule neurons: a sequential requirement for new mRNA and protein synthesis, ICE-like protease activity, and reactive oxygen species. Journal of Neuroscience 16:4696-4706.

Schweichel JU, Merker HJ (1973) The morphology of various types of cell death in prenatal tissues. Teratology 7:253-266.

Schweighofer N, Doya K, Kuroda S (2004) Cerebellar aminergic neuromodulation: towards a functional understanding. Brain Res Brain Res Rev 44:103-116

Segal RA, Takahashi H, McKay RD (1992) Changes in neurotrophin responsiveness during the development of cerebellar granule neurons. Neuron 9:1041-1052.

Seidenbecher CI, Langnaese K, Sanmarti-Vila L, Boeckers TM, Smalla KH, Sabel BA, Garner CC, Gundelfinger ED, Kreutz MR (1998) Caldendrin, a novel neuronal calcium-binding protein confined to the somato-dendritic compartment. J Biol Chem 273:21324-21331.

Sgaier SK, Millet S, Villanueva MP, Berenshteyn F, Song C, Joyner AL (2005) Morphogenetic and cellular movements that shape the mouse cerebellum; insights from genetic fate mapping. Neuron 45:27-40.

Shi Y (2002) Mechanisms of caspase activation and inhibition during apoptosis. Mol Cell 9:459-470.

Shi Y (2004) Caspase activation: revisiting the induced proximity model. Cell 117:855-858.

Shoji Y, Uedono Y, Ishikura H, Takeyama N, Tanaka T (1995) DNA damage induced by tumour necrosis factor-alpha in L929 cells is mediated by mitochondrial oxygen radical formation. Immunology 84:543-548.

Sidman RL, Green MC, Appel SH (1965) Catalog of the neurological mutants of the mouse. Cambridge, MA: Harvard University Press.

Slemmer JE, De Zeeuw CI, Weber JT (2005) Don't get too excited: mechanisms of glutamate-mediated Purkinje cell death. Progress in Brain Research 148:367-390.

Somlyo AP, Bond M, Somlyo AV (1985) Calcium content of mitochondria and endoplasmic reticulum in liver frozen rapidly in vivo. Nature 314:622-625.

Sotelo C (2004) Cellular and genetic regulation of the development of the cerebellar system. Progress in Neurobiology 72:295-339.

Sparagna GC, Gunter KK, Sheu SS, Gunter TE (1995) Mitochondrial calcium uptake from physiological-type pulses of calcium. A description of the rapid uptake mode. Journal of Biological Chemistry 270:27510-27515.

Stea A, Tomlinson WJ, Soong TW, Bourinet E, Dubel SJ, Vincent SR, Snutch TP (1994) Localization and functional properties of a rat brain alpha 1A calcium channel reflect similarities to neuronal Q- and P-type channels. Proc Natl Acad Sci USA 91:10576-10580.

Stys PK, Waxman SG, Ransom BR (1991) Na(+)-Ca2+ exchanger mediates Ca^{2+} influx during anoxia in mammalian central nervous system white matter. Annals of Neurology 30:375-380.

Sudbrak R, Brown J, Dobson-Stone C, Carter S, Ramser J, White J, Healy E, Dissanayake M, Larregue M, Perrussel M, Lehrach H, Munro CS, Strachan T, Burge S, Hovnanian A, Monaco AP (2000) Hailey-Hailey disease is caused by mutations in ATP2C1 encoding a novel Ca(2+) pump. Human Molecular Genetics 9:1131-1140.

Suh YS, Oda S, Kang YH, Kim H, Rhyu IJ (2002) Apoptotic cell death of cerebellar granule cells in rolling mouse Nagoya. Neurosci Lett 325:1-4.

Susin SA, Lorenzo HK, Zamzami N, Marzo I, Snow BE, Brothers GM, Mangion J, Jacotot E, Costantini P, Loeffler M, Larochette N, Goodlett DR, Aebersold R,

Siderovski DP, Penninger JM, Kroemer G (1999) Molecular characterization of mitochondrial apoptosis-inducing factor. Nature 397:441-446.

Tabuchi A, Nakaoka R, Amano K, Yukimine M, Andoh T, Kuraishi Y, Tsuda M (2000) Differential activation of brain-derived neurotrophic factor gene promoters I and III by Ca^{2+} signals evoked via L-type voltage-dependent and N-methyl-D-aspartate receptor Ca^{2+} channels. J Biol Chem 275:17269-17275.

Tabuchi A, Funaji K, Nakatsubo J, Fukuchi M, Tsuchiya T, Tsuda M (2003) Inactivation of aconitase during the apoptosis of mouse cerebellar granule neurons induced by a deprivation of membrane depolarization. Journal of Neuroscience Research 71:504-515.

Tan Y, Chen C-H, Lawrence D, Carpenter DO (2004) Ortho-substituted PCBs kill cells by altering membrane structure. Toxicological Sciences 80:54-59.

Tanaka O, Sakagami H, Kondo H (1995) Localization of mRNAs of voltage-dependent Ca(2+)-channels: four subtypes of alpha 1- and beta-subunits in developing and mature rat brain. Brain Res Mol Brain Res 30:1-16.

Tedford HW, Zamponi GW (2006) Direct G protein modulation of Cav2 calcium channels. Pharmacol Rev 58:837-862.

Thayer SA, Usachev YM, Pottorf WJ (2002) Modulating Ca2+ clearance from neurons. Front Biosci 7:1255-1279.

Thornberry NA, Lazebnik Y (1998) Caspases: enemies within. Science 281:1312-1316.

Tian L, Wen YQ, Li HZ, Xiong HB, Wang JJ (1999) The excitatory effects of histamine on cerebellar cortical Purkinje cells in the rat. Sheng Li Xue Bao 51:219-223.

Tremper-Wells B, Vallano ML (2005) Nuclear calpain regulates Ca^{2+}-dependent signaling via proteolysis of nuclear Ca2+/calmodulin-dependent protein kinase type IV in cultured neurons. J Biol Chem 280:2165-2175.

Tsou K, Brown S, Sanudo-Pena MC, Mackie K, Walker JM (1998) Immunohistochemical distribution of cannabinoid CB1 receptors in the rat central nervous system. Neuroscience 83:393-411.

Van Petegem F, Clark KA, Chatelain FC, Minor DL, Jr. (2004) Structure of a complex between a voltage-gated calcium channel beta-subunit and an alpha-subunit domain. Nature 429:671-675.

Vergun O, Sobolevsky AI, Yelshansky MV, Keelan J, Khodorov BI, Duchen MR (2001) Exploration of the role of reactive oxygen species in glutamate neurotoxicity in rat hippocampal neurones in culture. J Physiol 531:147-163.

Voogd J, Feirabend HKP, Schoen JHR (1990) Cerebellum and precerebellar nuclei. In: The human nervous sytem (Paxinos G, ed) pp 321-388. San Diego, CA: Academic Press.

Voogd J, Glickstein M (1998) The anatomy of the cerebellum. Trends Neurosci 21:370-375.

Vyssokikh MY, Brdiczka D (2003) The function of complexes between the outer mitochondrial membrane pore (VDAC) and the adenine nucleotide translocase in regulation of energy metabolism and apoptosis. Acta Biochim Pol 50:389-404.

Wakamori M, Yamazaki K, Matsunodaira H, Teramoto T, Tanaka I, Niidome T, Sawada K, Nishizawa Y, Sekiguchi N, Mori E, Mori Y, Imoto K (1998) Single tottering mutations responsible for the neuropathic phenotype of the P-type calcium channel. J Biol Chem 273:34857-34867.

Walker D, De Waard M (1998) Subunit interaction sites in voltage-dependent Ca^{2+} channels: role in channel function. Trends Neurosci 21:148-154.

Wallace VA (1999) Purkinje-cell-derived Sonic hedgehog regulates granule neuron precursor cell proliferation in the developing mouse cerebellum. Current Biology 9:445-448.

Wallig MA, Chan CM, Gillet NA (2002) Specific methods for detection and quantification of apoptosis in tissue section. In: Apoptosis methods in pharmacology and toxicology. Approaches to measurement and quantification (Davis MA, ed), pp 59-76. Totowa, NJ: Humana press

Ward MW, Kogel D, Prehn JH (2004) Neuronal apoptosis: BH3-only proteins the real killers? J Bioenerg Biomembr 36:295-298.

Weber JT (2004) Calcium homeostasis following traumatic neuronal injury. Current Neurovascular Research 1:151-171.

Wechsler-Reya RJ, Scott MP (1999) Control of neuronal precursor proliferation in the cerebellum by Sonic Hedgehog. Neuron 22:103-114.

Werth JL, Thayer SA (1994) Mitochondria buffer physiological calcium loads in cultured rat dorsal root ganglion neurons. J Neurosci 14:348-356.

Westenbroek RE, Sakurai T, Elliott EM, Hell JW, Starr TV, Snutch TP, Catterall WA (1995) Immunochemical identification and subcellular distribution of the alpha 1A subunits of brain calcium channels. J Neurosci 15:6403-6418.

Wetts R, Herrup K (1983) Direct correlation between Purkinje and granule cell number in the cerebella of lurcher chimeras and wild-type mice. Brain Research 312:41-47.

Wilson RI, Nicoll RA (2001) Endogenous cannabinoids mediate retrograde signalling at hippocampal synapses. Nature 410:588-592.

Wolter KG, Hsu YT, Smith CL, Nechushtan A, Xi XG, Youle RJ (1997) Movement of Bax from the cytosol to mitochondria during apoptosis. J Cell Biol 139:1281-1292.

Woodfield K, Ruck A, Brdiczka D, Halestrap AP (1998) Direct demonstration of a specific interaction between cyclophilin-D and the adenine nucleotide translocase confirms their role in the mitochondrial permeability transition. Biochem J 336 (Pt 2):287-290.

Xu J, Chuang DM (1987) Serotonergic, adrenergic and histaminergic receptors coupled to phospholipase C in cultured cerebellar granule cells of rats. Biochem Pharmacol 36:2353-2358.

Yan GM, Ni B, Weller M, Wood KA, Paul SM (1994) Depolarization or glutamate receptor activation blocks apoptotic cell death of cultured cerebellar granule neurons. Brain Res 656:43-51.

Yoon WJ, Won SJ, Ryu BR, Gwag BJ (2003) Blockade of ionotropic glutamate receptors produces neuronal apoptosis through the Bax-cytochrome C-caspase pathway: the causative role of Ca^{2+} deficiency. Journal of Neurochemistry 85:525-533.

Yoshida T, Hashimoto K, Zimmer A, Maejima T, Araishi K, Kano M (2002) The cannabinoid CB1 receptor mediates retrograde signals for depolarization-induced suppression of inhibition in cerebellar Purkinje cells. J Neurosci 22:1690-1697.

Yuan J, Yankner BA (2000) Apoptosis in the nervous system. Nature 407:802-809.

Yuan J, Lipinski M, Degterev A (2003) Diversity in the mechanisms of neuronal cell death. Neuron 40:401-413.

Zamzami N, Kroemer G (2001) The mitochondrion in apoptosis: how Pandora's box opens. Nat Rev Mol Cell Biol 2:67-71.

Zhang L, Goldman JE (1996) Generation of cerebellar interneurons from dividing progenitors in white matter. Neuron 16:47-54.

Zhou YD, Turner TJ, Dunlap K (2003) Enhanced G protein-dependent modulation of excitatory synaptic transmission in the cerebellum of the Ca^{2+} channel-mutant mouse, tottering. J Physiol 547:497-507.

Zhuchenko O, Bailey J, Bonnen P, Ashizawa T, Stockton DW, Amos C, Dobyns WB, Subramony SH, Zoghbi HY, Lee CC (1997) Autosomal dominant cerebellar ataxia (SCA6) associated with small polyglutamine expansions in the alpha 1A-voltage-dependent calcium channel. Nat Genet 15:62-69.

Zorov DB, Bannikova SY, Belousov VV, Vyssokikh MY, Zorova LD, Isaev NK, Krasnikov BF, Plotnikov EY (2005) Reactive oxygen and nitrogen species: friends or foes? Biochemistry-Russia 70:215-221.

Zwingman TA, Neumann PE, Noebels JL, Herrup K (2001) Rocker is a new variant of the voltage-dependent calcium channel gene Cacna1a. J Neurosci 21:1169-1178.

VITA

Name: Bhupinder Bawa

Address: Department of Veterinary Integrative Biosciences, College of Veterinary Medicine and Biomedical Sciences, Texas A&M University, VMA Building Room 107, 4458 TAMU, College Station, TX 77843-4458

Email Address: bsbawa@rediffmail.com

Education:

M.V.Sc., 2002, Veterinary Anatomy & Histology, Punjab Agricultural University, India

B.V.Sc & A.H., 1995, Punjab Agricultural University, India, 2000

Professional Experience

Research Associate 2002-2003, Punjab Agricultural University, India

Publications:

1) Bellum S, Bawa B, Thuett KA, Stoica G, Abbott LC (2007) Changes in biochemical processes in cerebellar granule cells of mice exposed to methylmercury. International Journal of Toxicology, 26:261–269.